Development of functional assays for human neuropeptide Y ($Y_{1,2,4,5}$) receptors exploiting GTPase activity and (bio)luminescence as readout

Dissertation

zur Erlangung des Doktorgrades der Naturwissenschaften (Dr. rer. nat.)
der Naturwissenschaftlichen Fakultät IV – Chemie und Pharmazie –
der Universität Regensburg

vorgelegt von
Nathalie Pop
aus Sathmar
2010

Die vorliegende Arbeit entstand im Rahmen des Graduiertenkollegs „Medizinische Chemie: Molekulare Erkennung – Ligand-Rezeptor-Wechselwirkungen“ (GRK 760) in der Zeit von Januar 2006 bis Juli 2010 unter der Leitung von Herrn Prof. Dr. Armin Buschauer, Herrn Prof. Dr. Günther Bernhardt und Herrn Prof. Dr. Roland Seifert am Institut für Pharmazie der Naturwissenschaftlichen Fakultät IV – Chemie und Pharmazie der Universität Regensburg.

Das Promotionsgesuch wurde eingereicht im Juli 2010.

Tag der mündlichen Prüfung: 06. August 2010

Prüfungsausschuss:	Prof. Dr. J. Heilmann	(Vorsitzender)
	Prof. Dr. A. Buschauer	(Erstgutachter)
	Prof. Dr. G. Bernhardt	(Zweitgutachter)
	Prof. Dr. A. Göpferich	(Drittprüfer)

Für meine Familie

„Wir wollen die Gegenwart mit Hoffnung gestalten, weil uns die Zukunft gewiss ist“

(Peter Hahne)

An dieser Stelle bedanke ich mich bei:

Herrn Prof. Dr. Armin Buschauer für die Möglichkeit an diesem spannenden und vielseitigen Projekt in seinem Arbeitskreis arbeiten zu dürfen, für seine Hilfsbereitschaft sowie seine konstruktive Kritik bei der Durchsicht dieser Arbeit.

Herrn Prof. Dr. Günther Bernhardt für seine fachliche Anleitung, sein Interesse an den Projekten, seine Hilfsbereitschaft und die kritische Durchsicht der Arbeit.

Herrn Prof. Dr. Roland Seifert (Medizinische Hochschule Hannover) für seine wissenschaftlichen Anregungen, sein Interesse sowie seine konstruktive Kritik bei der Entwicklung der GTPase assays für den Y_2 und Y_4 Rezeptor.

Frau Prof. Dr. Chiara Cabrele (Ruhruniversität Bochum) für die Synthese der benötigten Peptide, ihre Hilfsbereitschaft und die stets gute Zusammenarbeit.

Herrn Dr. Viacheslav O. Nikolaev (Universität Würzburg) für die Bereitstellung des Plasmids pcDNA3-EYFP-Epac2B(murine)-ECFP.

Herrn Dr. J. Daniels (Glaxo Wellcome) für die Bereitstellung des Liganden GW1229.

Herrn Dr. Dietmar Gross für die Einarbeitung in die Konfokalmikroskopie und seine stete Hilfsbereitschaft.

Frau Dr. Katharina Wenzel-Seifert für ihre Hilfsbereitschaft bei Fragen zur Klonierung und PCR.

Herrn Dr. Erich Schneider, Herrn Dr. David Schnell und Herrn Dr. Patrick Igel für ihre wertvolle Unterstützung und die anregenden Diskusionen vor allem auf dem Gebiet der GTPase.

Herrn Dr. Max Keller für die Aufreinigung von Peptiden mittels HPLC und die stets gute Zusammenarbeit.

Herrn Dr. Albert Brennauer und Herrn Nikola Pluym für die Bereitstellung von Y_2 Antagonisten sowie Herrn Dr. Liantao Li für die Synthese des Y_5 Antagonisten CGP 71683A.

Frau Dr. Anja Kraus und Herrn Dr. Patrick Igel für die Bereitstellung von Substanzen zur Testung am Y_4 Rezeptor.

Frau Dr. Edith Hofinger und Herrn Dr. Ralf Ziemek für die freundliche Unterstützung bei molekularbiologischen Arbeiten und dem Erlernen der Zellkultur in der Anfangszeit der Promotion.

Frau Evi Schreiber, Frau Susanne Bollwein, Frau Brigitte Wenzel für die Unterstützung auf dem Gebiet der Zellkultur und die gute Zusammenarbeit.

Frau Gertraud Wilberg für die Unterstützung auf dem Gebiet der Sf9 Zellkultur, die Einarbeitung in die SDS-Page und Western Blot und für ihre Hilfsbereitschaft.

Frau Martina Wechler, Frau Silvia Heinrich, Frau Karin Reindl und Herrn Peter Richthammer für ihre Unterstützung bei organisatorischen und technischen Problemen.

meinen ForschungspraktikantInnen Verena Venjakob, Daniela Schlosser, Nina Kraupner und Stefan Weidinger für die Testung von Substanzen, Durchführung von Western Blots und PCRs sowie meinen Wahlpflichtstudentinnen Alexa Schenke und Carolin Lichtinger für die Durchführung von Kristallviolett assays, Stefanie Surner für die Durchführung von PCRs sowie Jessica Wagner und Barbara Fink für die Hilfe bei Membranpräparationen und Western Blots.

Frau Daniela Erdmann, Frau Janina Hamberger, Frau Irena Brunskole, Herrn Miroslaw Lopuch, Herrn Dr. Johannes Mosandl, Herrn Dr. Martin Göttle, Herrn Dr. Patrick Igel für ihre tatkräftige Unterstützung bei Membranpräparationen.

allen hier namentlich nicht genannten Kollegen unseres Lehrstuhls für ihre Kollegialität und Hilfsbereitschaft sowie auch der Nachbarlehrstühle für das gute Arbeitsklima.

dem Graduiertenkolleg 760 der DFG für die finanzielle Unterstützung und wissenschaftliche Förderung.

<u>Desweiteren geht mein besonderer Dank an:</u>

Daniela Erdmann, Janina Hamberger, Johannes Mosandl und Tobias Scheuerer für ihre Freundschaft und Geduld in den letzten gemeinsamen Jahren in Regensburg.

Peter Jarzyna, Martin Göttle, Dietmar Gross und Erich Schneider für die besondere Stütze, die sie mir während der Promotion waren.

Annette Holler und Karin Schmidbauer für ihre Freundschaft und ihr beständiges unglaubliches Interesse (als nicht-Naturwissenschaftlerinnen) an der Entwicklung meiner Arbeit.

Christina Wirth, Kristin Kölbl, Marlen Schmidt, Susanne Eichhorn und Johannes Wessel für die schöne gemeinsame „Wohnzeit“ in Regensburg.

meinen wunderbaren Eltern und meinem ebenso wunderbaren Bruder, Christian, für ihre beständige und selbstlose Unterstützung nicht nur in Zeiten der Promotion.

Publications

Keller, M., Pop, N., Hutzler, C., Beck-Sickinger, A.G., Bernhardt, G., Buschauer, A., Guanidine -acylguanidine bioisosteric approach in the design of radioligands: Synthesis of a tritium-labeled N^G-propionylargininamide ([^{3}H]-UR-MK114) as a highly potent and selective neuropeptide Y Y_1 receptor antagonist. **J. Med. Chem.** (2008), doi: 10.1021/jm801018u

Poster presentations

Pop N., Seifert R., Bernhardt G., Buschauer A., Functional reconstitution of the human neuropeptide Y Y_2 and Y_4 receptors with $G_{i/o}$-proteins in Sf9 insect cells, **Conference of the German Pharmaceutical Society (DPhG), Jena (Germany), September 2009**

Pop N., Seifert R., Bernhardt G., Buschauer A., Functional reconstitution of the human neuropeptide Y Y_4 receptor with $G_{i/o}$-proteins in Sf9 insect cells, **4th International Summer School "Medicinal Chemistry", Regensburg (Germany), September 2008**

Pop N., Bernhardt G., Buschauer A., Development of a FRET based cAMP assay for the human NPY Y_1 receptor, **Annual Meeting of the GDCh, Fachgruppe Medizinische Chemie, "Frontiers in Medicinal Chemistry", Regensburg (Germany), March 2008**

Keller M., Pop N., Schneider E., Hoefelschweiger B.K., Brennauer A., Gross D., Wolfbeis O.S., Bernhardt G., Dove S. and Buschauer A., Fluorescence labeled NPY Y_1 receptor antagonists, **Conference of the German Pharmaceutical Society (DPhG), Erlangen (Germany), October 2007, and Annual Meeting of the GDCh, Fachgruppe Medizinische Chemie, "Frontiers in Medicinal Chemistry", Regensburg (Germany), March 2008**

Lopuch M., Pop N., Keller M., Cwik M., Bernhardt G., Buschauer A., Stable expression of neuropeptide Y receptor type 1 tagged with cyan and yellow fluorescent protein – investigations using radiochemistry and fluorescence-based methods, **4th International Summer School "Medicinal Chemistry", Regensburg (Germany), September 2008**

Contents

Abbreviations

aa	amino acid
AC	adenylyl cyclase
AcNPV	*Autographa californica* nuclear polyhedrosis virus
AKT	family of protein kinases B
ATP	adenosine 5`-triphosphate
bp	base pair(s)
BRET	bioluminescence resonance energy transfer
BSA	bovine serum albumine
cAMP	cyclic 3`:5`-adenosine monophosphate
cDNA	copy DNA
CHO cells	chinese hamster ovary cells
CIP	calf intestinal phosphatise
CNS	central nervous system
DAG	1,2-diacylglycerol
DMSO	dimethylsufloxide
DTT	dithiothreitol
EC_{50}	agonist concentration which induces 50 % of the maximum effect
EDTA	ethylenediaminetetraacetic acid (Ca^{2+}-chelator)
Epac	exchange protein directly activated by cAMP
E_{max}	efficacy (maximal response)
FACS	fluorescence activated cell sorter
FCS	fetal calf serum
Fl-1, FL-2, Fl-3, Fl-4	fluorescence channels of the flow cytometer
FLAG	octapeptide epitope for the labelling of proteins
FLIPR	fluorescence imaging plate reader
FRET	fluorescence resonance energy transfer
$G\alpha_{i1}$, $G\alpha_{i2}$, $G\alpha_{i3}$, $G\alpha_{o1}$	α-subunits of the G-proteins that inhibit adenylyl cyclase
$G\alpha_{q/11}$	α-subunits of the G-proteins that stimulate phospholipase C
$G\alpha_{qi5}$	chimeric α-subunit of $G\alpha_{q/11}$ and the carboxyl terminus of $G\alpha_i$ to redirect the signalling of $G\alpha_i$ coupled receptors towards calcium release
Gβγ	βγ-subunits of a heterotrimeric G-protein
GDP	guanosine 5`-diphosphate
GPCR	G protein-coupled receptor
GTP	guanosine 5`-triphosphate
GTPγS	guanosine 5`-[γ-thio]triphosphate
HEC-1B cells	human endometrial carcinoma cells
HEK 293 cells	human embryonic kidney cells
His_6	hexahistidine tag
IC_{50}	antagonist concentration which suppresses 50 % of an agonist induced effect

i.c.v.	intracerebroventricular
i.p.	intraperitoneal
IP_3	inositoltriphosphate
i.v.	intravenous
LAF	laminar air flow (for sterile working banks)
LB	lysogeny broth (for cultivation of E. *coli*)
MAPK	mitogen-activated protein kinase
mtAEQ	mitochondrially targeted aequorin
NPY	neuropeptide Y
PBS	phosphate buffered saline
PCR	polymerase chain reaction
P_i	inorganic phosphate
PLC	phospholipase C
PMSF	phenylmethylsulfonylfluoride
PP	pancreatic polypeptide
PYY	peptide YY
RGS	regulator of G protein signalling
RIA	radio immuno assay
s.c.	subcoutaneous
SDS	sodiumdodecylsulfate
SDS Page	sodiumdodecylsulfate polyacrylamide gel electrophoresis
S.E.M.	standard error of the mean
Sf9	insect cell line of *Spodoptera frugiperda*
SOC	salt optimized + carbon broth (for transformation of E. *coli*)
SPA	scintillation proximity assay
SRC	proto-oncogenic tyrosin kinases
TAE	tris-acetat-EDTA buffer
TBE	tris-borat-EDTA buffer
TM	transmembrane domain
Tris	tris(hydroxymethyl)aminomehtan
Y_1, Y_2, Y_3, Y_4, Y_5, y_6, Y_7	neuropeptide Y receptor subtypes

Chapter 1

1 General introduction

1.1 G protein-coupled receptors

G protein-coupled receptors (GPCRs) constitute the largest known gene superfamily (≈ 2 %) of the human genome with up to approximately 800 members. Over half of these representatives are olfactory, leaving ≈ 380 unique functional nonolfactory/nonsensory GPCRs of which about only 40 are known as targets of modern drugs. Nevertheless, up to 30 % of all marketed prescription drugs act on GPCRs (Jacoby *et al.*, 2006; Lagerström and Schiöth, 2008). Thus, G protein-coupled receptors offer an interesting field with high potential for drug discovery.

Though, the physiological agonists are extremely versatile, ranging from light, ions, amines, peptides to proteins (Bockaert and Pin, 1999), GPCRs can be phylogenetically divided into five main families termed glutamate, rhodopsin, adhesion, frizzled/taste2 and secretin (Fredriksson *et al.*, 2003). The common structural features of the G protein-coupled receptor superfamily are seven membrane-spanning helices connected by three alternating intracellular and extracellular loops and flanked by an extracellular N-terminus and an intracellular C-terminus, respectively. Due to the high abundance in retina the bovine rhodopsin was the first mammalian GPCR to be crystallized by Palczewski in 2000, providing the first insight into the three-dimensional architecture of a G protein-coupled receptor (Palczewski *et al.*, 2000). Further crystal structures have been resolved recently for the human β_2-adrenoceptor (hβ_2AR) (Rasmussen *et al.*, 2007; Rosenbaum *et al.*, 2007), the turkey β_1AR (Warne *et al.*, 2008) and the human adenosine 2A receptor (Jaakola *et al.*, 2008), which was only possible by diverse receptor modifications like truncation, use of an antibody or construction of a receptor/T4-lysozyme fusion protein as stabilizing elements in combination with receptor bound inverse

agonists or antagonists. These efforts were amongst others performed to elucidate receptor conformation upon activation by ligand binding and coupling to heterotrimeric G proteins, the mediators of intracellular effects (cf. section 1.3). However, in contrast to their original denomination, GPCRs do not only signal via heterotrimeric G proteins, but interaction with β-arrestin after receptor phosphorylation is part of the major signaling process (Violin and Lefkowitz, 2007; Rajagopal *et al.*, 2010), which comprises e.g. regulation of kinases - like MAPKs, SRC or AKT – and of the receptor itself by desensitization and internalization. Therefore, GPCRs lately are also named seven transmembrane receptors (7TMRs). The present work focuses on GPCR signaling via heterotrimeric G proteins. A detailed illustration of the G protein activation/deactivation cycle is shown in section 1.3.

1.2 The neuropeptide Y (NPY) multiligand/multireceptor system

1.2.1 The neuropeptide Y family of peptides

Neuropeptide Y (NPY) represents together with peptide YY (PYY) and the pancreatic polypeptide (PP) a ligand family of neuroendocrine hormones, consisting of 36 amino acids each with C-terminal amidation (**Fig. 1.1**). NPY is one of the most abundant neuropeptides in the brain (Gray and Morley, 1986), additionally it is also expressed in the peripheral nervous system and plays an important role in the regulation of many physiological processes, such as food intake, thermogenesis, mood, memory, blood pressure and reproduction (Berglund *et al.*, 2003). At the same time NPY is also extremely well conserved among species (Larhammar, 1996). By contrast, PYY shows greater variability, and PP is the most rapidly evolving member of the NPY peptide family with only 50 % identity within mammals. PYY and PP are hormones that are released in the gastrointestinal tract in response to meals to regulate pancreatic and gastric secretion (Tatemoto, 1982; Hazelwood, 1993). PYY is additionally present in neurons (Ekblad and Sundler, 2002). Each of the NPY receptors shows its individual ligand binding profile for the members of the NPY family of peptides (**Table 1.1**).

```
          1         10          20          30
hNPY      YPSKPDNPGEDAPAEDMARYYSALRHYINLITRQRY-NH2
hPYY      YPIKPEAPGEDASPEELNRYYASLRHYLNLVTRQRY-NH2
hPP       APLEPVYPGDNATPEQMAQYAADLRRYINMLTRPRY-NH2
```

Fig. 1.1: Alignment of the human NPY, PYY and PP amino acid sequence; Constant positions in all species for the three peptides are underlined. The seven constant residues within the NPY-family are indicated (boxed).

1.2.2 NPY receptors

NPY receptors belong to the rhodopsin like GPCR superfamily and have a common main signaling pathway via $G_{i/o}$ proteins (Michel *et al.*, 1998). Subtypes in humans comprise the Y_1, Y_2, Y_4, Y_5 and y_6, with the y_6 being non-functional because of a frameshift mutation (single base deletion) in the third intracellular loop leading to a truncated receptor protein after the 6^{th} transmembrane region (Rose *et al.*, 1997). The average sequence homology between the subtypes is relatively low (27-31 %). NPY receptors play a role in a plethora of physiological processes. Some examples of current NPY investigation fields are their implication in depression (Painsipp *et al.*, 2009a; Painsipp *et al.*, 2009b), alcohol dependence (Thorsell, 2007; Wetherill *et al.*, 2008) or pain modulation (Gibbs and Hargreaves, 2008). Besides the pharmacological aspect as a target the Y_1 receptor e.g. is also regarded as a tumor marker in breast cancer as it is overexpressed in malignant tissues (Amlal *et al.*, 2006). However, the most prominent effect mediated by the NPY multiligand/multireceptor system still remains its involvement in regulating energy homeostasis. For example, Y_1 or Y_5 receptor selective agonists stimulate feeding (Gerald *et al.*, 1996; Mullins *et al.*, 2001; Henry *et al.*, 2005) and antagonists produce anti-obesity effects. In contrast, Y_2 or Y_4 receptor selective agonists show inhibition of food intake (Batterham *et al.*, 2002; Asakawa *et al.*, 2003), though these findings were controversially discussed (Tschöp *et al.*, 2004). As obesity and resulting co-morbidities are increasing health problems there has been a special interest in NPY receptor ligands (cf. section 1.2.3). In **Table 1.1** an overview of the most important properties of NPY receptors is given (for a survey of Y receptor antagonists see section 1.2.3.)

Table 1.1: Overview of NPY receptors adapted from (Merten and Beck-Sickinger, 2006)

Y_1R	
Expression pattern	Cerebral cortex, vascular smooth muscle cells, colon, human adipocytes
Signal transduction	$G_{i/o} \rightarrow$ cAMP↓; $[Ca^{2+}]$↑
Physiological functions	Analgesia, anxiolysis, circadian rhythm regulation, endocrine regulation, increase feeding, sedative, vasoconstriction
Ligand binding profile (agonists)	NPY ≈ PYY ≈ [Leu^{31},Pro^{34}]NPY > NPY_{2-36} ≈ NPY_{3-36} ≥ PP ≈ NPY_{13-36}
Selective agonists	[Phe^{7},Pro^{34}]NPY; [Leu^{31},Pro^{34}]NPY/PYY; [Arg^{6},Pro^{34}]NPY

Y_2R	
Expression pattern	Nerve fibers, hippocampus, intestine, blood vessels
Signal transduction	$G_{i/o} \rightarrow cAMP\downarrow$; $[Ca^{2+}]\uparrow$
Physiological functions	Angiogenesis, anxiogenesis, enhanced memory, decreased neurotransmitter secretion, decrease feeding, anticonvulsant
Ligand binding profile (agonists)	$PYY > PYY_{3-36} \approx NPY_{3-36} \approx NPY_{2-36} \approx NPY_{13-36} >> [Leu^{31},Pro^{34}]NPY$
Selective agonists	NPY_{3-36}; NPY_{13-36}; $[Ahx_{5-24}]NPY$
Y_4R	
Expression pattern	Hypothalamus, skeletal muscle, thyroid gland, stomach, small intestine, colon
Signal transduction	$G_{i/o} \rightarrow cAMP\downarrow$; $[Ca^{2+}]\uparrow$
Physiological functions	Pancreatic secretion, gall bladder contraction, LH secretion, decrease feeding
Ligand binding profile (agonists)	$PP \geq GW1229 > PYY \geq NPY > NPY_{2-36}$
Selective agonists	PP; GW1229
Y_5R	
Expression pattern	Hypothalamus, cerebral cortex, intestine, ovary, spleen, pancreas, skeletal muscle
Signal transduction	$G_{i/o} \rightarrow cAMP\downarrow$; $[Ca^{2+}]\uparrow$
Physiological functions	Circadian rhythm regulation, increase feeding, anticonvulsant, reproduction
Ligand binding profile (agonists)	$NPY \approx PYY \approx NPY_{2-36} \approx [Leu^{31},Pro^{34}]NPY > hPP > [D\text{-}Trp^{32}]NPY > NPY_{13-36} > rPP$
Selective agonists	$[Ala^{31},Aib^{32}]NPY$; $[Leu^{31},Pro^{34}]NPY$; $[D\text{-}Trp^{34}]NPY$

1.2.3 NPY receptor ligands

Starting from the endogenous ligands, NPY, PYY and PP, structure-affinity/activity relationships have been intensely studied by peptide modifications such as amino acid replacements, truncations, cyclizations or building chimera. Thereby, selective peptidergic agonists (listed in **Table 1.1**) have been widely accepted as reference compounds for the characterization of NPY receptors (Beck-Sickinger *et al.*, 1992; Cabrele and Beck-Sickinger, 2000; Cabrele *et al.*, 2000). Likewise, essential structures from the endogenous ligands were identified for the binding to each receptor. Thus, the small-molecule antagonist reported for the Y_1R, BIBP 3226 (Rudolf *et al.*, 1994) (**Fig. 1.2**), is considered a mimic of the C-terminus, i.e. Arg^{35} and Tyr^{36} in NPY (Sautel *et al.*, 1996). The first non-peptidic antagonist was HE-90481 (Michel and Motulsky, 1990). Likewise, BIIE 0246 (Doods *et al.*, 1999; Dumont *et al.*, 2000) and CGP 71683A (Criscione *et al.*, 1998) (**Fig. 1.3**) represented the first selective and potent antagonists for the Y_2R and the Y_5R, respectively. In the following, an overview of the development of Y receptor ligands of the last five years is given. As reviewed by Sato *et al.* (2009b), the major motivation to design new compounds for neuropeptide Y receptors was the treatment of obesity. Due to the lack of oral availability and inability to penetrate across the blood brain barrier NPY receptors could not be easily addressed in vivo with the classical substances. However these have been useful pharmacological tools for the characterization of YRs.

Fig. 1.2 shows a selection of developed novel potent and selective Y_1 receptor antagonists, all of which show promising results in the inhibition of feeding and the reduction of body weight in animal models, however only if applied systemically, i.e. intracerebroventricularly, intravenously or intraperitoneally (i.c.v., i.v. or i.p.). In order to advance into clinical trial, there is still a need for substances with suitable pharmacokinetic profiles and physicochemical properties.

Beside the aim to treat obesity several compounds have been developed as pharmacological tools. For example, Keller *et al.* designed a tritium labeled N^G-propionylargininamide ([^{3}H]-UR-MK114) that is a BIBP 3226 derivative (Keller *et al.*, 2008). Moreover, there have been reports on agonists with peptidic structures for PET or SPECT imaging of breast cancer (Guerin *et al.*, 2010; Khan *et al.*, 2010) and a carboxyfluorescein labeled small peptide derivative for tumour diagnostics and therapy (Zwanziger *et al.*, 2009).

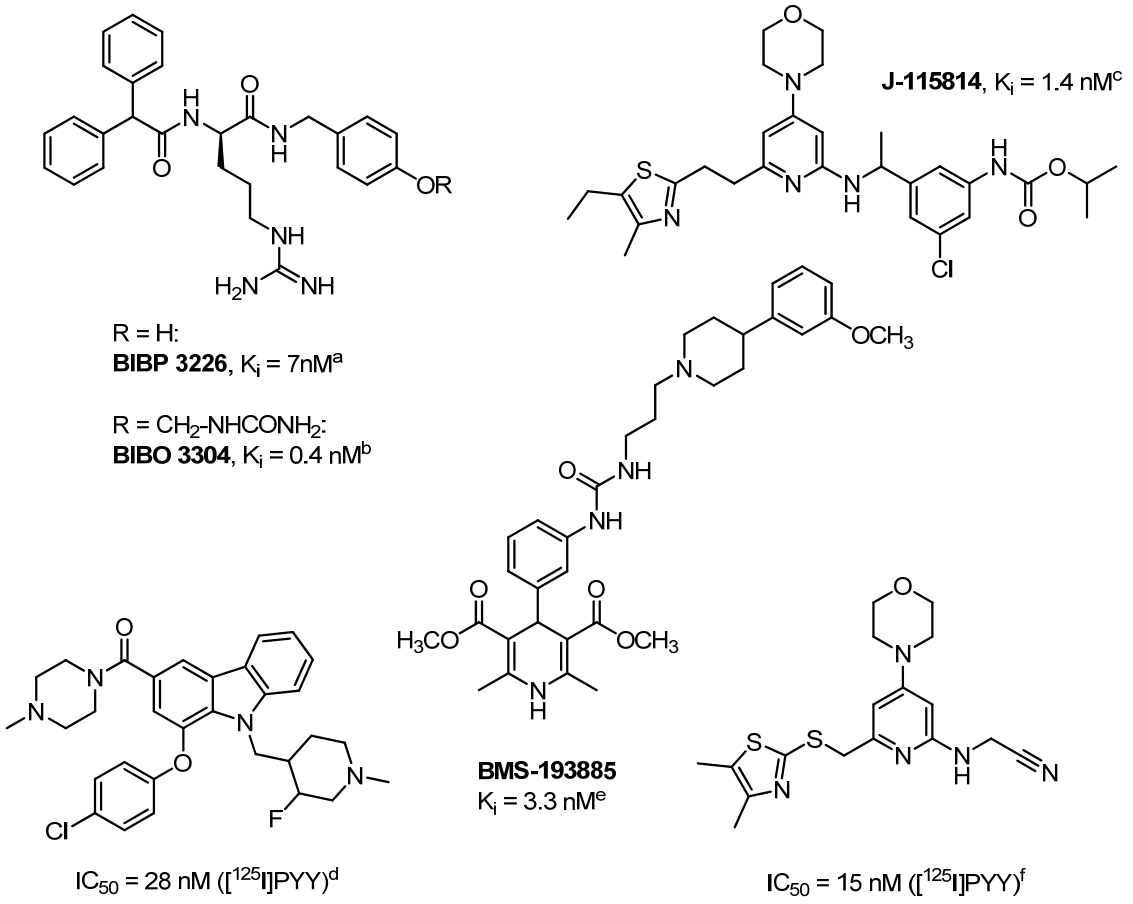

Fig. 1.2: Selection of non-peptidic Y_1 antagonist; [a](Rudolf *et al.*, 1994), [b](Wieland *et al.*, 1998), [c](Kanatani *et al.*, 2001), [d](Leslie *et al.*, 2007), [e](Antal-Zimanyi *et al.*, 2008), [f](Kameda *et al.*, 2009)

Several novel compounds different in structure from the peptidomimetic BIIE 0246 have been designed for the Y_2 receptor (**Fig. 1.3**). Here the situation is similar as for the Y_1R, namely the development of many potent and selective substances has been successful (for review see (Sato *et al.*, 2009b). These compounds were demonstrated to penetrate into the brain (Brothers *et al.*, 2010) when administered i.p. or subcutaneuosly (s.c.) Apart from the synthesis of small molecules the attempt has been pursued to conjugate peptidic Y_2R agonists (based on the C-terminus of PYY) with polyethylene glycol (20 kDa) to achieve a higher stability and to modify the amino acid sequence for higher selectivity. Indeed, the substances showed reduction of food intake and body weight (DeCarr *et al.*, 2007; Lumb *et al.*, 2007; Ortiz *et al.*, 2007). Obinepitide, a Y_2/Y_4 dual peptide agonist is reported to be in clinical trial (Sato *et al.*, 2009b).

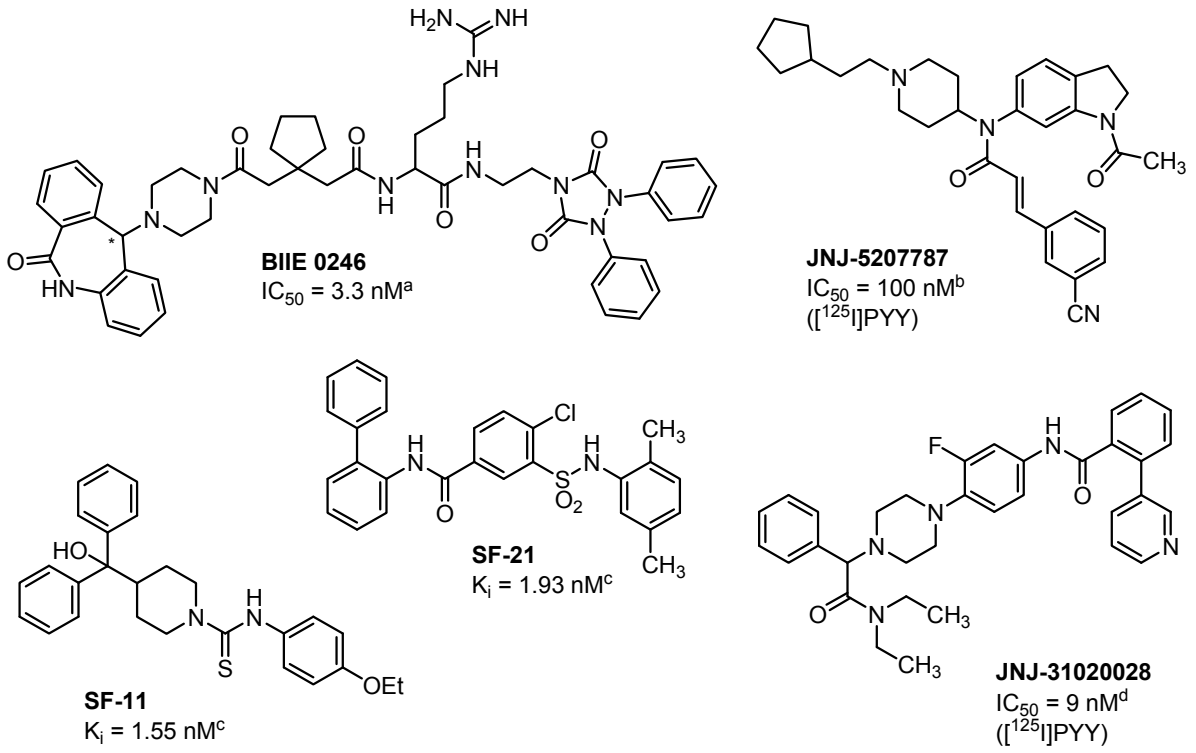

Fig. 1.3: Selection of non-peptidic Y_2 antagonists; [a](Doods *et al.*, 1999), [b](Bonaventure *et al.*, 2004), [c](Brothers *et al.*, 2010), [d](Shoblock *et al.*, 2010)

For the Y_4 receptor only UR-AK49, a weak antagonist, has been reported up to date (Ziemek *et al.*, 2007) (**Fig. 1.4**). In **Table 1.1** GW1229, based on the C-terminus of NPY, is mentioned as a selective and potent Y_4R agonist (Parker *et al.*, 1998; Schober *et al.*, 1998), although this compound is also active at the Y_1R as an antagonist. Furthermore, recent studies are focusing on peptidergic agonists as the Y_4R is known to mediate satiety via the release of PP in response to meals. For example, Sub[-Tyr-Arg-Leu-Arg-Tyr-NH_2]$_2$ - a peptide dimer based on NPY_{32-36} - has been reported to be a selective and highly potent Y_4 agonist, which inhibited food intake in mice after i.p. application (Balasubramaniam *et al.*, 2006). As already mentioned for the Y_2, the strategy to address Y_2 and Y_4 receptors at the same time with selective peptidergic agonists is pursued (Balasubramaniam *et al.*, 2007).

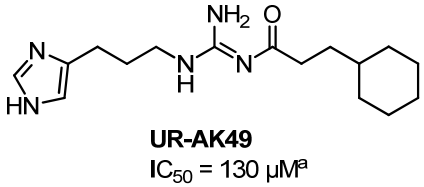

Fig. 1.4: UR-AK49, an acylguanidine with moderate Y_4 antagonistic activity; [a]Inhibition of hPP induced luminescence in CHO cells expressing the hY_4R, the chimeric G protein G_{qi5} and mitochondrially targeted apoaequorin.

The first non-peptidic Y_5 antagonist reported was CGP 71683A (Criscione *et al.*, 1998), whereas MK-0557 (Erondu *et al.*, 2006) was the first substance to be applied in clinical trial. As MK-0557 was well tolerated and showed small, but statistically significant reduction in body weight, several new compounds were designed (**Fig. 1.5**), (Ando *et al.*, 2009; Haga *et al.*, 2009; Sato *et al.*, 2009a) with promising pharmacological and pharmacokinetic properties so that proof-of-concept studies in humans are planned. Due to its expression in the limbic system, the Y_5R was hypothesized to modulate stress sensitivity. Indeed, Lu AA33810 was shown to exert anxiolytic- and antidepressant-like effects in rats (Walker *et al.*, 2009).

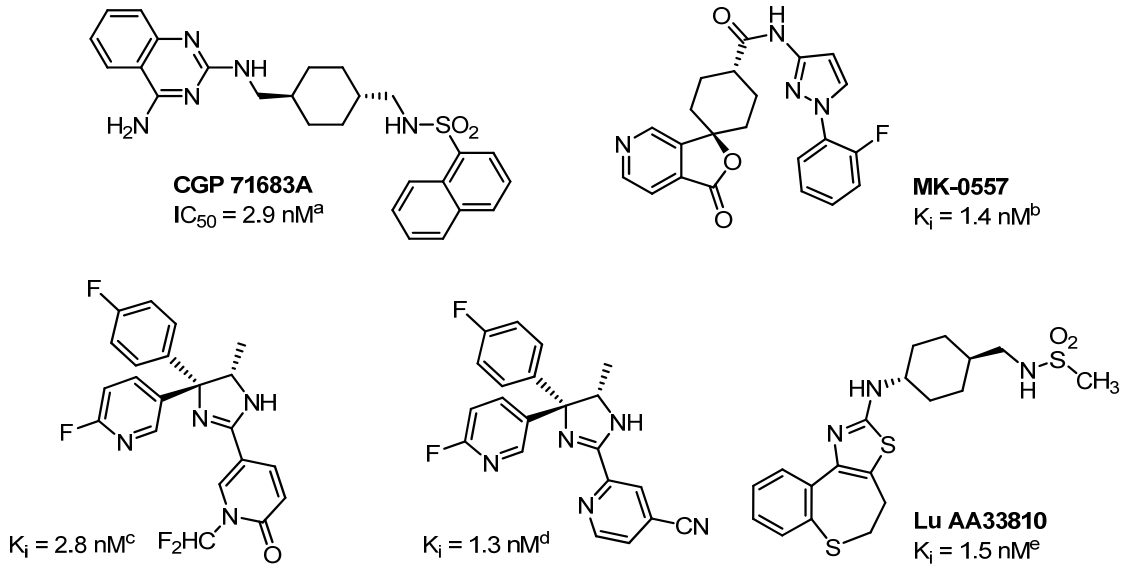

Fig. 1.5: Selection of Y_5R antagonists ; [a](Criscione *et al.*, 1998), [b](Erondu *et al.*, 2006), [c](Ando *et al.*, 2009), [d](Sato *et al.*, 2009a), [e](Walker *et al.*, 2009)

1.3 Development of novel functional assays for NPY receptors

Principally, for the pharmacological characterization of GPCR ligands, such as the substances presented in the previous section, in addition to binding data, the determination of the quality of action, agonistic potency or antagonistic activity is a must. There are numerous methods to determine potency and efficacy of ligands at the GPCR of interest, each of which has its specific applications, advantages and disadvantages. Therefore, a maximum of information on a given GPCR can only be obtained by combining complementary approaches.

For an overview of existing functional assays for NPY receptors the reader is referred to the introductory sections of chapters 4 to 6. This work aims at the development of new assay types presented in the current section exploiting GPCR signaling via various heterotrimeric G proteins.

As already mentioned (section 1.1), one of the prevailing signaling pathways of 7TMRs is coupling to heterotrimeric G proteins. Upon agonist binding a conformational change of the receptor takes place leading to association with a free inactive G protein consisting of a Gα-subunit and a Gβγ heterodimer, located on the cytosolic side of the membrane. Subsequently, Gα-bound GDP is released and replaced by GTP, which causes the dissociation of the ternary complex into the GPCR, the GTP-bound Gα-subunit and the Gβγ-dimer. The G protein subunits each activate effector proteins until the intrinsic GTPase activity of Gα cleaves the nucleotide into GDP and inorganic phosphate (P_i). Termination of the cycle is completed by the association of GDP-bound Gα with the Gβγ-dimer. The inactive G protein heterotrimer is available for another round of activation (**Fig. 1.6**).

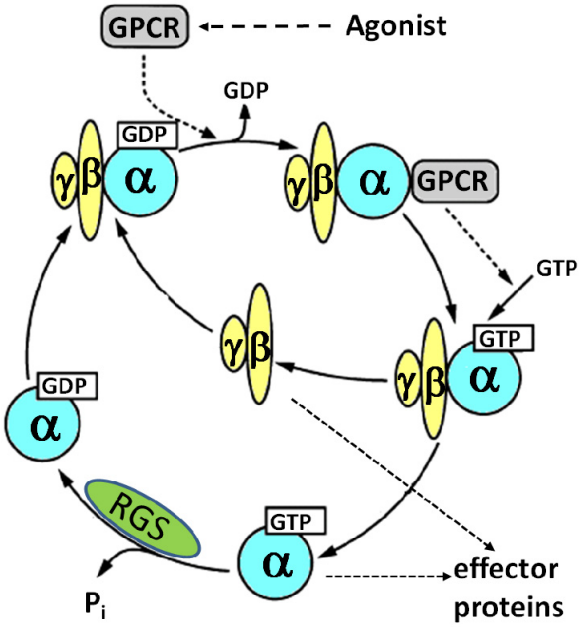

Fig. 1.6: G protein activation/ deactivation cycle after GPCR stimulation by an agonist; Adapted from (Seifert and Wieland, 2005)

There are four classes of G proteins with respect to the homology of their Gα sequences: G_s, $G_{i/o}$, $G_{q/11}$ and $G_{12/13}$ (Cabrera-Vera *et al.*, 2003; Milligan and Kostenis, 2006). G_s proteins activate adenylyl cyclase (AC), which results in the formation of 3′,5′-adenosine mono-phosphate (cAMP). Members of the $G_{i/o}$ class inhibit AC, while $G_{q/11}$ activate phospholipase Cβ (PLCβ), that catalyzes the formation of inositol-1,4,5-triphosphate (IP_3) and 1,2-diacylglycerol (DAG). $G_{12/13}$ proteins interact with guanine nucleotide exchange factors. The modulation of the mentioned second messengers leads to diverse downstream cellular signals, e.g. cAMP activates protein kinase A (PKA) resulting in the phosphorylation of various substrate proteins. Furthermore, exchange proteins directly activated by cAMP (Epac) as well as cAMP-gated ion channels are regulated. The inhibition of cAMP formation prevents these effects. Elevated IP_3 levels result in the release of intracellular calcium (Ca^{2+})

from the endoplasmic reticulum (ER), while DAG stimulates protein kinase C (PKC), which in turn stimulates various intracellular proteins by phosphorylation. Additionally, activated Gβγ-dimers can also trigger cellular effects, for instance, by interacting with AC, PLCβ or certain ion channels.

Gα-subunits as well as Gβγ-heterodimers are anchored to the cell membrane by lipidation of their N-termini. The interaction of Gα with a GPCR is defined by the amino acid sequence of its C-terminus, which is recognized by the receptor.

A large and diverse family of proteins – the regulators of G protein signaling (RGS) – has its part in the G protein cycle by accelerating the GTPase activity of the Gα-subunit (Ross and Wilkie, 2000; Willars, 2006) by stabilization of the transition state of GTP cleavage. Thus, RGS proteins function as negative regulators of G protein signaling.

1.3.1 FRET based cAMP assay for the human NPY Y_1 receptor

In case of the NPY receptors, coupling to $G_{i/o}$ proteins, the inhibition of cAMP formation has to be measured to determine receptor activation. Therefore, pre-stimulation with e.g. forskolin, a direct activator of adenylyl cyclase, is required to see an effect. Classical assay formats for YRs are based, for example, on measuring cAMP radioimmunologically or spectroscopically after enzymatic conversion of the second messenger to NADPH. To avoid such hazardous and laborious approaches in monitoring cAMP levels, several sensors have been developed from structures of known interaction partners of the second messenger, which are, e.g., exchange protein, directly activated by cAMP 1 (Epac1) and Epac2 (de Rooij *et al.*, 1998; Bos, 2003). Such proteins contain a catalytic domain regulated by a cAMP binding site. Upon binding of the second messenger, the conformation of Epac is changed, releasing the catalytic part. Because of this unfolding of the protein (the termini are supposed to move away from each other) the cyan and yellow fluorescent proteins (CFP and YFP) have been fused to the ends and cAMP has been measured by means of fluorescence resonance energy transfer (FRET) (Ponsioen *et al.*, 2004). For FRET to take place, the applied fluorophores have to overlap in their emission and absorption spectra, as shown for CFP and YFP as an example in **Fig. 1.7 A**. Moreover, they have to be in close proximity to each other, i.e. 1-10 nm, which means that in case of CFP-Epac-YFP, the FRET efficiency decreases upon cAMP formation. A further development, devoid of the catalytic domain of Epac, is the Epac cAMP sensor (Epac-camps) (Nikolaev *et al.*, 2004; Nikolaev *et al.*, 2005), which contains a cAMP binding site flanked by CFP and YFP (**Fig. 1.7 B**). This protein was used in an

approach to establish a FRET based assay in SK-N-MC cells endogenously expressing the hY_1R (chapter 3).

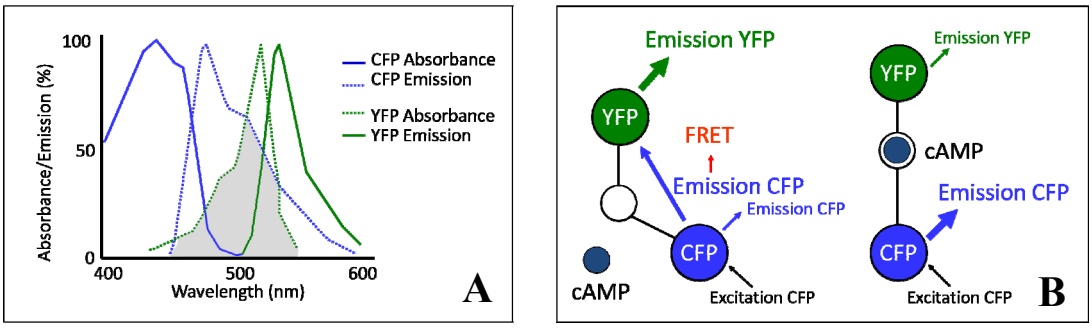

Fig. 1.7: Absorbance and emission spectra of CFP and YFP (A) and the principle of Epac-camps (B)

1.3.2 Fluorescence and luminescence based calcium assays for the human NPY Y_5 receptor

Conklin et al (Conklin *et al.*, 1993) have shown that the G protein specificity of a GPCR depends on its C-terminal amino acid sequence. Subsequently, several G protein chimera were constructed, e.g., consisting of $G\alpha_q$ with the last amino acids replaced by those of $G\alpha_{i2}$ (Conklin *et al.*, 1996), thus being able to re-direct receptor signaling to the PLC pathway. Such chimeric G proteins have already been successfully applied in high throughput screening (HTS) at $G_{i/o}$ coupling receptors (Coward *et al.*, 1999; Dautzenberg, 2005; Dautzenberg *et al.*, 2005). Ca^{2+} chelating dyes such as fluo-4 or the ratiometric fura-2 are used to measure the intracellular Ca^{2+} mobilization in flow cytometric or spectrofluorimetric assays as already established, e.g., for the hY_2 and the hY_4 receptors, stably co-expressed with $G\alpha_{qi5}$ in CHO cells (Ziemek *et al.*, 2006; Ziemek *et al.*, 2007). Because such fluorescence based assays suffer from dye leakage from the cells, which results in decreased signal-to-noise ratios during experiments, another approach based on luminescence with the photoprotein aequorin targeted to the mitochondria (see below) is favorable (Ziemek *et al.*, 2006; Ziemek *et al.*, 2007). Aequorin is a luciferase, which is reconstituted as a holoprotein with its chromophore cofactor coelenterazine (a luciferin). Upon binding of Ca^{2+}, coelenterazine is oxidized to coelenteramide, and CO_2, and luminescence occurs (λ_{max} = 470 nm) (Shimomura and Johnson, 1978; Jones *et al.*, 1999). The advantages of aequorin as an intracellular calcium indicator are its high sensitivity, low background, as well as absence of toxicity and its large linear dynamic range (Dupriez *et al.*, 2002). For functional GPCR assays cytoplasmically expressed and mitochondrially targeted aequorin (cytAEQ and mtAEQ) have been applied,

both giving the same functional data (Stables *et al.*, 1997; Stables *et al.*, 2000), whereas substantially stronger luminescence was obtained with mtAEQ.

1.3.3 Steady-state GTPase assay for the human NPY Y_2 and Y_4 receptors

The steady-state GTPase assay aims at directly measuring receptor activation, which subsequently results in the activation of the G protein cycle and the cleavage of [γ-^{32}P]GTP. This is favorable for GPCRs coupling to $G_{i/o}$ proteins, such as the NPY receptors, as no pre-stimulation is necessary.

For such assays membranes containing the respective GPCR, appropriate G proteins are required and in some cases the coexpression of RGS proteins turned out to be useful. To generate such membranes, the baculovirus/Sf9 cell expression system is used, which is well established for many GPCRs (Massotte, 2003; Aloia *et al.*, 2009). The Sf9 cell line is derived from *Spodoptera frugiperda* ovarian tissue and can be infected by the highly species-specific baculovirus *Autographa californica* nuclear polyhedrosis virus (AcNPV), which was used for expression purposes. Recombinant baculovirus containing receptor cDNA had to be generated. Because the genome of AcNPV is too large to easily insert foreign genes, a transfer vector (pVL1392) is used. The foreign gene is inserted into the vector in such a way that its expression is controlled by the strong late phase polyhedrin promoter. Polyhedrin, the matrix protein in which virus particles are embedded, can be replaced by the cDNA of interest. Upon co-transfection into Sf9 cells (**Fig.1.8**), the transfer vector and the linearized baculovirus DNA undergo homologous recombination, yielding viable recombinant baculovirus.

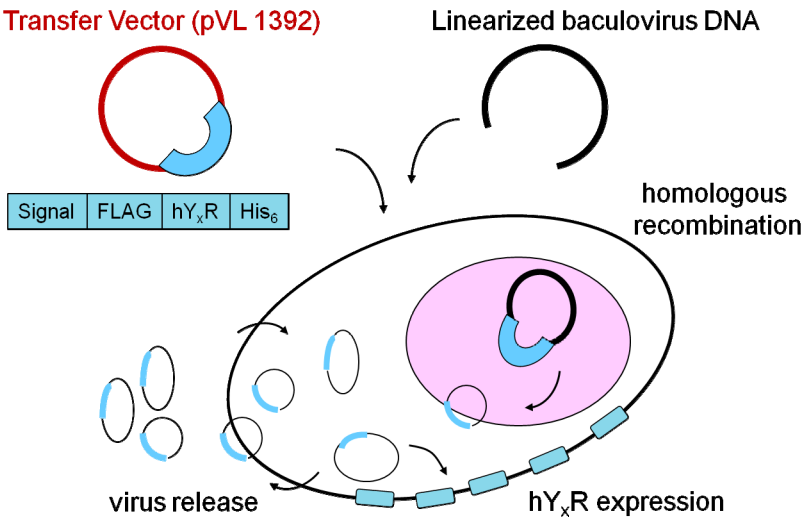

Fig. 1.8: Generation of recombinant hY$_x$R-baculoviruses and protein expression

By the infection of Sf9 cells with such viruses high GPCR or G protein expression levels can be achieved (Seifert *et al.*, 1998; Massotte, 2003; Schneider *et al.*, 2009). Co-infection with up to four baculoviruses, thereby combining the receptor of interest with diverse Gα-, Gβγ-subunits and RGS proteins, is tolerated by the cells (Kleemann *et al.*, 2008). Thus, for example G protein selectivity of the GPCR of interest can be studied.

From functional experiments and immunoblot analyses it can be concluded that Sf9 cells do not express any constitutively active GPCRs, i.e. receptors, that isomerize to the activated form in the absence of agonists, and that signaling of mammalian GPCRs via endogenous G protein is limited (Quehenberger *et al.*, 1992; Wenzel-Seifert *et al.*, 1998; Brys *et al.*, 2000; Seifert *et al.*, 2003). This was considered as an excellent starting point for the establishment of functional assays with high signal-to-noise ratios for the molecular pharmacological investigation of NPY receptor ligands and for studying constitutive receptor activity.

1.4 References

Aloia AL, Glatz RV, McMurchie EJ and Leifert WR (2009) GPCR expression using baculovirus-infected Sf9 cells. *Methods Mol Biol* **552**:115-129.

Amlal H, Faroqui S, Balasubramaniam A and Sheriff S (2006) Estrogen up-regulates neuropeptide Y Y_1 receptor expression in a human breast cancer cell line. *Cancer Res* **66**:3706-3714.

Ando M, Sato N, Nagase T, Nagai K, Ishikawa S, Takahashi H, Ohtake N, Ito J, Hirayama M, Mitobe Y, Iwaasa H, Gomori A, Matsushita H, Tadano K, Fujino N, Tanaka S, Ohe T, Ishihara A, Kanatani A and Fukami T (2009) Discovery of pyridone-containing imidazolines as potent and selective inhibitors of neuropeptide Y Y_5 receptor. *Bioorg Med Chem* **17**:6106-6122.

Antal-Zimanyi I, Bruce MA, Leboulluec KL, Iben LG, Mattson GK, McGovern RT, Hogan JB, Leahy CL, Flowers SC, Stanley JA, Ortiz AA and Poindexter GS (2008) Pharmacological characterization and appetite suppressive properties of BMS-193885, a novel and selective neuropeptide Y_1 receptor antagonist. *Eur J Pharmacol* **590**:224-232.

Asakawa A, Inui A, Yuzuriha H, Ueno N, Katsuura G, Fujimiya M, Fujino MA, Niijima A, Meguid MM and Kasuga M (2003) Characterization of the effects of pancreatic polypeptide in the regulation of energy balance. *Gastroenterology* **124**:1325-1336.

Balasubramaniam A, Joshi R, Su C, Friend LA and James JH (2007) Neuropeptide Y (NPY) Y_2 receptor-selective agonist inhibits food intake and promotes fat metabolism in mice: combined anorectic effects of Y_2 and Y_4 receptor-selective agonists. *Peptides* **28**:235-240.

Balasubramaniam A, Mullins DE, Lin S, Zhai W, Tao Z, Dhawan VC, Guzzi M, Knittel JJ, Slack K, Herzog H and Parker EM (2006) Neuropeptide Y (NPY) Y_4 receptor selective agonists based on NPY(32-36): development of an anorectic Y_4 receptor selective agonist with picomolar affinity. *J Med Chem* **49**:2661-2665.

Batterham RL, Cowley MA, Small CJ, Herzog H, Cohen MA, Dakin CL, Wren AM, Brynes AE, Low MJ, Ghatei MA, Cone RD and Bloom SR (2002) Gut hormone PYY(3-36) physiologically inhibits food intake. *Nature* **418**:650-654.

Beck-Sickinger AG, Grouzmann E, Hoffmann E, Gaida W, van Meir EG, Waeber B and Jung G (1992) A novel cyclic analog of neuropeptide Y specific for the Y_2 receptor. *Eur J Biochem* **206**:957-964.

Berglund MM, Hipskind PA and Gehlert DR (2003) Recent developments in our understanding of the physiological role of PP-fold peptide receptor subtypes. *Exp Biol Med (Maywood)* **228**:217-244.

Bockaert J and Pin JP (1999) Molecular tinkering of G protein-coupled receptors: an evolutionary success. *EMBO J* **18**:1723-1729.

Bonaventure P, Nepomuceno D, Mazur C, Lord B, Rudolph DA, Jablonowski JA, Carruthers NI and Lovenberg TW (2004) Characterization of N-(1-Acetyl-2,3-dihydro-1H-indol-6-yl)-3-(3-cyano-phenyl)-N-[1-(2-cyclopen tyl-ethyl)-piperidin-4yl]acrylamide (JNJ-5207787), a small molecule antagonist of the neuropeptide Y Y_2 receptor. *J Pharmacol Exp Ther* **308**:1130-1137.

Bos JL (2003) Epac: a new cAMP target and new avenues in cAMP research. *Nat Rev Mol Cell Biol* **4**:733-738.

Brothers SP, Saldanha SA, Spicer TP, Cameron M, Mercer BA, Chase P, McDonald P, Wahlestedt C and Hodder PS (2010) Selective and brain penetrant neuropeptide Y Y_2 receptor antagonists discovered by whole-cell high-throughput screening. *Mol Pharmacol* **77**:46-57.

Brys R, Josson K, Castelli MP, Jurzak M, Lijnen P, Gommeren W and Leysen JE (2000) Reconstitution of the human $5\text{-}HT_{1D}$ receptor-G-protein coupling: evidence for constitutive activity and multiple receptor conformations. *Mol Pharmacol* **57**:1132-1141.

Cabrele C and Beck-Sickinger AG (2000) Molecular characterization of the ligand-receptor interaction of the neuropeptide Y family. *J Pept Sci* **6**:97-122.

Cabrele C, Langer M, Bader R, Wieland HA, Doods HN, Zerbe O and Beck-Sickinger AG (2000) The first selective agonist for the neuropeptide Y Y_5 receptor increases food intake in rats. *J Biol Chem* **275**:36043-36048.

Cabrera-Vera TM, Vanhauwe J, Thomas TO, Medkova M, Preininger A, Mazzoni MR and Hamm HE (2003) Insights into G Protein Structure, Function, and Regulation. *Endocr Rev* **24**:765-781.

Conklin BR, Farfel Z, Lustig KD, Julius D and Bourne HR (1993) Substitution of three amino acids switches receptor specificity of $G_q\alpha$ to that of $G_i\alpha$. *Nature* **363**:274-276.

Conklin BR, Herzmark P, Ishida S, Voyno-Yasenetskaya TA, Sun Y, Farfel Z and Bourne HR (1996) Carboxyl-terminal mutations of $G_q\alpha$ and $G_s\alpha$ that alter the fidelity of receptor activation. *Mol Pharmacol* **50**:885-890.

Coward P, Chan SD, Wada HG, Humphries GM and Conklin BR (1999) Chimeric G proteins allow a high-throughput signaling assay of G_i-coupled receptors. *Anal Biochem* **270**:242-248.

Criscione L, Rigollier P, Batzl-Hartmann C, Rueger H, Stricker-Krongrad A, Wyss P, Brunner L, Whitebread S, Yamaguchi Y, Gerald C, Heurich RO, Walker MW, Chiesi M, Schilling W, Hofbauer KG and Levens N (1998) Food intake in free-feeding and energy-deprived lean rats is mediated by the neuropeptide Y_5 receptor. *J Clin Invest* **102**:2136-2145.

Dautzenberg FM (2005) Stimulation of neuropeptide Y-mediated calcium responses in human SMS-KAN neuroblastoma cells endogenously expressing Y_2 receptors by co-expression of chimeric G proteins. *Biochem Pharmacol* **69**:1493-1499.

Dautzenberg FM, Higelin J, Pflieger P, Neidhart W and Guba W (2005) Establishment of robust functional assays for the characterization of neuropeptide Y (NPY) receptors: identification of 3-(5-benzoyl-thiazol-2-ylamino)-benzonitrile as selective NPY type 5 receptor antagonist. *Neuropharmacology* **48**:1043-1055.

de Rooij J, Zwartkruis FJ, Verheijen MH, Cool RH, Nijman SM, Wittinghofer A and Bos JL (1998) Epac is a Rap1 guanine-nucleotide-exchange factor directly activated by cyclic AMP. *Nature* **396**:474-477.

DeCarr LB, Buckholz TM, Milardo LF, Mays MR, Ortiz A and Lumb KJ (2007) A long-acting selective neuropeptide Y_2 receptor PEGylated peptide agonist reduces food intake in mice. *Bioorg Med Chem Lett* **17**:1916-1919.

Doods H, Gaida W, Wieland HA, Dollinger H, Schnorrenberg G, Esser F, Engel W, Eberlein W and Rudolf K (1999) BIIE0246: a selective and high affinity neuropeptide Y Y_2 receptor antagonist. *Eur J Pharmacol* **384**:R3-5.

Dumont Y, Cadieux A, Doods H, Pheng LH, Abounader R, Hamel E, Jacques D, Regoli D and Quirion R (2000) BIIE0246, a potent and highly selective non-peptide neuropeptide Y Y_2 receptor antagonist. *Br J Pharmacol* **129**:1075-1088.

Dupriez VJ, Maes K, Le Poul E, Burgeon E and Detheux M (2002) Aequorin-based functional assays for G-protein-coupled receptors, ion channels, and tyrosine kinase receptors. *Receptors Channels* **8**:319-330.

Ekblad E and Sundler F (2002) Distribution of pancreatic polypeptide and peptide YY. *Peptides* **23**:251-261.

Erondu N, Gantz I, Musser B, Suryawanshi S, Mallick M, Addy C, Cote J, Bray G, Fujioka K, Bays H, Hollander P, Sanabria-Bohorquez SM, Eng W, Langstrom B, Hargreaves RJ, Burns HD, Kanatani A, Fukami T, MacNeil DJ, Gottesdiener KM, Amatruda JM, Kaufman KD and Heymsfield SB (2006) Neuropeptide Y_5 receptor antagonism does not induce clinically meaningful weight loss in overweight and obese adults. *Cell Metab* **4**:275-282.

Fredriksson R, Lagerström MC, Lundin LG and Schiöth HB (2003) The G-protein-coupled receptors in the human genome form five main families. Phylogenetic analysis, paralogon groups, and fingerprints. *Mol Pharmacol* **63**:1256-1272.

Gerald C, Walker MW, Criscione L, Gustafson EL, Batzl-Hartmann C, Smith KE, Vaysse P, Durkin MM, Laz TM, Linemeyer DL, Schaffhauser AO, Whitebread S, Hofbauer KG, Taber RI, Branchek TA and Weinshank RL (1996) A receptor subtype involved in neuropeptide-Y-induced food intake. *Nature* **382**:168-171.

Gibbs JL and Hargreaves KM (2008) Neuropeptide Y Y_1 receptor effects on pulpal nociceptors. *J Dent Res* **87**:948-952.

Gray TS and Morley JE (1986) Neuropeptide Y: anatomical distribution and possible function in mammalian nervous system. *Life Sci* **38**:389-401.

Guerin B, Dumulon-Perreault V, Tremblay MC, Ait-Mohand S, Fournier P, Dubuc C, Authier S and Benard F (2010) [Lys(DOTA)4]BVD15, a novel and potent neuropeptide Y analog designed for Y_1 receptor-targeted breast tumor imaging. *Bioorg Med Chem Lett* **20**:950-953.

Haga Y, Sakamoto T, Shibata T, Nonoshita K, Ishikawa M, Suga T, Takahashi H, Takahashi T, Ando M, Murai T, Gomori A, Oda Z, Kitazawa H, Mitobe Y, Kanesaka M, Ohe T, Iwaasa H, Ishii Y, Ishihara A, Kanatani A and Fukami T (2009) Discovery of trans-N-[1-(2-fluorophenyl)-3-pyrazolyl]-3-oxospiro[6-azaisobenzofuran-1(*3H*),1'-cyclohexane]-4'-carboxamide, a potent and orally active neuropeptide Y Y_5 receptor antagonist. *Bioorg Med Chem* **17**:6971-6982.

Hazelwood RL (1993) The pancreatic polypeptide (PP-fold) family: gastrointestinal, vascular, and feeding behavioral implications. *Proc Soc Exp Biol Med* **202**:44-63.

Henry M, Ghibaudi L, Gao J and Hwa JJ (2005) Energy metabolic profile of mice after chronic activation of central NPY Y_1, Y_2, or Y_5 receptors. *Obes Res* **13**:36-47.

Jaakola VP, Griffith MT, Hanson MA, Cherezov V, Chien EY, Lane JR, Ijzerman AP and Stevens RC (2008) The 2.6 angstrom crystal structure of a human A2A adenosine receptor bound to an antagonist. *Science* **322**:1211-1217.

Jacoby E, Bouhelal R, Gerspacher M and Seuwen K (2006) The 7 TM G-protein-coupled receptor target family. *ChemMedChem* **1**:761-782.

Jones K, Hibbert F and Keenan M (1999) Glowing jellyfish, luminescence and a molecule called coelenterazine. *Trends Biotechnol* **17**:477-481.

Kameda M, Kobayashi K, Ito H, Miyazoe H, Tsujino T, Nakama C, Kawamoto H, Ando M, Ito S, Suzuki T, Kanno T, Tanaka T, Tahara Y, Tani T, Tanaka S, Tokita S and Sato N (2009) Optimization of a series of 2,4-diaminopyridines as neuropeptide Y Y_1 receptor antagonists with reduced hERG activity. *Bioorg Med Chem Lett* **19**:4325-4329.

Kanatani A, Hata M, Mashiko S, Ishihara A, Okamoto O, Haga Y, Ohe T, Kanno T, Murai N, Ishii Y, Fukuroda T, Fukami T and Ihara M (2001) A typical Y_1 receptor regulates feeding behaviors: effects of a potent and selective Y_1 antagonist, J-115814. *Mol Pharmacol* **59**:501-505.

Keller M, Pop N, Hutzler C, Beck-Sickinger AG, Bernhardt G and Buschauer A (2008) Guanidine-acylguanidine bioisosteric approach in the design of radioligands: synthesis of a tritium-labeled N^G-propionylargininamide ([^{3}H]-UR-MK114) as a highly potent and selective neuropeptide Y Y_1 receptor antagonist. *J Med Chem* **51**:8168-8172.

Khan IU, Zwanziger D, Bohme I, Javed M, Naseer H, Hyder SW and Beck-Sickinger AG (2010) Breast-cancer diagnosis by neuropeptide Y analogues: from synthesis to clinical application. *Angew Chem Int Ed Engl* **49**:1155-1158.

Kleemann P, Papa D, Vigil-Cruz S and Seifert R (2008) Functional reconstitution of the human chemokine receptor CXCR4 with G_i/G_o-proteins in Sf9 insect cells. *Naunyn Schmiedebergs Arch Pharmacol* **378**:261-274.

Lagerström MC and Schiöth HB (2008) Structural diversity of G protein-coupled receptors and significance for drug discovery. *Nat Rev Drug Discov* **7**:339-357.

Larhammar D (1996) Evolution of neuropeptide Y, peptide YY and pancreatic polypeptide. *Regul Pept* **62**:1-11.

Leslie CP, Di Fabio R, Bonetti F, Borriello M, Braggio S, Dal Forno G, Donati D, Falchi A, Ghirlanda D, Giovannini R, Pavone F, Pecunioso A, Pentassuglia G, Pizzi DA, Rumboldt G and Stasi L (2007) Novel carbazole derivatives as NPY Y_1 antagonists. *Bioorg Med Chem Lett* **17**:1043-1046.

Lumb KJ, DeCarr LB, Milardo LF, Mays MR, Buckholz TM, Fisk SE, Pellegrino CM, Ortiz AA and Mahle CD (2007) Novel selective neuropeptide Y_2 receptor PEGylated peptide agonists reduce food intake and body weight in mice. *J Med Chem* **50**:2264-2268.

Massotte D (2003) G protein-coupled receptor overexpression with the baculovirus-insect cell system: a tool for structural and functional studies. *Biochimica et Biophysica Acta* **1610**:77-89.

Merten N and Beck-Sickinger AG (2006) Molecular ligand-receptor interaction of the NPY/PP peptide family. *EXS*:35-62.

Michel MC, Beck-Sickinger A, Cox H, Doods HN, Herzog H, Larhammar D, Quirion R, Schwartz T and Westfall T (1998) XVI. International Union of Pharmacology recommendations for the nomenclature of neuropeptide Y, peptide YY, and pancreatic polypeptide receptors. *Pharmacol Rev* **50**:143-150.

Michel MC and Motulsky HJ (1990) HE 90481: A competitive nonpeptidergic antagonist at neuropeptide Y receptors. *Ann N Y Acad Sci* **611**:392-394.

Milligan G and Kostenis E (2006) Heterotrimeric G-proteins: a short history. *Br J Pharmacol* **147 Suppl 1**:S46-55.

Mullins D, Kirby D, Hwa J, Guzzi M, Rivier J and Parker E (2001) Identification of potent and selective neuropeptide Y Y_1 receptor agonists with orexigenic activity in vivo. *Mol Pharmacol* **60**:534-540.

Nikolaev VO, Bunemann M, Hein L, Hannawacker A and Lohse MJ (2004) Novel single chain cAMP sensors for receptor-induced signal propagation. *J Biol Chem* **279**:37215-37218.

Nikolaev VO, Gambaryan S, Engelhardt S, Walter U and Lohse MJ (2005) Real-time monitoring of the PDE2 activity of live cells: hormone-stimulated cAMP hydrolysis is faster than hormone-stimulated cAMP synthesis. *J Biol Chem* **280**:1716-1719.

Ortiz AA, Milardo LF, DeCarr LB, Buckholz TM, Mays MR, Claus TH, Livingston JN, Mahle CD and Lumb KJ (2007) A novel long-acting selective neuropeptide Y_2 receptor polyethylene glycol-conjugated peptide agonist reduces food intake and body weight and improves glucose metabolism in rodents. *J Pharmacol Exp Ther* **323**:692-700.

Painsipp E, Herzog H and Holzer P (2009a) Evidence from knockout mice that neuropeptide-Y Y_2 and Y_4 receptor signaling prevents long-term depression-like behaviour caused by immune challenge. *J Psychopharmacol*.

Painsipp E, Sperk G, Herzog H and Holzer P (2009b) Delayed stress-induced differences in locomotor and depression-related behaviour in female neuropeptide-Y Y_1 receptor knockout mice. *J Psychopharmacol*.

Palczewski K, Kumasaka T, Hori T, Behnke CA, Motoshima H, Fox BA, Le Trong I, Teller DC, Okada T, Stenkamp RE, Yamamoto M and Miyano M (2000) Crystal structure of rhodopsin: A G protein-coupled receptor. *Science* **289**:739-745.

Parker EM, Babij CK, Balasubramaniam A, Burrier RE, Guzzi M, Hamud F, Mukhopadhyay G, Rudinski MS, Tao Z, Tice M, Xia L, Mullins DE and Salisbury BG (1998) GR231118 (1229U91) and other analogues of the C-terminus of neuropeptide Y are potent neuropeptide Y Y_1 receptor antagonists and neuropeptide Y Y_4 receptor agonists. *Eur J Pharmacol* **349**:97-105.

Ponsioen B, Zhao J, Riedl J, Zwartkruis F, van der Krogt G, Zaccolo M, Moolenaar WH, Bos JL and Jalink K (2004) Detecting cAMP-induced Epac activation by fluorescence resonance energy transfer: Epac as a novel cAMP indicator. *EMBO Rep* **5**:1176-1180.

Quehenberger O, Prossnitz ER, Cochrane CG and Ye RD (1992) Absence of G_i proteins in the Sf9 insect cell. Characterization of the uncoupled recombinant N-formyl peptide receptor. *J Biol Chem* **267**:19757-19760.

Rajagopal S, Rajagopal K and Lefkowitz RJ (2010) Teaching old receptors new tricks: biasing seven-transmembrane receptors. *Nat Rev Drug Discov* **9**:373-386.

Rasmussen SG, Choi HJ, Rosenbaum DM, Kobilka TS, Thian FS, Edwards PC, Burghammer M, Ratnala VR, Sanishvili R, Fischetti RF, Schertler GF, Weis WI and Kobilka BK (2007) Crystal structure of the human β_2 adrenergic G-protein-coupled receptor. *Nature* **450**:383-387.

Rose PM, Lynch JS, Frazier ST, Fisher SM, Chung W, Battaglino P, Fathi Z, Leibel R and Fernandes P (1997) Molecular genetic analysis of a human neuropeptide Y receptor. The human homolog of the murine "Y_5" receptor may be a pseudogene. *J Biol Chem* **272**:3622-3627.

Rosenbaum DM, Cherezov V, Hanson MA, Rasmussen SG, Thian FS, Kobilka TS, Choi HJ, Yao XJ, Weis WI, Stevens RC and Kobilka BK (2007) GPCR engineering yields high-resolution structural insights into β_2-adrenergic receptor function. *Science* **318**:1266-1273.

Ross EM and Wilkie TM (2000) GTPase-activating proteins for heterotrimeric G proteins: regulators of G protein signaling (RGS) and RGS-like proteins. *Annu Rev Biochem* **69**:795-827.

Rudolf K, Eberlein W, Engel W, Wieland HA, Willim KD, Entzeroth M, Wienen W, Beck-Sickinger AG and Doods HN (1994) The first highly potent and selective non-peptide neuropeptide Y Y_1 receptor antagonist: BIBP3226. *Eur J Pharmacol* **271**:R11-13.

Sato N, Ando M, Ishikawa S, Jitsuoka M, Nagai K, Takahashi H, Sakuraba A, Tsuge H, Kitazawa H, Iwaasa H, Mashiko S, Gomori A, Moriya R, Fujino N, Ohe T, Ishihara A, Kanatani A and Fukami T (2009a) Discovery of tetrasubstituted imidazolines as potent and selective neuropeptide Y Y_5 receptor antagonists: reduced human ether-a-go-go related gene potassium channel binding affinity and potent antiobesity effect. *J Med Chem* **52**:3385-3396.

Sato N, Ogino Y, Mashiko S and Ando M (2009b) Modulation of neuropeptide Y receptors for the treatment of obesity. *Expert Opin Ther Pat* **19**:1401-1415.

Sautel M, Rudolf K, Wittneben H, Herzog H, Martinez R, Munoz M, Eberlein W, Engel W, Walker P and Beck-Sickinger AG (1996) Neuropeptide Y and the nonpeptide antagonist BIBP 3226 share an overlapping binding site at the human Y_1 receptor. *Mol Pharmacol* **50**:285-292.

Schneider EH, Schnell D, Papa D and Seifert R (2009) High constitutive activity and a G-protein-independent high-affinity state of the human histamine H_4-receptor. *Biochemistry* **48**:1424-1438.

Schober DA, Van Abbema AM, Smiley DL, Bruns RF and Gehlert DR (1998) The neuropeptide Y Y_1 antagonist, 1229U91, a potent agonist for the human pancreatic polypeptide-preferring (NPY Y_4) receptor. *Peptides* **19**:537-542.

Seifert R, Lee TW, Lam VT and Kobilka BK (1998) Reconstitution of β_2-adrenoceptor-GTP-binding-protein interaction in Sf9 cells-high coupling efficiency in a β_2-adrenoceptor-$G_s\alpha$ fusion protein. *Eur J Biochem* **255**:369-382.

Seifert R, Wenzel-Seifert K, Burckstummer T, Pertz HH, Schunack W, Dove S, Buschauer A and Elz S (2003) Multiple differences in agonist and antagonist pharmacology between human and guinea pig histamine H_1-receptor. *Journal of Pharmacology and Experimental Therapeutics* **305**:1104-1115.

Seifert R and Wieland T (2005) *G protein-coupled receptors as drug targets: analysis of activation and constitutive activity*. Wiley-VCH, Weinheim.

Shimomura O and Johnson FH (1978) Peroxidized coelenterazine, the active group in the photoprotein aequorin. *Proc Natl Acad Sci U S A* **75**:2611-2615.

Shoblock JR, Welty N, Nepomuceno D, Lord B, Aluisio L, Fraser I, Motley ST, Sutton SW, Morton K, Galici R, Atack JR, Dvorak L, Swanson DM, Carruthers NI, Dvorak C, Lovenberg TW and Bonaventure P (2010) In vitro and in vivo characterization of JNJ-31020028 (N-(4-{4-[2-(diethylamino)-2-oxo-1-phenylethyl]piperazin-1-yl}-3-fluorophe nyl)-2-pyridin-3-ylbenzamide), a selective brain penetrant small molecule antagonist of the neuropeptide Y Y_2 receptor. *Psychopharmacology (Berl)* **208**:265-277.

Stables J, Green A, Marshall F, Fraser N, Knight E, Sautel M, Milligan G, Lee M and Rees S (1997) A bioluminescent assay for agonist activity at potentially any G-protein-coupled receptor. *Anal Biochem* **252**:115-126.

Stables J, Mattheakis LC, Chang R and Rees S (2000) Recombinant aequorin as reporter of changes in intracellular calcium in mammalian cells. *Methods Enzymol* **327**:456-471.

Tatemoto K (1982) Isolation and characterization of peptide YY (PYY), a candidate gut hormone that inhibits pancreatic exocrine secretion. *Proc Natl Acad Sci U S A* **79**:2514-2518.

Thorsell A (2007) Neuropeptide Y (NPY) in alcohol intake and dependence. *Peptides* **28**:480-483.

Tschöp M, Castaneda TR, Joost HG, Thone-Reineke C, Ortmann S, Klaus S, Hagan MM, Chandler PC, Oswald KD, Benoit SC, Seeley RJ, Kinzig KP, Moran TH, Beck-sickinger AG, Koglin N, Rodgers RJ, Blundell JE, Ishii Y, Beattie AH, Holch P, Allison DB, Raun K, Madsen K, Wulff BS, Stidsen CE, Birringer M, Kreuzer OJ, Schindler M, Arndt K, Rudolf K, Mark M, Deng XY, Whitcomb DC, Halem H, Taylor J, Dong J, Datta R, Culler M, Craney S, Flora D, Smiley D and Heiman ML (2004) Physiology: does gut hormone PYY_{3-36} decrease food intake in rodents? *Nature* **430**:1 p following 165; discussion 162 p following 165.

Violin JD and Lefkowitz RJ (2007) β-Arrestin-biased ligands at seven-transmembrane receptors. *Trends Pharmacol Sci* **28**:416-422.

Walker MW, Wolinsky TD, Jubian V, Chandrasena G, Zhong H, Huang X, Miller S, Hegde LG, Marsteller DA, Marzabadi MR, Papp M, Overstreet DH, Gerald CP and Craig DA (2009) The novel neuropeptide Y Y_5 receptor antagonist Lu AA33810 [N-[[trans-4-[(4,5-dihydro[1]benzothiepino[5,4-d]thiazol-2-yl)amino]cycloh exyl]methyl]-methanesulfonamide] exerts anxiolytic- and antidepressant-like effects in rat models of stress sensitivity. *J Pharmacol Exp Ther* **328**:900-911.

Warne T, Serrano-Vega MJ, Baker JG, Moukhametzianov R, Edwards PC, Henderson R, Leslie AG, Tate CG and Schertler GF (2008) Structure of a β_1-adrenergic G-protein-coupled receptor. *Nature* **454**:486-491.

Wenzel-Seifert K, Hurt CM and Seifert R (1998) High constitutive activity of the human formyl peptide receptor. *J Biol Chem* **273**:24181-24189.

Wetherill L, Schuckit MA, Hesselbrock V, Xuei X, Liang T, Dick DM, Kramer J, Nurnberger JI, Jr., Tischfield JA, Porjesz B, Edenberg HJ and Foroud T (2008) Neuropeptide Y receptor genes are associated with alcohol dependence, alcohol withdrawal phenotypes, and cocaine dependence. *Alcohol Clin Exp Res* **32**:2031-2040.

Wieland HA, Engel W, Eberlein W, Rudolf K and Doods HN (1998) Subtype selectivity of the novel nonpeptide neuropeptide Y Y_1 receptor antagonist BIBO 3304 and its effect on feeding in rodents. *Br J Pharmacol* **125**:549-555.

Willars GB (2006) Mammalian RGS proteins: multifunctional regulators of cellular signalling. *Semin Cell Dev Biol* **17**:363-376.

Ziemek R, Brennauer A, Schneider E, Cabrele C, Beck-Sickinger AG, Bernhardt G and Buschauer A (2006) Fluorescence- and luminescence-based methods for the determination of affinity and activity of neuropeptide Y_2 receptor ligands. *European Journal of Pharmacology* **551**:10-18.

Ziemek R, Schneider E, Kraus A, Cabrele C, Beck-Sickinger AG, Bernhardt G and Buschauer A (2007) Determination of affinity and activity of ligands at the human neuropeptide Y Y_4 receptor by flow cytometry and aequorin luminescence. *Journal of Receptor and Signal Transduction Research* **27**:217-233.

Zwanziger D, Bohme I, Lindner D and Beck-Sickinger AG (2009) First selective agonist of the neuropeptide Y_1-receptor with reduced size. *J Pept Sci* **15**:856-866.

Chapter 2

2 Scope and Objectives

During the last decades obesity and its co-morbidities like hypertension, diabetes type II, coronary heart disease, have emerged as severe diseases in the modern world, causing immense expenses in a country's health systems. With the NPY receptor family playing a major role in appetite regulation and energy expenditure, ongoing efforts are focusing on the development of potent and orally available ligands of the Y receptors to solve the aforementioned problem, with more or less promising results (Sato *et al.*, 2009). To date, the Y_2R and Y_5R are the only members of the NPY receptor family, at which small molecular antagonists fulfill, as outlined above, the demands concerning pharmacodynamic and pharmacokinetic properties (see section 1.3). Appropriate Y_4R antagonists are unknown so far. Regarding the wide field of additional physiological effects, e.g. regulation of mood, cognition, pain, circadian rhythm and angiogenesis, with high potential for drug discovery, sensitive and reliable methods for both screening and detailed molecular pharmacological studies are needed to accelerate ongoing investigations.

Due to the common signaling pathway of NPY receptors, namely the coupling to $G_{i/o}$ proteins, classical ligand screening assays are based on the radioimmuno detection of cAMP formation in cells (CHO, HEK293), expressing the GPCR of interest. Thereby, the stimulation of adenylyl cyclase by forskolin is needed to reveal inhibitory effects of Y receptor agonists. In the present work a further development of this assay format and more straightforward ways of determining ligand potencies and efficacies were pursued:

- With the application of Epac-camps (Nikolaev *et al.*, 2004), a promising cAMP sensor, a sophisticated in vitro assay based on fluorescence resonance energy transfer (FRET), should be developed in SK-N-MC cells, endogenously expressing the hY_1R. Epac is an engineered protein consisting of a cAMP binding site flanked by enhanced cyan fluorescent protein (CFP) and enhanced yellow fluorescent protein (YFP). Increased cAMP concentrations in the cell due to extracellular stimuli, should lead to the binding of the second messenger and subsequently to a change in its conformation moving the fluorophores apart and thereby eliminating FRET. The change in donor and acceptor fluorescence should be measurable depending on the concentration of intracellular cAMP. This concept would enable the avoidance of radioactivity and even live cell imaging by confocal laser scanning microscopy (CLSM). As a starting point, single cell imaging should prove the functionality of Epac-camps as a cAMP sensor. However, the final goal was to establish an HTS assay system by means of fluorescence spectroscopy using a fluorescence plate reader (96-well format).

- By analogy to the well established luminescence based aequorin assay for the hY_2R and the hY_4R developed in our work group (Ziemek *et al.*, 2006; Ziemek *et al.*, 2007), HEC-1B-hY_5 cells should be stably transfected with the genes encoding chimeric G proteins (Conklin *et al.*, 1996) and, subsequently after assuring the Ca^{2+} signal, with the gene encoding the fluorescent protein aequorin, targeted to the mitochondria. The above mentioned assay format is desirable because of the direct readout (increasing intracellular calcium) upon receptor stimulation and a usually very high signal-to-noise ratio. The HEC-1B-hY_5 cell line, previously established in our work group (Moser *et al.*, 2000), was considered suitable for this purpose. The chimeric G protein, $G\alpha_{qi5}$, had to be modified by PCR to $G\alpha_{qi9}$ to potentially increase receptor coupling. After stable transfection of the cells, initially a spectrofluorimetric and a flow cytometric fluorescence based calcium assay should be established and modified to allow luminescence based aequorin assays.

- Finally, a steady-state GTPase assay, which is well established for many other GPCRs (Massotte, 2003; Wieland and Seifert, 2005), should be developed for the hY_2R and the hY_4R, using the baculovirus/Sf9 system, which is especially suited for $G_{i/o}$ coupled receptors, because e.g. GTP hydrolysis following receptor activation is measured. In such a system there is no need of pre-stimulation by forskolin. Due to the proximal readout, amplification steps that would complicate stoichiometry are not included.

This ensures that e.g. partial agonists can be discriminated from full agonists. Furthermore, with a steady-state GTPase assay constitutive receptor activity can be identified, and if so, an appropriate system for the screening of inverse agonists is available. In the baculovirus/Sf9 system GPCRs, G proteins and regulators of G protein signaling (RGS) proteins can be deliberately combined and the engineered Sf9 membranes can be characterized biochemically, e.g. with respect to expression levels and ratios of relevant proteins by immunoblotting, and pharmacologically using standard ligands. Finally, investigations on the impact of receptor N-glycosylation are feasible by culturing infected insect cells in the presence of the GlcNAc-1P-transferase, tunicamycin.

2.1 References

Conklin BR, Herzmark P, Ishida S, Voyno-Yasenetskaya TA, Sun Y, Farfel Z and Bourne HR (1996) Carboxyl-terminal mutations of $G_q\alpha$ and $G_s\alpha$ that alter the fidelity of receptor activation. *Mol Pharmacol* **50**:885-890.

Massotte D (2003) G protein-coupled receptor overexpression with the baculovirus-insect cell system: a tool for structural and functional studies. *Biochimica et Biophysica Acta* **1610**:77-89.

Moser C, Bernhardt G, Michel J, Schwarz H and Buschauer A (2000) Cloning and functional expression of the hNPY Y_5 receptor in human endometrial cancer (HEC-1B) cells. *Can J Physiol Pharmacol* **78**:134-142.

Nikolaev VO, Bunemann M, Hein L, Hannawacker A and Lohse MJ (2004) Novel single chain cAMP sensors for receptor-induced signal propagation. *J Biol Chem* **279**:37215-37218.

Sato N, Ogino Y, Mashiko S and Ando M (2009) Modulation of neuropeptide Y receptors for the treatment of obesity. *Expert Opin Ther Pat* **19**:1401-1415.

Wieland T and Seifert R (2005) Methodological approaches, in *G-protein coupled receptors as drug targets (Methods and principles in medicinal chemistry)* (Seifert R, Wieland, T. ed) pp 81-120, Weinheim.

Ziemek R, Brennauer A, Schneider E, Cabrele C, Beck-Sickinger AG, Bernhardt G and Buschauer A (2006) Fluorescence- and luminescence-based methods for the determination of affinity and activity of neuropeptide Y_2 receptor ligands. *European Journal of Pharmacology* **551**:10-18.

Ziemek R, Schneider E, Kraus A, Cabrele C, Beck-Sickinger AG, Bernhardt G and Buschauer A (2007) Determination of affinity and activity of ligands at the human neuropeptide Y Y_4 receptor by flow cytometry and aequorin luminescence. *Journal of Receptor and Signal Transduction Research* **27**:217-233.

Chapter 3

3 Towards a FRET based functional cAMP assay for the human NPY Y_1 receptor in SK-N-MC cells

3.1 Introduction

The first fluorescent indicator for cAMP used in real-time measurements in live cells was a cAMP-dependent protein kinase in which the catalytic (C) and regulatory (R) subunits were each labeled with fluorescein or rhodamine, respectively, enabling fluorescence resonance energy transfer (FRET) in the holoenzyme complex R2C2 (Adams *et al.*, 1991). Binding of cAMP to the R subunit results in the dissociation of the C subunits, thereby eliminating energy transfer. This modified protein kinase had to be microinjected into the cells so that the procedure was compromised e. g. by handling a large protein (≈ 170 kDa), unequal distribution within the cells or toxicity due to the large amount. With the cloning of the gene encoding green fluorescent protein (GFP) from Aequorea Victoria and the engineering of mutants (such as CFP or YFP) with altered spectral properties (Tsien, 1998) the development of a genetically encoded PKA-based biosensor for cAMP has been facilitated (Zaccolo *et al.*, 2000; Zaccolo and Pozzan, 2002). Namely, the construct consisted of the regulatory RII subunit fused to CFP and the catalytical C subunit was tagged with YFP, so that a co-transfection of cells had to be performed. Thus, the expression of the proteins had to be carefully matched in order to yield reliable FRET measurements. However, with the catalytically active site of C-YFP an overexpression could affect downstream targets. The A kinase activity reporter (AKAR) consisted of a fusion protein of CFP, the phosphoamido binding domain, the consensus substrate sequence for PKA and YFP (Zhang *et al.*, 2001), an optimized derivative of which has been applied in a primary high-troughput screening (see below). Upon PKA activation by cAMP, the substrate sequence of AKAR is phosphorylated

and bound by its neighbouring domain. This conformational change brings the two fluorophores into close proximity to each other, enabling FRET. Measuring YFP and CFP emission (535/455 nm) upon CFP excitation (440 nm) the ratio of the fluorescence intensities can be calculated. In this case, the change in the ratios was between 25 to 50 %. Further single molecule biosensors for cAMP are, as already mentioned in section 1.3.1, derived from the exchange protein directly activated by cAMP (Epac). Either the whole Epac protein (DiPilato *et al.*, 2004; Ponsioen *et al.*, 2004) or a truncated version of Epac, consisting of the cAMP binding site (Nikolaev *et al.*, 2004), are sandwiched between CFP and YFP. Though, emphasis was put on real-time imaging of cAMP in living cells by monitoring changes in the CFP/YFP ratio after stimulation of the cells, there have been some attempts to use the FRET based sensors in primary HTS (96-well format), i. e. for initial testing of compounds at a single concentration, in combination with subsequent secondary assays. For that purpose either AKAR3 or the indicator of cAMP using epac 3 were expressed as cAMP probes (Allen *et al.*, 2006). Live cell plate reading was accomplished in the 96-well format by excitation at 420 nm and emission recording at 475 and 535 nm. Maximal changes in the ratio were ≈ 25 % and ≈ 43 %, respectively, after applying 50 μM of forskolin (FSK) and 100 μM of isobutylmethylxanthin (IBMX, a phosphodiesterase (PDE) inhibitor, to prevent cellular cAMP degradation). Motivated by these reports from literature, the development of a functional FRET based cAMP assay for the human NPY Y_1 receptor, using Epac2-camps (see below) in SK-N-MC cells, was aimed at.

3.2 Materials and Methods

3.2.1 Materials

The plasmid encoding Epac2-camps, pcDNA3-EYFP-Epac2B(murine)-ECFP (abbreviated as pcDNA3-Epac2-camps) was a kind gift from Dr. V. O. Nikolaev (University of Würzburg, Germany) and was subcloned into the pcDNA3.1(+)Zeo vector by J. Mosandl (University of Regensburg, Germany) using the restriction sites *Hind*III and *Not*I. The plasmids for the enhanced cyan fluorescent protein, pECFP-N1 and the enhanced yellow fluorescent protein pEYFP-N1 were from Clontech (Saint-Germain-en-Laye, France). Forskolin (ICN Biomedicals, Eschwege, Germany) was prepared as a stock solution (10 mM) in DMSO and kept at -20 °C. Dilutions were prepared in 50 % DMSO. The phosphodiesterase (PDE) inhibitor IBMX (Sigma, Deisenhofen, Germany) was used as a 10 mM solution in 50 % ethanol.

3.2.2 Cell culture

SK-N-MC cells were maintained in EMEM containing NEAA, 2.2 g/l $NaHCO_3$, 110 mg/l sodium pyruvate and 10 % FCS (Biochrom, Berlin, Germany). Subculturing was performed every week by 1:10 dilution. Cells transfected with pcDNA3.1(+)Zeo-epac2-camps were kept under selection with 300 µg/ml of zeocin (Cayla SAS, Toulouse, France) (see next section).

3.2.3 Chemosensitivity assay

The chemosensitivity assay was performed according to Bernhardt et al. (Bernhardt *et al.*, 1992). Briefly, SK-N-MC cells were seeded 100 µl/well in transparent 96-well plates (Greiner, Frickenhausen, Germany) to a density of approximately 15 cells/microscopic field (magnification 320x). After 2-3 days the culture medium was removed by suction and 200 µl new medium containing increasing concentrations of zeocin were added. Two rows (16 wells) per plate contained vehicle instead of antibiotic as control. Zeocin was added as 1000-fold concentrated feed solutions. Two rows per plate were used for the incubation with each concentration. Approximately every 24 hours cells from a plate were fixed with glutardialdehyde (Merck, Darmstadt, Germany) and stored in a refrigerator. At the end of the experiment the cells were stained with 0.02 % crystal violet (Serva, Heidelberg, Germany) simultaneously. Plates were rinsed with water to remove excess dye, and cell-bound crystal

violet was extracted with 70 % ethanol for three hours under shaking. Subsequently, absorbance was measured at 578 nm using a Biotek 309 Autoreader (Tecnomara, Fernwald, Germany). Growth curves were constructed using the Prism 5.01 software (GraphPad, San Diego, CA). Absorbance values were transformed into corrected T/C values, expressing the net growth of the treated cells, relative to the growth of the vehicle control. Cytotoxic effects were comparable at all concentrations applied, thus 300 µg/ml zeocin were used for the selection of transfectants.

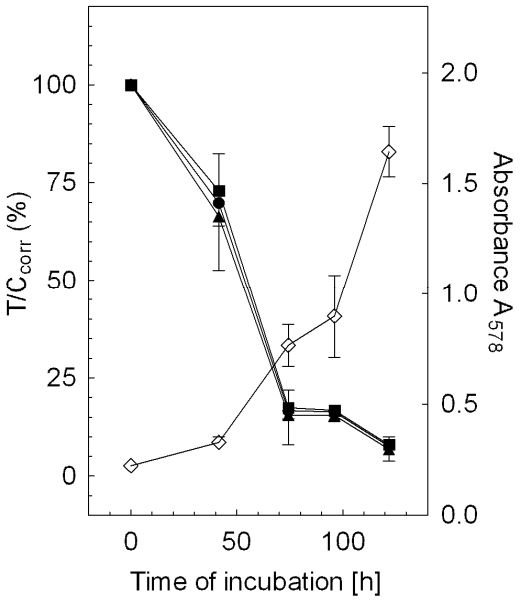

Fig. 3.1: Incubation of SK-N-MC cells with various concentrations of zeocin; Millipore water was used as negative control. ◊ vehicle; zeocin concentration: ● 300 µg/ml, ■ 400 µg/ml and ▲ 500 µg/ml.

3.2.4 Transfection of SK-N-MC cells

For stable transfection, cells were seeded in a 24-well plate (Greiner, Frickenhausen, Germany) and 1 µg of pcDNA3.1(+)Zeo-Epac2-camps was applied with FuGENE®6 (Roche, Mannheim, Germany) at a ratio of 4:9 according to the manufacturer's instructions. After two days, culture medium was replaced by zeocin (300 µg/ml) containing medium.

For confocal microscopy cells were seeded either in 8-well Lab-Tek (Nunc, Wiesbaden, Germany) or in µ-slide 8-well (Ibidi, Martinsried, Germany) chamber slides, and one day prior to the experiments transiently transfected with 0.6 µg of DNA and 1.5 µl of lipofectamine 2000 (Invitrogen, Karlsruhe, Germany) per well following the manufacturer's instruction.

3.2.5 Spectrofluorimetry

For spectrofluorimetry SK-N-MC cells and SK-N-MC cells, stably expressing Epac2-camps, were let grow to confluency in a 25-cm^2 culture flask. On the day of experiment, cells were detached with trypsin/EDTA, washed with loading buffer (Gessele, 1998) (120 mM NaCl, 5 mM KCl, 2 mM $MgCl_2$, 1.5 mM $CaCl_2$ (all from Merck), 25 mM HEPES (Sigma), 10 mM glucose (Merck) at pH 7.4) and adjusted to 10^6 cells/ml.

Measurements were performed in a Varian Cary Eclipse fluorescence spectrometer at a constant temperature of 25 °C (slit width: 5 nm, scan rate: slow, PMT voltage: high). The excitation wavelength was 436 nm, and fluorescence emission was scanned from 450 nm to 560 or 600 nm. Quartz UV cuvettes (Hellma, Müllheim, Germany) contained 3 ml of cell suspension under continuous stirring. Cells were treated with IBMX and FSK and incubated under stirring. For applied concentrations see section 3.3.1.

Recorded spectra were smoothed with SigmaPlot™ using the negative exponential function (sampling proportion 0.05, polynomial degree 1). Fluorescence intensities at the emission maxima (at 485 and 535 nm) were determined from the smoothed curves and CFP/YFP ratios were calculated.

3.2.6 Cell sorting

Due to decreasing expression of Epac2-camps after several passages (10), SK-N-MC-Epac2-camps cells were subjected to cell sorting with a fluorescence activated cell sorter FACSCalibur™ (Becton Dickinson, Heidelberg Germany) to enrich transfectants in the culture. Therefore, cells were centrifuged at 300 g for 5 min and re-suspended at a density of $2 \cdot 10^6$ cells/ml in sterile phosphate buffered saline (see 5.2.6). The fluidic system of the flow cytometer was disinfected by flushing with 70 % ethanol for 30 min and washed subsequently with sterile PBS for additional 30 min. The collection tubes were prepared by incubation with sterile PBS containing 4 % BSA overnight. The solution was discarded and the collection tubes were filled with 5 ml of EMEM supplemented with 20 % FCS before installation into the sorting unit of the flow cytometer. The argon laser was used to excite the YFP domain of the Epac2-camps protein. Instrument settings were FSC: E-1, SSC: 350V and FL-1 > 360 V using the single cell sorting mode. 30 – 40 ml of diluted sorted cells were centrifuged for 10 min at 300 g and re-suspended in 500 µl of EMEM containing 20 % FCS on a 24-well plate. The sorted cells were expanded and maintained in EMEM supplemented with 5 % FCS and 300 µg/ml zeocin. However, Epac2-camps expression declined again after 7 passages (**Fig. 3.2**).

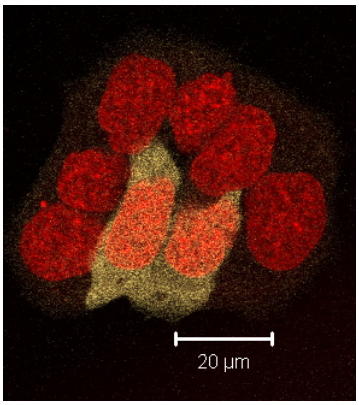

Fig. 3.2: SK-N-MC-Epac2-camps (7. P. after sorting), nuclei stained with DRAQ5™; C-Apochromat 40x/1.2W, Ar 458, HFT 514/633, BP 530-600, HeNe 633, HFT 514/633, LP 650

3.2.7 Confocal microscopy

For confocal microscopy, stable or transiently transfected SK-N-MC cells were seeded in 8-well chamber slides (3.2.4). At the day of image acquisition the culture medium was replaced with Leibovitz L15 medium (Sigma), supplemented with 5 % FCS. DRAQ5™ (Biostatus Limited, Leicestershire, UK) was used as a nuclear stain at a final concentration of 1 µM (**Fig. 3.2**). Images were acquired with a Carl Zeiss Axiovert 200M LSM510 confocal laser scanning microscope (CLSM) equipped with the Zeiss Meta system. Instrument settings (laser excitation wavelengths, beam paths, filter combinations) are described in the legends of the respective figures. Spectra were recorded with the Meta detector of the microscope, i. e. the sample was excited with the 458 nm beam of the Argon laser, light emitted from the fluorophores is split into its component wavelengths. Every 10.7 nm is sent to a separate PMT of the Meta detector. Spectra were extracted from intracellular regions of interest (ROIs). For the calculation of CFP/YFP ratios, the intensities at 483 and 526 nm were used. Cells were treated with 10-fold concentrated IBMX and FSK solutions as indicated in **Table 3.3**.

3.3 Results and discussion

3.3.1 Spectrofluorimetry

Fluorescence spectra of SK-N-MC and untreated SK-N-MC-Epac2-camps cells are shown in **Fig. 3.3 A**. After background correction, the spectrum of SK-N-MC-Epac2-camps cells showed the expected two emission maxima at 485 (CFP) and 530 nm (YFP), respectively. Incubation of the cells with 100 µM FSK (20 min) (**Fig. 3.3 B** curve 2) and 50 µM IBMX (15 min) and 100 µM FSK (20 min) (**Fig. 3.3 B** curve 3) raised the CFP signal, and concomitantly the CFP/YFP ratio by 7.1, respectively 14.2 % (**Table 3.1**). This is in

accordance with literature as a maximum ratio change of Epac2-camps expressing HEK-β_1AR cells upon isoprenaline stimulation was reported to amount to approx. 15 % (Nikolaev *et al.*, 2004).

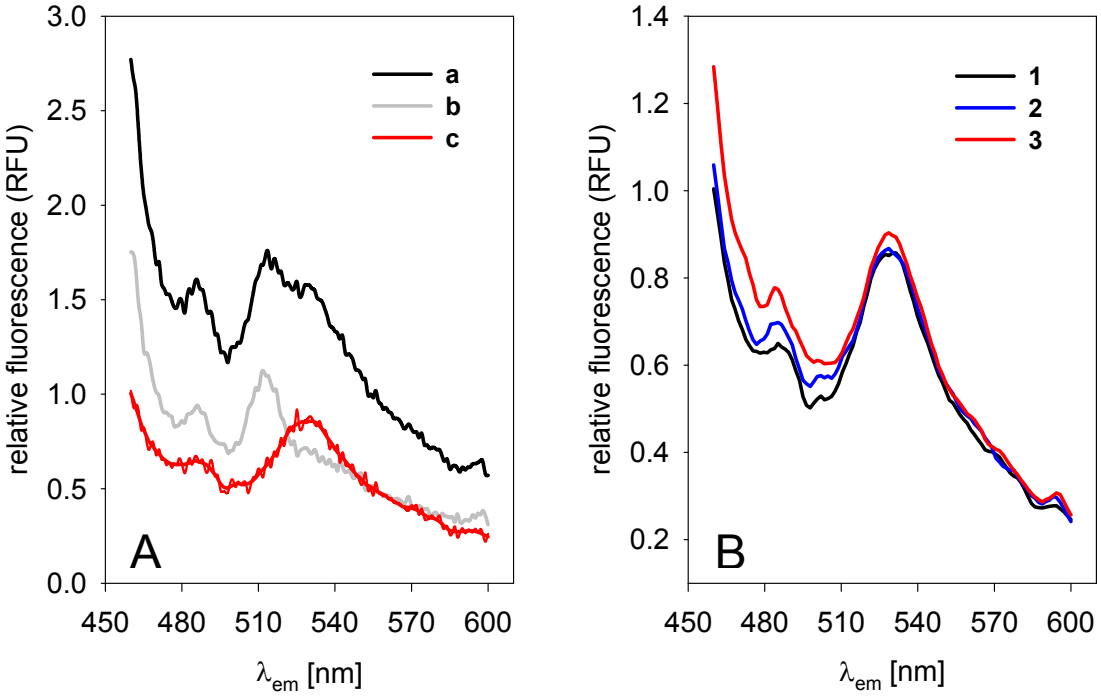

Fig. 3.3: Fluorescence spectra of SK-N-MC wild-type and SK-N-MC-Epac2-camps cells; **A**: Background corrected spectrum of SK-N-MC-Epac2-camps cells (c) was calculated by substracting the autofluorescence of wild type cells (b) from the spectrum of SK-N-MC-Epac2-camps cells (a). **B**: Background corrected, smoothed fluorescence spectra of untreated SK-N-MC-Epac2-camps cells (1), in the presence of 100 µM forskolin (2) and in the presence of 1 mM IBMX and 100 µM forskolin (3); Fluorescence values at the emission peaks (485 nm and 530 nm) were used for analysis.

Table 3.1: CFP/YFP ratios of SK-N-MC-Epac2-camps cells calculated from the maxima at 485 and 530 nm, respectively

	untreated	FSK	IBMX, FSK
Ratio (CFP/YFP)	0.759	0.813	0.866
dRatio (relative to untreated cells)	-	0.054	0.108

To confirm these results, the experiment was repeated. However, as already mentioned in section 3.2.6, due to declining Epac2-camps expression, the difference in background corrected spectra became very small (**Fig. 3.4**), and stimulation of the cells with FSK and treatment with IBMX failed to give reproducible results (**Table 3.2**).

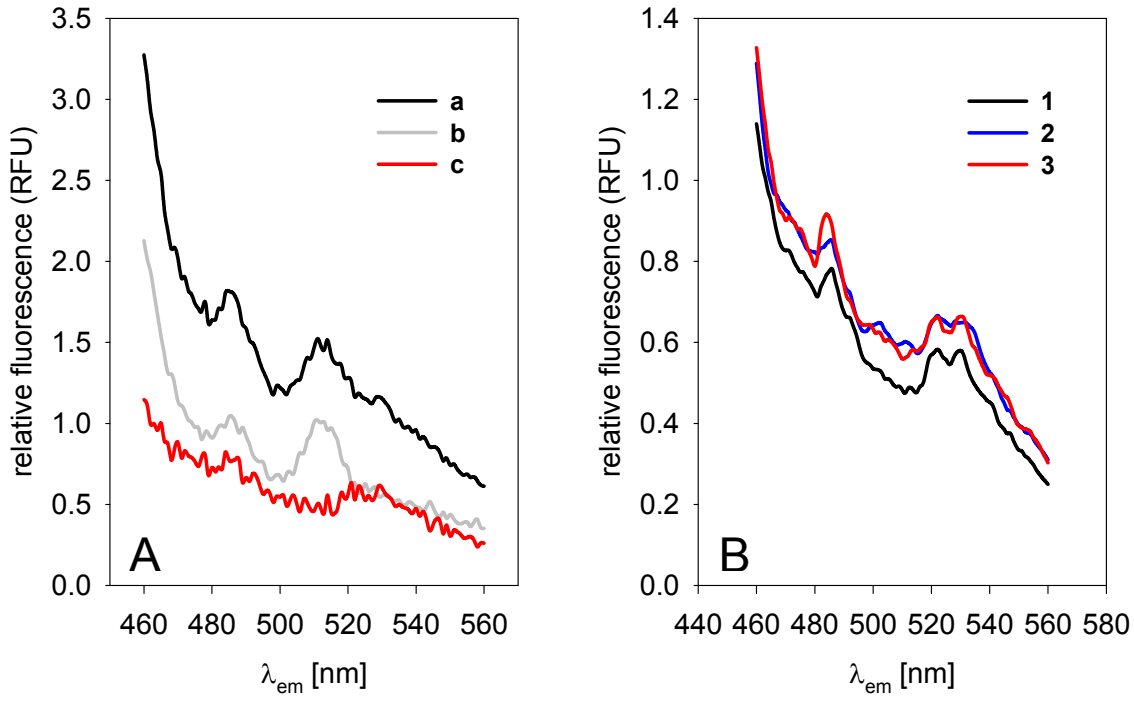

Fig. 3.4: Fluorescence spectra of SK-N-MC wild-type and SK-N-MC-Epac2-camps cells; **A**: Background corrected spectrum of SK-N-MC-Epac2-camps cells (c) was calculated by substracting the autofluorescence of wild-type cells (b) from the spectrum of SK-N-MC-Epac2-camps cells (a). **B**: Background corrected, smoothed fluorescence spectra of untreated SK-N-MC-Epac2-camps cells (1), in the presence of 100 µM forskolin (2) and in the presence of 50 µM IBMX and 100 µM forskolin (3). Fluorescence values at the emission peaks (485 nm and 530 nm) were used for analysis.

Table 3.2: CFP/YFP ratios of SK-N-MC-Epac2-camps cells calculated from the maxima at 485 and 530 nm, respectively

	untreated	FSK	IBMX, FSK
Ratio (CFP/YFP)	1.337	1.311	1.368
dRatio (relative to untreated cells)	-	- 0.026	0.031

3.3.2 Confocal microscopy

Initially, evaluation of Epac2-camps was planned to be done by confocal microscopy. However, due to technical problems with the microscope, these experiments were performed after spectrofluorimetry. The fluorescent proteins CFP and YFP alone (**Fig. 3.5**) and in combination (**Fig. 3.6**) were expressed transiently in SK-N-MC cells, and fluorescence spectra were recorded with the CLSM upon excitation at 458 nm (argon laser). The shapes of the spectra are comparable with those found in literature (see also section 1.3.1). Obviously, in particular the spectrum of co-expressed CFP and YFP showed no FRET as the emission

peaks were approximately the same, which was not the case in the spectrum of SK-N-MC-Epac2-camps cells (**Fig. 3.7 A**). There, the YFP peak was considerably higher. To determine autofluorescence, spectra of SK-N-MC wild-type cells were recorded as well (**Fig. 3.7 B**). However, only minimal fluorescence was detected. **Fig. 3.7 C** shows the phase contrast image of SK-N-MC wild-type cells in comparison to the confocal image (**Fig. 3.7 B**).

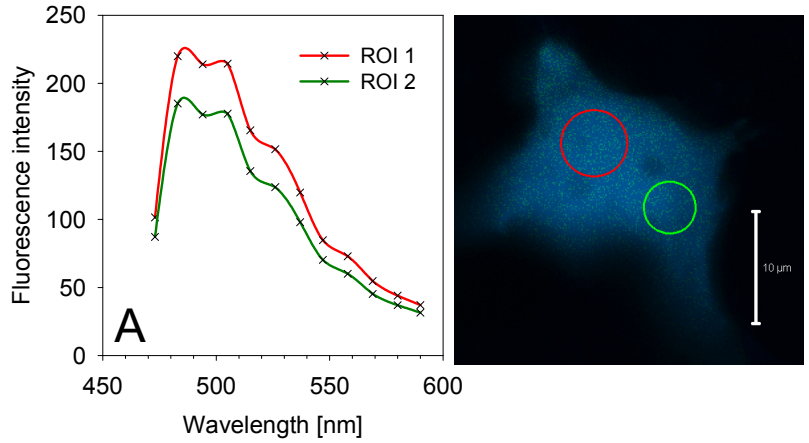

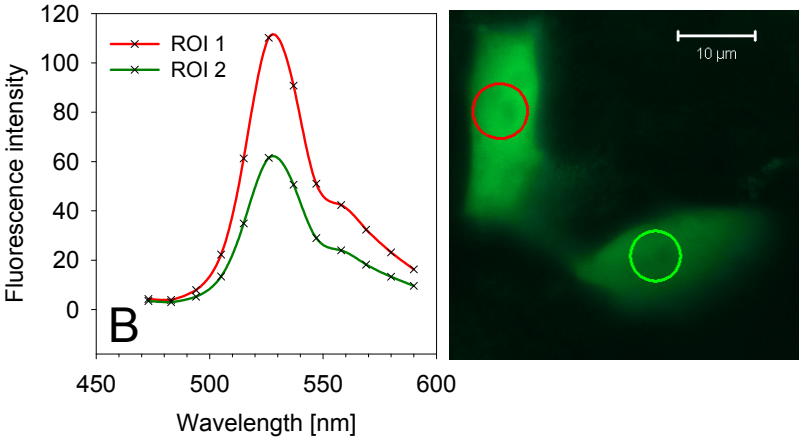

Fig. 3.5: Fluorescence spectra of SK-N-MC cells expressing CFP (A), YFP (B); Spectra were extracted from regions of interest (ROI) shown in the corresponding images.
C-Apochromat 40x/1.2W,
A: Ar 458, ChS: 467-596
B: Ar 458, ChS: 467-596

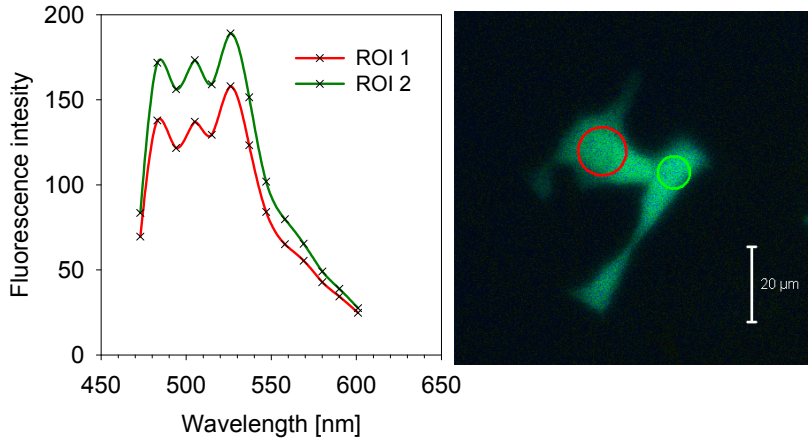

Fig. 3.6: Fluorescence spectra of SK-N-MC cells expressing CFP and YFP; Spectra were extracted from regions of interest (ROI) shown in the corresponding images.
C-Apochromat 40x/1.2W,
Ar 458, ChS: 467-606

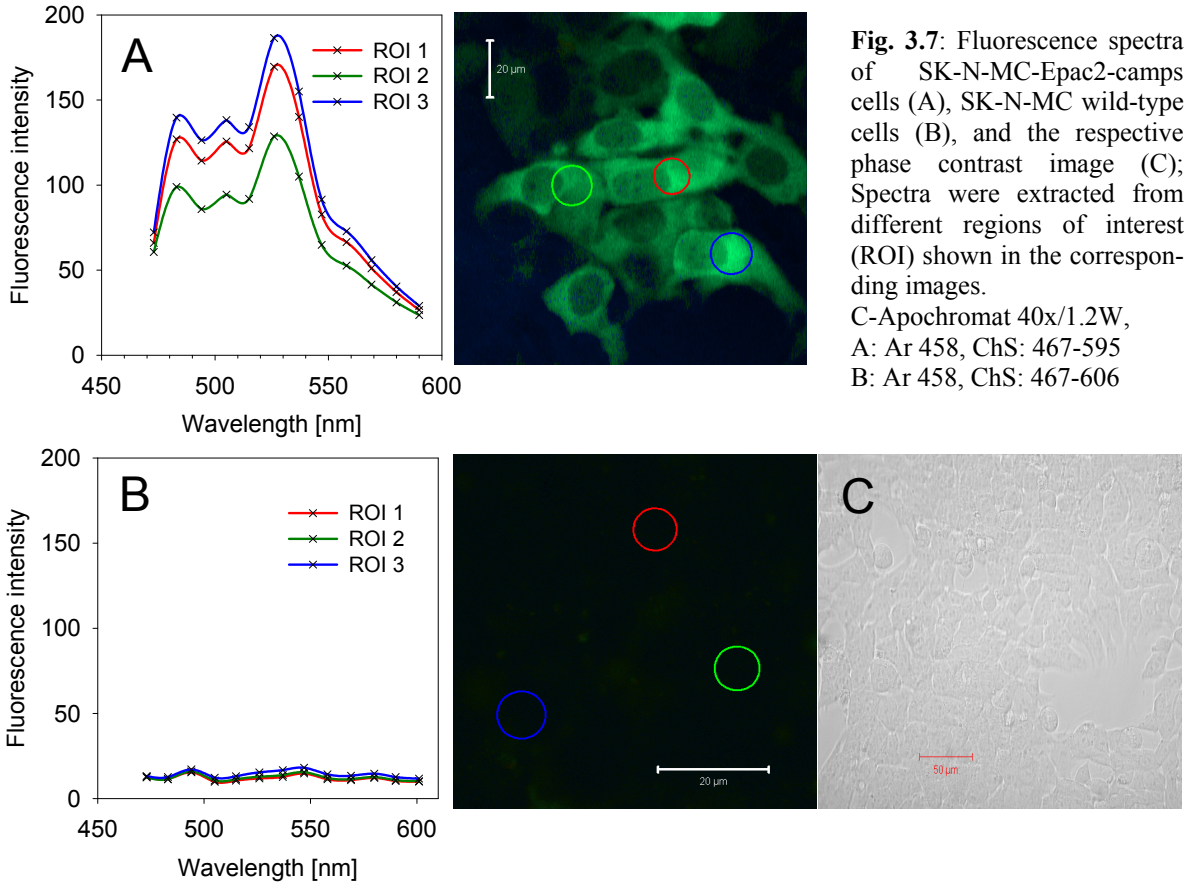

Fig. 3.7: Fluorescence spectra of SK-N-MC-Epac2-camps cells (A), SK-N-MC wild-type cells (B), and the respective phase contrast image (C); Spectra were extracted from different regions of interest (ROI) shown in the corresponding images.
C-Apochromat 40x/1.2W,
A: Ar 458, ChS: 467-595
B: Ar 458, ChS: 467-606

SK-N-MC-Epac2-camps cells were treated with different concentrations of IBMX and FSK (as indicated in **Table 3.3**). 5 µM FSK are used in the enzymatic cAMP assay established in our work group (Gessele, 1998). At this concentration and 100 µM IBMX the cAMP production in SK-N-MC cells amounts to ca. 38 µM. Epac2-camps is already saturated at a concentration of 2 µM of cAMP to 90 %. Thus, with 5 µM FSK there should be an unequivocal change in the ratio of CFP/YFP intensity. In **Table 3.3** the results from one experiment are given. Data were averaged from four cells, each. Fluorescence spectra of the same cells were recorded during the experiment. The change in the ratios was up to 32 % for FSK treatment for 10 min. Intriguingly, this change decreased to half of the value after another 5 min, and the cells treated with the PDE inhibitor and FSK showed poor FRET response. The experiment was repeated twice. However, no sensible results were obtained. Thus, the initial idea to develop a FRET based assay for the 96-well plate format was not pursued any longer.

Table 3.3: Ratios of CFP- and YFP-fluorescence calculated from spectra of differently treated SK-N-MC-Epac2-camps cells

Treatment	Ratio (483/526)	dRatio (483/526)
-	0.553 ± 0.003	-
FSK 10 µM, 10 min	0.815 ± 0.022	0.262 ± 0.025
FSK 10 µM, 15 min	0.668 ± 0.018	0.115 ± 0.015
-	0.721 ± 0.023	-
IBMX 100 µM, 10 min FSK 5 µM, 13 min	0.667 ± 0.023	-0.054 ± 0.029
-	0.672 ± 0.012	-
IBMX 100 µM, 10 min FSK 5 µM, 17 min	0.717 ± 0.033	0.044 ± 0.026

Means ± S.E.M. (n = 4 cells from one image), dRatio (483/526) is relative to untreated cells

3.4 Summary and conclusions

The promising concept of measuring cAMP with biosensors such as Epac2-camps was evaluated with the aim to develop a HTS for hY_1R in SK-N-MC cells. For this purpose, the cells were transfected with pcDNA3.1(+)Zeo-Epac2-camps. Stable transfection was not accomplished, because protein expression declined after as few as 7 passages, even after flow cytometric cell sorting. Transient tranfection was satisfactory for confocal microscopy. In a spectrofluorimetric assay, SK-N-MC-Epac2-camps cells showed the expected spectrum with emission peaks at 485 and 530 nm. However, these initial promising results, i.e. changes in the ratio of CFP/YFP intensities upon FSK and IBMX treatment, could not be confirmed. This is partly due to the poor protein expression by the transfectants. In confocal microscopy, spectra of CFP, YFP and Epac2-camps expressed in SK-N-MC cells had the expected shapes and peaks. Intriguingly, the CFP/YFP FRET change upon treatment with IBMX and FSK showed no usable results, although spectra were recorded from identical cells, untreated and treated, respectively. The FRET efficiency of Epac2-camps determined by acceptor photobleaching was 15 %, of which the change in the CFP/YFP fluorescence ratio upon isoprenalin stimulation of HEK-β_1AR cells was again only 15 % (Nikolaev *et al.*, 2004). This amounts approximately to 2 – 3 % of the total fluorescence. Most probably, such small signals can hardly be exploited for HTS.

3.5 References

Adams SR, Harootunian AT, Buechler YJ, Taylor SS and Tsien RY (1991) Fluorescence ratio imaging of cyclic AMP in single cells. *Nature* **349**:694-697.

Allen MD, DiPilato LM, Rahdar M, Ren YR, Chong C, Liu JO and Zhang J (2006) Reading dynamic kinase activity in living cells for high-throughput screening. *ACS Chem Biol* **1**:371-376.

Bernhardt G, Reile H, Birnbock H, Spruss T and Schonenberger H (1992) Standardized kinetic microassay to quantify differential chemosensitivity on the basis of proliferative activity. *J Cancer Res Clin Oncol* **118**:35-43.

DiPilato LM, Cheng X and Zhang J (2004) Fluorescent indicators of cAMP and Epac activation reveal differential dynamics of cAMP signaling within discrete subcellular compartments. *Proc Natl Acad Sci U S A* **101**:16513-16518.

Gessele K (1998) Zelluläre Testsysteme zur pharmakologischen Charakterisierung neuer Neuropeptid Y-Rezeptorantagonisten, Doctoral thesis, University of Regensburg, Germany

Nikolaev VO, Bunemann M, Hein L, Hannawacker A and Lohse MJ (2004) Novel single chain cAMP sensors for receptor-induced signal propagation. *J Biol Chem* **279**:37215-37218.

Ponsioen B, Zhao J, Riedl J, Zwartkruis F, van der Krogt G, Zaccolo M, Moolenaar WH, Bos JL and Jalink K (2004) Detecting cAMP-induced Epac activation by fluorescence resonance energy transfer: Epac as a novel cAMP indicator. *EMBO Rep* **5**:1176-1180.

Tsien RY (1998) The green fluorescent protein. *Annu Rev Biochem* **67**:509-544.

Zaccolo M, De Giorgi F, Cho CY, Feng L, Knapp T, Negulescu PA, Taylor SS, Tsien RY and Pozzan T (2000) A genetically encoded, fluorescent indicator for cyclic AMP in living cells. Nat Cell Biol 2:25-29.

Zaccolo M and Pozzan T (2002) Discrete microdomains with high concentration of cAMP in stimulated rat neonatal cardiac myocytes. Science 295:1711-1715.

Zhang J, Ma Y, Taylor SS and Tsien RY (2001) Genetically encoded reporters of protein kinase A activity reveal impact of substrate tethering. Proc Natl Acad Sci U S A 98:14997-15002.

Chapter 4

4 Towards fluorescence and luminescence based functional assays for the human NPY Y_5 receptor in HEC-1B-hY_5 cells

4.1 Introduction

4.1.1 Redirecting receptor signaling via chimeric G proteins

Historically, cAMP inhibition of the Y_5R after forskolin stimulation was measured radioimmunologically (Gerald *et al.*, 1995; Gerald *et al.*, 1996; Bischoff *et al.*, 2001). Meanwhile modern assays such as a homogenous cAMP kit ((HTRF), Cisbio Bioassays, Bagnols-sur-Cèze Cedex, France) based on time-resolved FRET (TR-FRET) are in use (Kakui *et al.*, 2006; Walker *et al.*, 2009). In the latter, after lysis of the cells, endogeneous cAMP competes with e.g. phycobilin conjugated cAMP (acceptor) for the binding site of a cryptate-labeled cAMP antibody (donor), thereby eliminating FRET. Though this approach exhibits high sensitivity, reproducibility and precision (De los Frailes and Diez, 2009), it has the disadvantage of high costs regarding small scale laboratory use. The same is true for GTPγ^{35}S binding assays based on scintillation proximity with membranes of mY_5R expressing HEK293 cells (Dautzenberg *et al.*, 2005).

Ca^{2+} mobilization is the most versatile and convenient way to measure signals within cells. The two main technologies to quantify intracellular Ca^{2+} in high throughput screening (HTS) mode use Ca^{2+}-sensitive dyes (fluorescent assays) or photoproteins (luminescence assays) (De los Frailes and Diez, 2009). The hY_5R has been shown to elicit Ca^{2+} signals upon stimulation, when expressed in LMTK cells heterologously. This system was used for determination of Y_5 ligand activities (Criscione *et al.*, 1998; Kanatani *et al.*, 2000). Moreover, a combination of

the receptor with chimeric G proteins like $G\alpha_{qi5}$, $G\alpha_{qi9}$ or $G\alpha_{q/z5}$ in CHO, HEK293 or COS-7 cells was efficient for this purpose (Dautzenberg *et al.*, 2005; Sato *et al.*, 2008; Ando *et al.*, 2009; Walker *et al.*, 2009).

So far, bioluminescence assays for the Y_5 receptor have not been described. Advantages of an aequorin assay are for example: no dye leakage, no requirement for excitation light, no photo-bleaching, no auto-fluorescence or biological degradation problems. Menon *et al*. also reported on a significant decrease in the number of false-positives with the aequorin assay (Menon *et al.*, 2008). Therefore, the HEC-1B-hY_5 cell line (established at our work group) was used first to establish fluorescence based Ca^{2+} assays, becoming feasible via chimeric G proteins. Subsequently exploitation of mitochondrially targeted aequorin (mtAEQ) as calcium sensor was probed.

4.2 Materials and Methods

4.2.1 Preparation of media and agar plates

LB medium containing 1 % bacto tryptone (Difco, Detroit, MI), 0.5 % yeast extract (Carl Roth GmbH, Karlsruhe, Germany) and 1 % NaCl (Merck, Darmstadt, Germany) was prepared in millipore water, and the pH was adjusted to 7.0. For sterilization the medium was autoclaved at 121 °C for 20 min and then stored at 4 °C until use. Selective amp-LB medium was prepared by adding ampicillin (Sigma, Deisenhofen, Germany) from a sterile stock solution in millipore water (100 mg/ml) to the LB medium to yield the final concentration of 100 µg/ml.

For the preparation of selective agar plates, 1.5 % agar (Carl Roth GmbH) was added to 1000 ml of LB medium. After sterilization by autoclaving, the medium was cooled to 60-65 °C, ampicillin was added (as described above) and plates were prepared under LAF conditions. Selective plates were stored at 4 °C for 8 to 12 weeks.

SOC medium contained 2.5 mM KCl (Merck), 10 mM $MgCl_2$ (Merck) and 10 mM $MgSO_4$ (Merck) in LB medium. After autoclaving a sterile glucose (Merck) solution was added to yield a final concentration of 20 mM.

4.2.2 Preparation of competent E. coli

Competent cells were prepared using the *E. coli* TOP10 strain (Invitrogen, Karlsruhe, Germany). 5 ml of an overnight culture were grown in LB medium. Then 200 ml of sterile LB medium were inoculated with 2 ml of the overnight culture. Cells were grown with shaking (190 rpm) at 37 °C to an OD_{600} of 0.2. The bacterial suspension was aliquoted into 8 pre-chilled, sterile polypropylene tubes and left on ice for 10 min. Cells were collected by centrifugation at 1500 g for 7 min at 4 °C, the supernatant was discarded and each cell pellet was re-suspended in 5 ml of ice-cold $CaCl_2$ solution containing 60 mM $CaCl_2$ (Merck), 10 mM PIPES (Gerbu, Gaiberg, Germany) and 15 % glycerol (Merck) at pH 7.0. Cells were centrifuged for 5 min at 1000 g, re-suspended in 5 ml of ice-cold $CaCl_2$ solution and incubated on ice for 30 min. After another centrifugation step at 1000 g for 5 min, the supernatant was poured off, and each pellet was re-suspended in 1 ml of ice-cold $CaCl_2$ solution. 100 µl aliquots of cell suspension were pipetted into 1.5 ml microfuge tubes and left on ice for another 2 h. Finally, competent cells were frozen in liquid nitrogen and stored at -80 °C.

4.2.3 Transformation of E. coli

For chemical transformation, 200 µl of a suspension of competent cells were thawed on ice and the plasmid DNA or the ligation product was added prior to incubation on ice for 30 min. Cells were heat-shocked by transferring the tubes into a 42 °C warm water bath for 90 min. For recovery and the expression of the antibiotic resistance gene needed for the positive selection of the transformants, 1 ml of SOC medium, pre-warmed to 37 °C, was added, and the bacteria were incubated for 45 min at 37 °C with shaking (200 rpm).

20 µl of the transformant suspension were plated onto selective agar and the plates were incubated overnight at 37 °C. Colonies were picked and used for overnight cultures in selective medium.

4.2.4 Preparation of plasmid DNA

4.2.4.1 Miniprep

For the preparations of DNA small scale alkaline lysis procedures were performed according to the protocol described by Birnboim and Doly (1979). Buffers were prepared as follows:

Buffer P1: 50 mM Tris·HCl (Serva, Heidelberg, Germany), 10 mM titriplex III (Merck) and 100 µg/ml RNase A (MBI Fermentas, St. Leon-Rot, Germany) in millipore water, pH 8.0
Buffer P2: 0.2 M NaOH (Merck) and 1 % SDS (Sigma) in millipore water
Buffer P3: 3 M KAc (Merck) in millipore water, pH 5.5
5 ml of amp-LB selective medium were inoculated with bacteria from an isolated colony and incubated overnight at 37 °C under vigorous shaking (200 rpm). 1.5 ml of this culture was centrifuged for 30 s at 13,000 rpm (Eppendorf Centrifuge 5415 R, Eppendorf, Hamburg, Germany). The supernatant was discarded and the cell pellet was re-suspended in 100 µl of P1. For the degradation of bacterial RNA the suspension was incubated for 5 min at room temperature. Addition of 200 µl of P2 resulted in cell lysis. The solution was mixed gently by inverting the tubes several times, before another 5 min of incubation on ice. Addition of 150 µl of ice-cold P3 and further incubation for 10 min led to neutralization of the lysate and precipitation of SDS, denaturation of proteins and chromosomal DNA. Separation of the precipitate from solution was achieved by centrifugation at 13,000 rpm for 15 min. Further purification of the plasmid in the supernatant resulted from the addition of 400 µl of phenol-chloroform-isoamylalcohol (25:24:1) (Carl Roth GmbH), vigorous vortexing and separation of the phases by centrifugation at 13000 rpm for 3 min. The aqueous phase was transferred into a new tube and plasmid DNA was precipitated by addition of 1 ml of ice-cold ethanol (Mallinckrodt Baker, Griesheim, Germany) and centrifugation at 13000 rpm for 20 min. Finally, the pellet was washed with 1 ml of ethanol (70 %), air dried and dissolved in 10 µl of millipore water. The DNA solutions were stored at -20 °C.
Usually Mini-Preps were done in parallel (3 x 1.5 ml of each preparation) and the solutions were pooled to obtain larger amounts of plasmid DNA for analytical purposes.

4.2.4.2 Maxiprep

For large scale plasmid preparation, the Qiagen Plasmid Maxi Purification Kit (Qiagen, Hilden, Germany) was used according to the manufacturer's instructions.

4.2.4.3 Determination of DNA concentration and sequencing

Usually, a 1:70 dilution of Mini-Prep or Maxi-Prep DNA was prepared and spectra were recorded with a Cary 100 UV-Vis spectrophotometer (Varian, Darmstadt, Germany). DNA concentration was determined according to the following equation: c [µg/ml] = 50 · A_{260} · dilution factor, according to the assumption that a double stranded DNA solution of 50 µg/ml

has an absorbance of 1.0 at 260 nm when the path length is 1 cm. Sequencing was performed by Entelechon (Regensburg, Germany).

4.2.4.4 Restriction enzyme digestion and dephosphorylation of plasmid ends

For the subcloning of PCR products and restriction enzyme analysis of plasmid DNA the enzymes *Bam*HI (MBI Fermentas, St. Leon-Rot, Germany) and *Eco*RV (MBI Fermentas) were used. The reaction buffer (SuRE/Cut buffer B, Roche) was chosen to assure 100 % activity for each enzyme. Usually samples were digested in 20 µl of reaction volumes containing 2 µl of reaction buffer, 1 µl of each enzyme (10 U) and 0.5 – 2.0 µg of DNA. The reaction was carried out for one hour at 37 °C in an Eppendorf reaction vessel and enzymes were heat inactivated for 15 min at 70 °C.

In order to avoid self ligation of digested plasmid, the DNA ends were dephosphorylated with calf intestine phosphatase (CIP; Boehringer Mannheim, Mannheim, Germany) by incubation at 37 °C for 1 h. Heat inactivation of the CIP followed for 20 min at 80 °C. Required CIP units for reaction were calculated according to the amount of digested plasmid DNA (1 pmol DNA ends correspond for 0.05 U of CIP).

4.2.4.5 Agarose gel electrophoresis

Agarose gels were prepared by dissolving 0.75 or 1.0 g of agarose (pegGOLD Universal-Agarose, Peqlab, Erlangen, Germany) under heating and stirring in 50 ml of TAE buffer (used as a dilution from a 50x concentrated stock solution containing 242 g Tris base (usb, Cleveland, OH), 57 ml of glacial acetic acid (Merck) and 100 ml of EDTA solution (0.5 M, pH 8.0; Merck) in 1000 ml of millipore water). To visualize DNA, 2 µl of an ethidium bromide (Janssen Chimica, Beerse, Belgium) solution (10 mg/ml) were added. The warm agarose solution was poured into the gel chamber and let gel for 30 min.

Prior to electrophoresis, TAE buffer was filled into the gadget, 6x DNA loading dye (MBI Fermentas) was added to the samples from PCR or restriction enzyme digestion and the mixtures were pipetted into the pockets. For analytical gels usually 5 µl of PCR product or digested DNA mixed with 1 µl of loading dye were applied. For quantitative gels after restriction enzyme digestion volumes up to 30 µl were pipetted into gels with larger pockets. As reference, 5-10 µl of the MassRuler^{TM} DNA ladder Mix (#SM0403; MBI Fermentas) were used.

Electrophoresis was performed 60-90 min at 90 V until the track dye moved 2/3 of the gel length. Then, the gel tray was removed from the electrophoresis chamber and DNA bands were visualized by illumination with UV light at 254 nm (Gel Doc 2000; Bio-Rad Laboratories, München, Germany). Quantity One (Bio-Rad) software was used for data analysis.

DNA concentration of the sample was roughly estimated by comparing the intensities of the bands with the intensity of the band of the DNA ladder corresponding to the sample in size according to the manufacturer´s information.

4.2.4.6 Purification of PCR product and recovery of DNA fragments from agarose gels

DNA from PCRs was desalted and the polymerase was removed with the QIAquick PCR Purification Kit (Qiagen, Hilden, Germany). After restriction enzyme digestion DNA fragments were first separated by agarose gel electrophoresis. Bands with the correct sizes were excised from the gel under UV light (λ_{ex} 254 nm) and extracted with the QIAEX II Gel Extraction Kit (Qiagen) according to the manufacturer's instructions. Depending on the volume of the PCR reaction mixtures, DNA was eluted with 10-50 µl of millipore water. Subsequent to purification, DNA concentration was assessed as described (cf. section 4.2.4.5).

4.2.5 Preparation of chimeric $G\alpha_{qi9}$ by PCR

The nucleotide sequence of $G\alpha_{qi5}$ encodes a chimeric Gα-protein representing $G\alpha_q$ with the last 5 C-terminal amino acids changed into the sequence of $G\alpha_{i2}$, thereby enabling G_i-coupled receptors to signal via calcium mobilization. Since Dautzenberg et al. reported that the human and the murine Y_5 receptor would exclusively couple to $G\alpha_{qi9}$ (Dautzenberg *et al.*, 2005), $G\alpha_{qi5}$ was further modified by PCR. With the antisense primer the triplet CTG, encoding the 9th amino acid (counted from the C-terminus), was exchanged (AAC) so that lysine was mutated into asparagine, which is the corresponding amino acid in $G\alpha_i$ in that position. In PCR reactions 100 ng of the plasmid pcDNA3.1/Hygro-$G\alpha_{qi5}$, prepared by R. Ziemek (Dept. of Pharmaceutical Chemistry II, University of Regensburg, Germany), was used as template. The primers were obtained from MWG (Ebersberg, Germany).

Gqi9-(T7)-sense	5' - TAA TAC GAC TCA CTA TAG GGA GAC CCA AGC TGG - 3'
Gqi9-EcoRV-anti:	5' - CGC GAT ATC ATG CAT TCA GAA GAG GCC ACA GTC CTT AAG GTT GTT CTG CAG GAT GGT - 3'

If not stated otherwise, all other reagents were from MBI Fermentas Life Sciences,. PCR reaction mixtures contained 2.5 U of recombinant *Pfu* DNA Polymerase, 10 µl 10x *Pfu* buffer without $MgSO_4$, 3.5 mM $MgSO_4$, dNTP Mix (0.2 mM each) and primers (0.5 µM each) in a final volume of 100 µl. 10 % DMSO was added to prevent annealing of template cDNA. PCR reactions were performed in a Mastercycle gradient Thermocycler (Eppendorf, Hamburg, Germany).

Cycling parameters were:

(1)	initial denaturation	95 °C, 3 min
(2)	denaturation	95 °C, 1 min
(3)	annealing	60 °C, 2 min
(4)	extension	72 °C, 2 min
(5)	final extension	72 °C, 5 min
(6)	hold	4 °C

Steps (2) to (4) were repeated 24 times.

The expected size of PCR product was 1167 bp, which was found in agarose gel electrophoresis subsequently, as shown in **Fig. 4.1**.

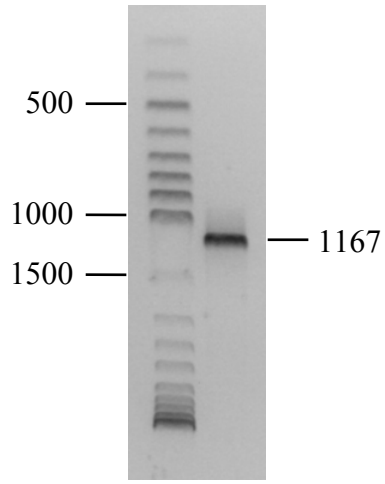

Fig. 4.1: Agarose gel (2%) electrophoresis of PCR product $G\alpha_{qi9}$; Numbers indicate the sizes of bands in the DNA ladder in base pairs (bp).

4.2.6 Subcloning of pcDNA3.1/Hygro-Gα$_{qi9}$

The PCR product and the template pcDNA3.1/Hygro-$G\alpha_{qi5}$ were digested and the plasmid ends were additionally dephosphorylated as described in 4.2.4.4. After electrophoresis (**Fig. 4.2 A**), the amount of DNA was assessed, bands were excised from the agarose gel and DNA fragments were extracted. 240 ng of plasmid was incubated with each a 5- and 2-fold molar excess of insert for ligation. Reactions in mixtures containing 5 Weiss units of T4 DNA ligase (MBI Fermentas), 2 µl of 10x ligation buffer (MBI Fermentas) and water in a final volume of 20 µl were carried out overnight at room temperature. After transformation of the ligation products in competent *E. coli* minipreps of plasmids were prepared. Restriction enzyme analysis was performed with *Bam*HI and *Eco*RV (**Fig. 4.2 B**). Sequencing proved the insertion of the PCR product $G\alpha_{qi9}$ with three mutations (A1051C, A1052T and C1053G counted from the ATG of the gene) compared to pcDNA3.1/Hygro-$G\alpha_{qi5}$ prepared by R. Ziemek (Ziemek, 2006).

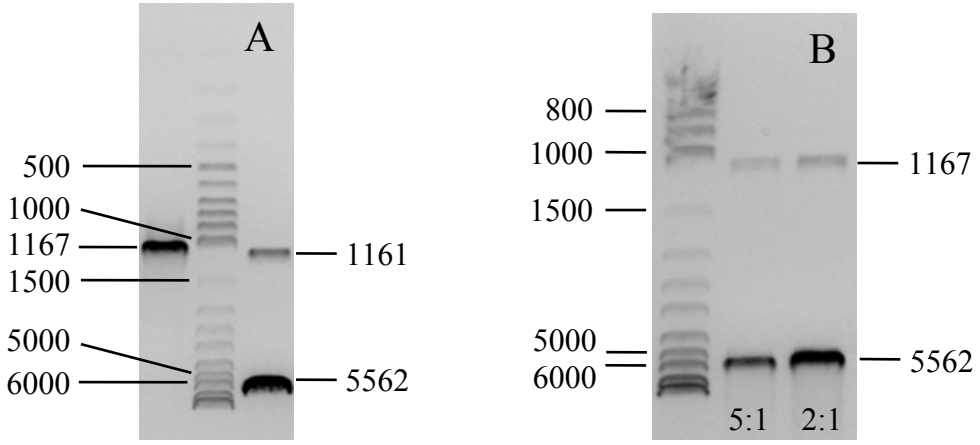

Fig. 4.2: Restriction enzyme digestion of PCR product $G\alpha_{qi9}$ and pcDNA3.1/Hygro-$G\alpha_{qi5}$ (A) and restriction enzyme analysis of minipreps (pcDNA3.1/Hygro-$G\alpha_{qi9}$) from ligation reactions with different molar ratios of insert to plasmid as indicated below lanes (B)

4.2.7 Cell culture and chemosensitivity assay

HEC-1B-hY_5 cells (Moser *et al.*, 2000) were maintained in EMEM containing NEAA, 2.2 g/l $NaHCO_3$, 110 mg/l sodium pyruvate, 10 % FCS (Biochrom, Berlin, Germany) and 400 µg/ml G418. Subculturing was performed weekly by 1:10 dilution.

For transfection pcDNA3.1/Hygro-$G\alpha_{qi5/9}$ and pcDNA3.1/Zeocin-mtAEQ were used, which encode the hygromycin and the zeocin resistence gene, respectively. The cells were tested for their sensitivity to the antibiotics, hygromycin B (MoBiTec GmbH, Göttingen, Germany) and zeocin (Cayla SAS, Toulouse, France), in a chemosensitivity assay as described in section 3.2.3. At all tested concentrations, hygromycin showed similar cytotoxicity (**Fig. 4.3 A**), so that a concentration of the antibiotic of 250 µg/ml was chosen for the selection of transfected cells. Zeocin showed cytotoxicity at a concentration of 100 µg/ml, which was used for the selection of transfectants (**Fig. 4.3 B**).

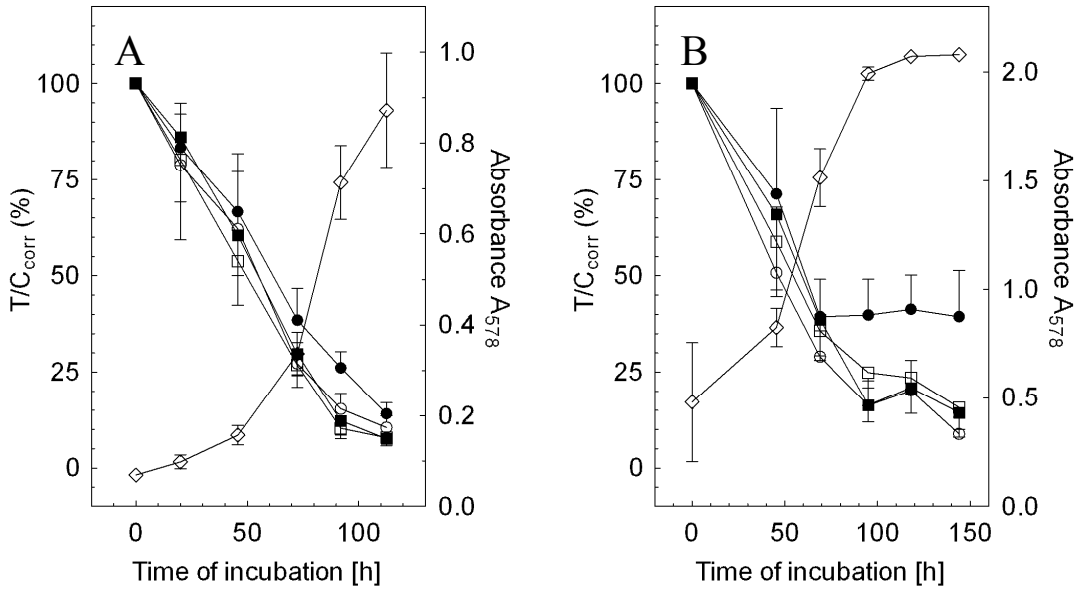

Fig. 4.3: Incubation of HEC-1B-hY_5 cells with various concentrations of hygromycin (A) and zeocin (B); Millipore water was used as negative control. A: ◊ vehicle; hygromycin concentration: ● 100 µg/ml, ○ 250 µg/ml, ■ 350 µg/ml and □ 500 µg/ml. B: ◊ vehicle; zeocin concentration: ● 50 µg/ml, ○ 100 µg/ml, ■ 200 µg/ml and □ 500 µg/ml

4.2.8 Transfection of HEC-1B-hY_5 cells with pcDNA3.1/Hygro-G$\alpha_{qi5/9}$

HEC-1B-hY_5 cells were seeded in 25-cm^2 cell culture flasks or in 24 well plates (Thermo Fisher Scientific GmbH, Bonn, Germany) and transfected with FuGENE 6 or FuGENE HD (Roche, Mannheim, Germany) according to the manufacturer's protocol and **Table 4.1**:

Table 4.1: Overview of transfection procedures for HEC-1B-hY_5 cells

Cells	Culture dish	pcDNA 3.1/Hygro-Gα_{qix}	Transfection reagent	DNA:FuGENE Ratio	Tested clone	See Fig.
HEC-1B-hY_5, 64. P	25 cm^2 flask	Gα_{qi5} 4 µg	FuGENE 6 9 µl	1 : 2.25	qi5	**4.4 – 4.6**
HEC-1B-hY_5, 119. P	24 well	Gα_{qi5} 0.4 µg	FuGENE HD 4 µl	1 : 10	H1	**4.7**
HEC-1B-hY_5, 119. P	24 well	Gα_{qi9} 0.4 µg	FuGENE HD 4 µl	1 : 10	J1	**4.7**
HEC-1B-hY_5, 29. P	24 well	Gα_{qi5} 1.5 µg	FuGENE HD 4.5 µl	1 :3	62a	**4.8**
HEC-1B-hY_5, 29. P	24 well	Gα_{qi9} 0.5 µg	FuGENE HD 4 µl	1 : 8	82	**4.8 – 4.9**

Usually, two days after transfection the culture medium was replaced with selective medium, which was exchanged every 4-5 days until the cells from control dishes had died and the colonies formed by the transfected cells were big enough for passaging. Subsequently the transfectants were tested in either flow cytometric or spectrofluorimetric calcium assays as described in the following sections.

4.2.9 Transfection of HEC-1B-hY$_5$-G$\alpha_{qi5/9}$ with pcDNA3.1/Zeo-mtAEQ

The mtAEQ cDNA was subcloned into the pcDNA3.1/Zeo vector by R. Ziemek. HEC-1B-hY$_5$-Gα_{qi5} (clone 62a) and HEC-1B-Gα_{qi9} (clone 82) cells were seeded in 24 well plates. Transfection was accomplished with 0.8 µg of plasmid DNA and 1.2 µl (clone 62a), respectively 1.8 µl (clone 82) of FuGENE 6 transfection reagent (Roche) according to the manufacturer's protocol. Transfectants were selected in the presence of 100 µg/ml zeocin and tested as described (cf. sections 4.2.8 and 4.2.12).

4.2.10 Flow cytometric calcium assay

The assay was essentially performed as described by Ziemek (2006). Cells were grown for 2-3 days to 70-90 % confluency, trypsined and EMEM 10 % FCS was added to inactivate trypsine before detaching the cells from the bottom of the flask. Afterwards cells were counted and centrifuged for 5 min at 300 g. Cell density was adjusted to $2.66 \cdot 10^6$ cells/ml in loading buffer (Gessele, 1998) containing 120 mM NaCl, 5 mM KCl, 2 mM $MgCl_2$, 1.5 mM $CaCl_2$ (all from Merck), 25 mM HEPES (Sigma) and 10 mM glucose (Merck) at pH 7.4. The dye suspension was prepared by mixing 3 µl of fluo-4-AM (Molecular Probes; 1 mM stock solution in anhydrous DMSO) with 5 µl of pluronic^{TM} F-127 (Molecular Probes; 20 % stock solution in DMSO) before the addition of 1 ml of loading buffer containing 2 % BSA (VWR International, Poole, England). 330 µl of the dye suspension were added to 1 ml of cell suspension resulting in a cell number of $2 \cdot 10^6$ cells/ml and a dye concentration of 0.7 µM.
Cells were incubated in the dark for 30 min at room temperature. After centrifugation at 300 g for 5 min and suspending of the pellet in fresh loading buffer to a density of $0.5 – 1 \cdot 10^6$ cells/ml, the cells were incubated again to enable the cleavage of the acetoxymethylester by intracellular esterases. Thereby, carboxylic groups are exposed and due to its negative charges the calcium chelator is trapped within the cells.
Measurements were performed in a purpose-built glass tube closed by a silicon septum as described (Schneider, 2005). This instrumentation allows injections into the samples during continuous flow cytometric measurements. A tube containing 1 ml of the cell suspension was

connected with a FacsCalibur™ flow cytometer (Becton Dickinson, Heidelberg, Germany) under permanent stirring, and recording was started. Instrument settings were: FSC: E-1, SSC: 280, FL-1: 350, flow: high.

During the first 30 s basal fluorescence was measured, then 10 µl of pNPY solution were injected with a Hamilton syringe, and data acquisition continued for another 90 s. Raw data were averaged with the WinMDI 2.8 software and then exported to SigmaPlot™ 11.0.1. Data were further smoothed (running average) with SigmaPlot™. The level of increase in fluorescence was calculated from the difference between the baseline (mean fluorescence of the first 25 s) and the highest value of the averaged curve. The amplitudes of the averaged signals were used to construct concentration response curves. The EC_{50} value was calculated using the equation of the four parameter logistics function.

10 µl of a tenfold solution of CGP 71638A (see structure in section 1.2.3), prepared in an equal mixture of DMSO and 10 mM HCl, was incubated with 990 µl of cell suspension for 1 min prior to measurement. Calcium response was triggered with various concentrations of pNPY as indicated in the figures in section 4.3.1.

4.2.11 Spectrofluorimetric calcium assay

The spectrofluorimetric calcium assay was performed with the ratiometric Ca^{2+} indicator fura-2 as described by Gessele (1998) for HEL cells. HEC-1B-hY5-Gα_{qix} cells were grown for 2-3 days to 70-80 % confluence, trypsinized and detached with EMEM 10 % FCS. Cells were counted, centrifuged at 300 g for 5 min and resuspended at $1.3 \cdot 10^6$ cells/ml in loading buffer. The dye suspension was prepared by mixing 4 µl of fura-2-AM (Molecular Probes; 1 mM stock solution in anhydrous DMSO) with 5 µl pluronic™ F-127 (Molecular Probes; 20 % stock solution in DMSO) before the addition of 1 ml of loading buffer containing 2 % BSA. 250 µl of the dye suspension were added to 750 µl of cell suspension resulting in a cell number of $1 \cdot 10^6$ cells/ml and a dye concentration of 1 µM. Cells were incubated for 30 min at room temperature in the dark, centrifuged at 300 g for 5 min, re-suspended in the same volume of loading buffer and incubated another 30 min at room temperature in the dark. Subsequently, the cells were washed twice with loading buffer, and the suspension was adjusted to a density of $1 \cdot 10^6$ cells/ml.

Measurements were performed in a Perkin Elmer LS 50 B spectrofluorimeter (Perkin Elmer, Überlingen, Germany) at 25 °C under continuous stirring (low). Instrument settings were: λ_{ex}: 340 nm and 380 nm (alternating) with slit: 10 nm and λ_{em}: 510 nm with slit: 10 nm.

For measurements, 1 ml of the cell suspension was transferred into disposable cuvettes containing 1 ml of loading buffer under continuous stirring. The baseline was recorded for 30 s before the agonist was added. Antagonists were incubated with the cells 30 s prior to measurement.

For the calculation of the calcium concentration the Grynkiewicz equation (Grynkiewicz *et al.*, 1985) was used:

$$[Ca^{2+}] = K_D \cdot \frac{(R - R_{min})}{(R_{max} - R)} \cdot SFB$$

Equation 4.1

Explanations:

K_D dissociation constant of fura-2-Ca^{2+} (= 225 nM)

R ratio of fluorescence intensity at 510 nm after excitation at 340 nm and 380 nm

R_{max} fluorescence ratio in presence of saturating Ca^{2+} concentration, determined by the addition of 10 µl of digitonin (2 % in water, Sigma), which caused lysis of the cells and saturation of the dye with the calcium ions of the loading buffer.

R_{min} fluorescence ratio of calcium free dye, which was achieved by the addition of 50 µl of EGTA solution (600 mM in 1 M Tris·HCl buffer, pH 8.7) to the lysed cells.

SFB correction factor; the ratio of fluorescence intensity at 510 nm after excitation at 380 nm of the Ca^{2+} free and the calcium saturated dye.

4.2.12 Aequorin assay

Cells were seeded into 25-cm^2 culture flasks and grown to 80-90 % confluency, trypsinized and adjusted to $10 \cdot 10^6$/ml in DMEM, supplemented with 1 % FCS and 2 µM coelenterazine h (Biotrend GmbH, Köln, Germany). The suspension was kept under gentle stirring in the dark for 2 h. Loading buffer (cf. section 4.2.10) was added to dilute the suspension (1:20), and the cells were incubated for another 3 h. This time period assures the complete reconstitution of the apoprotein aequorin with its cofactor colelenterazine h. 180 µl of cell suspension were pipetted per well into a white 96-well luminescence plate (Nunc, Wiesbaden, Germany). The plate was inserted into the GENios ProTM (Tecan, Salzburg, Austria) plate reader and 20 µl of 1 % triton-X-100 in loading buffer were injected per well. Upon addition of the non-ionic surfactant the cells are lysed and entering Ca^{2+} from the loading buffer triggers the oxidation of coelenterazine and thereby the emittance of light. Luminescence was recorded for 20 s in 200 ms integration steps (instrument setting: no attenuation).

4.3 Results and discussion

4.3.1 Flow cytometric calcium assay

Upon stimulation of hY_5R in HEC-1B-hY_5 cells lacking $G\alpha_{qi5}$, only small Ca^{2+} transients were recorded (at high concentrations of pNPY (100 nM); **Fig. 4.4**). This is in agreement with published results (Bischoff *et al.*, 2001). On the contrary, with $G\alpha_{qi5}$ expressing HEC-1B-hY_5 cells a robust Ca^{2+} signal was obtained in the flow cytometric fluo-4 assay (**Fig. 4.4** and **4.5**). From the amplitudes of the fluorescence signals a concentration response curve of pNPY was constructed. The calculated EC_{50} is in agreement with data from literature (Gerald *et al.*, 1996; Bischoff *et al.*, 2001; Dautzenberg *et al.*, 2005). Moreover, Ca^{2+} mobilization could be inhibited by the Y_5 receptor antagonist CGP 71683A (**Fig. 4.6**), indicating a Y_5R mediated effect.

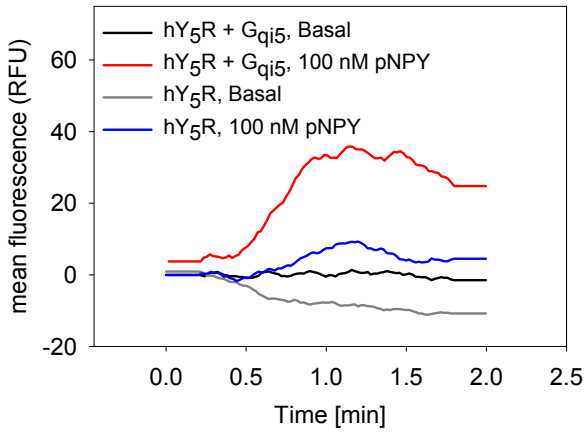

Fig. 4.4: Basal and stimulated (100 nM pNPY) fluorescence signal of Fluo-4 loaded HEC-1B-hY_5 and HEC-1B-hY_5-G_{qi5} cells

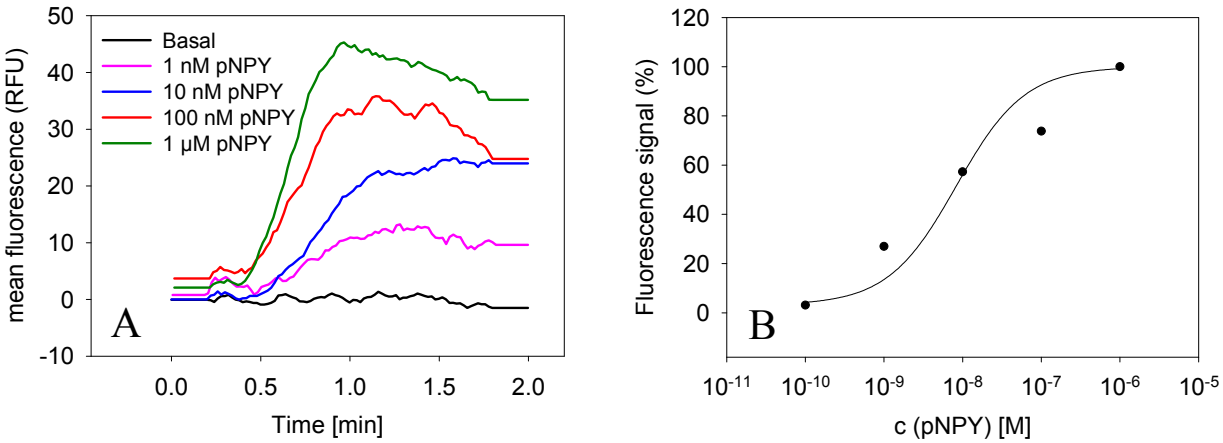

Fig. 4.5: Base line corrected fluorescence signals of Fluo-4 loaded HEC-1B-hY_5-$G\alpha_{qi5}$ cells with various concentrations of pNPY and concentration response curve of pNPY; Fluorescence was measured in the FL-1 channel of the flow cytometer. (A) The concentration response curve of pNPY (B) was constructed from the experiment shown in (A). Data were calculated from baseline corrected mean fluorescence signals related to the maximum signal with 1 µM pNPY. The determined EC_{50} value is 8.3 nM.

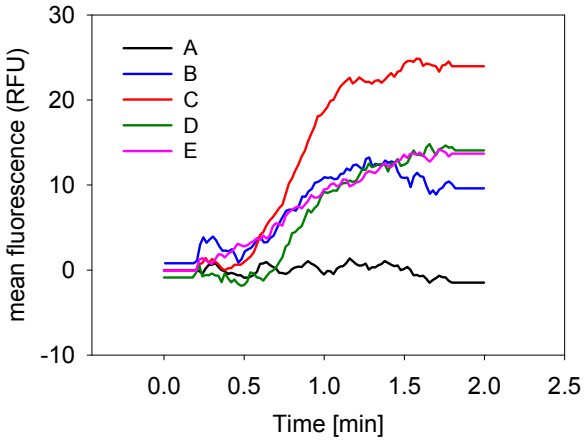

Fig. 4.6: Baseline corrected mean fluorescence signals of Fluo-4 loaded HEC-1B-hY_5-G_{qi5} cells from a flow cytometric calcium assay
A: Baseline
B: 1 nM pNPY
C: 10 nM pNPY
D: 1 nM pNPY, 100 nM CGP 71683A,
E: 10 nM pNPY, 1 µM CGP 71683A.

However, after several passages of the co-transfectants, no calcium signal was detectable (data not shown), probably because the expression of the chimeric G protein was not stable. Therefore, cells were newly transfected with $G\alpha_{qi5}$ and $G\alpha_{qi9}$, respectively. Mobilization of intracellular Ca^{2+} was mediated by both chimeric G proteins to approximately the same extent (**Fig. 4.7**). However, compared to the former experiment (**Fig. 4.5**) the amplitude of the calcium signal triggered by 100 nM pNPY was only about one-fifth (with $G\alpha_{qi5}$; **Fig. 4.7 A**) and one-fifteenth (with $G\alpha_{qi9}$, **Fig. 4.7 B**), respectively. This is presumably due to the high passage (119. P) of the HEC-1B-hY_5 cells used for the generation of the latter transfectants (**Table 4.1**), in which the expression level of the NPY Y_5 receptor was insufficient. Therefore, transfections were repeated with HEC-1B-hY_5 cells from a lower passage (29. P; **Table 4.1**).

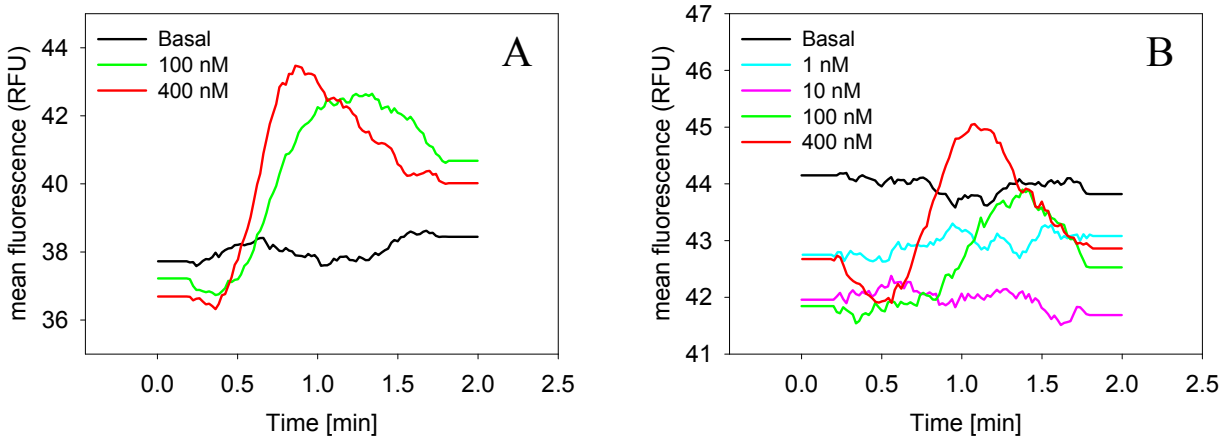

Fig. 4.7: Mean fluorescence signals of Fluo-4 loaded HEC-1B-hY_5-G_{qi5} (A) and HEC-1B-hY_5-G_{qi9} (B) cells from a flow cytometric calcium assay at varying pNPY concentrations

4.3.2 Spectrofluorimetric calcium assay

When stimulated with 1 µM pNPY, both, Fura-2 loaded HEC-1B-hY5-$G\alpha_{qi5}$ and HEC-1B-hY5-$G\alpha_{qi9}$ showed an increase in intracellular calcium by about 100 nM and 150 nM, respectively in spectrofluorimetric Ca^{2+} assays (**Fig. 4.8**). However, these Ca^{2+} transients are quite low, when compared to signals (600 nM) e.g. elicited in CHO-hY_2-$G\alpha_{qi5}$ by pNPY concentrations as low as 50 nM (Ziemek, 2006). In the absence of chimeric G proteins, hY_5R did not mediate Ca^{2+} mobilization, presumably, due to the fact that by spectrofluorimetry the mean signal of the total cell population is recorded, while the flow cytometric Fluo-4 assays allows for gating of the cells of interest.

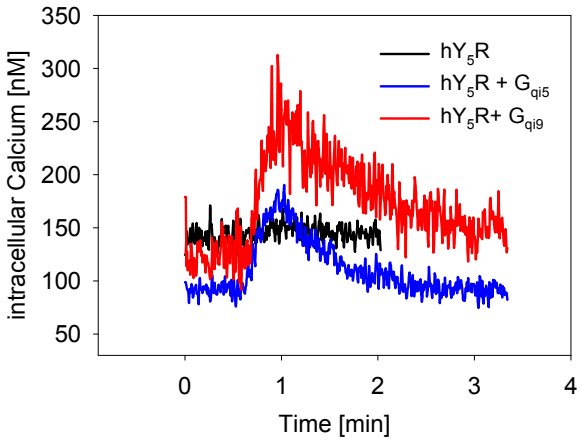

Fig. 4.8: Calcium mobilization in Fura-2 loaded HEC-1B-hY_5, HEC-1B-hY_5-G_{qi5} and HEC-1B-hY_5-G_{qi9} cells by 1 µM pNPY measured in a spectrofluorimetric calcium assay

HEC-1B-hY_5-$G\alpha_{qi9}$ cells were serially passaged over three weeks and tested for their calcium signal. As shown in **Fig. 4.9**, 1 µM pNPY elicited a robust response, however there was poor responsiveness to low concentrations of pNPY (A). Calcium signals were inhibited by the Y_5 antagonist (B).

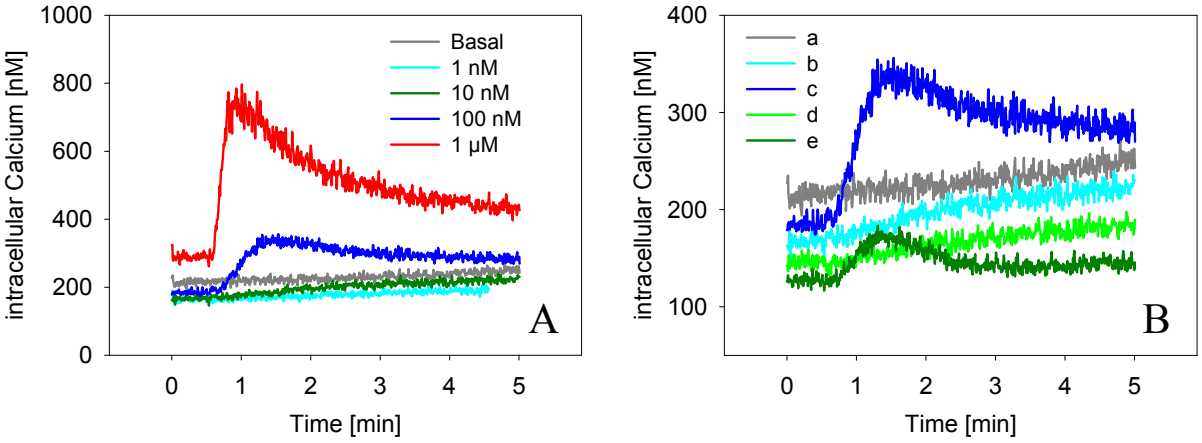

Fig. 4.9: Calcium mobilization in Fura-2 loaded HEC-1B-hY_5-G_{qi9} cells with varying pNPY concentrations in a spectrofluorimetric calcium assay (A) and in the presence of the Y_5 receptor antagonist CGP 71683A (B); a: Basal; b: 10 nM pNPY; c: 100 nM pNPY; d: 10 nM pNPY, 1 µM CGP 71683A; e: 100 nM pNPY, 1 µM CGP 71638A

4.3.3 Aequorin assay

HEC-1B-hY$_5$-Gα_{qi5}-mtAEQ and HEC-1B-hY$_5$-Gα_{qi9}-mtAEQ were tested for their expression of aequorin. Cells were loaded with the cofactor coelenterazine h to reconstitute the holoprotein. Upon injection of triton-X-100 at a final concentration of 0.1 %, the nonionic surfactant causes cell lysis, thereby allowing Ca^{2+} to enter with the loading buffer. Subsequently, if aequorin is expressed, the oxidation of the cofactor to coelenteramide takes place and luminescence occurs ($\lambda = 470$ nm). **Fig. 4.10** shows that only the cells expressing Gα_{qi9} were able to emit light, i.e. in this case the transfection was successful. In the aequorin assay triton-X-100 is used to lyse the cells after the Ca^{2+} signal, in order to determine the total luminescence within a well. Thus, by calculating fractional luminescence i.e. signal elicited by the ligand relative to total luminescence) the measurement becomes independent of variability in cell number. Regarding the fact that the testing was conducted at exactly the same conditions as the established assay, the light emitted from the HEC-1B-hY$_5$-Gα_{qi9}-mtAEQ cells corresponds to only about 4 % of the intensity of the "triton-X-signals" from CHO-hY$_{2/4}$-Gα_{qi5}-mt AEQ. Therefore, the development of such an assay was no longer pursued.

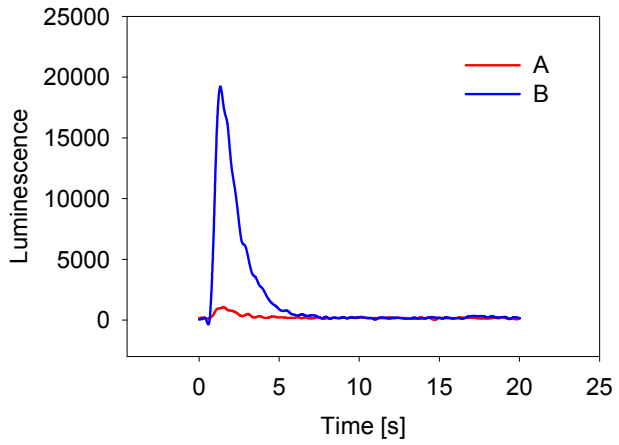

Fig. 4.10: Luminescence signal of HEC-1B-hY$_5$-Gα_{qi5}-mtAEQ (A) and HEC-1B-hY$_5$-Gα_{qi9}-mtAEQ (B) in response to 0.1 % triton-X-100

4.4 Summary and conclusions

With HEC-1B-hY_5 cells stably expressing the hY_5R a starting point was given to develop functional fluorescence- and bioluminescence-based Ca^{2+} assays. Therefore, the suitability of chimeric G proteins such as $G\alpha_{qi5}$ was investigated for their ability to redirect receptor signaling to the PLCβ pathway. By modification of a C-terminal amino acid by PCR, yielding $G\alpha_{qi9}$ a benefit effect concerning receptor coupling was expected. Initially, transfection with the chimeric G protein $G\alpha_{qi5}$ resulted in robust intracellular Ca^{2+} mobilization detected in a flow cytometric calcium assay with Fluo-4 loaded cells. The signal was receptor mediated as it could be blocked by the Y_5R selective antagonist CGP 71683A and a concentration response curve could be constructed yielding an EC_{50} in accordance with data reported in literature. Unfortunately, the expression of the chimeric G protein was not stable and the Ca^{2+} signal diminished after several passages of the cells. Further transfection experiments with $G\alpha_{qi5}$ respectively $G\alpha_{qi9}$ did not fulfil the expectations in terms of robust signals and high signal-to-noise ratios (especially regarding low pNPY concentrations) in flow cytometric (Fluo-4) or spectrofluorimetric (Fura-2) assays, irrespective of the number of passages of the parent HEC-1B-hY_5 cells. Thus, declining levels of receptor expression due to senescent cells are unlikely. Nevertheless, HEC-1B-hY_5-$G\alpha_{qi5/9}$ cells were further transfected with the pcDNA3.1/Zeo-mtAEQ to test the ability of these cells to express functionally active aequorin. Indeed, luminescence was measured, when co-transfected HEC-1B-hY_5-$G\alpha_{qi9}$ cells were treated with triton-X-100. However, compared to assays established for the hY_2R and the hY_4R this signal amounted to only about 4 % of the expected value. Nevertheless, optimizations in the generation and selection of stable HEC-1B-hY_5 transfectants might pave the way for versatile functional calcium assays.

4.5 References

Ando M, Sato N, Nagase T, Nagai K, Ishikawa S, Takahashi H, Ohtake N, Ito J, Hirayama M, Mitobe Y, Iwaasa H, Gomori A, Matsushita H, Tadano K, Fujino N, Tanaka S, Ohe T, Ishihara A, Kanatani A and Fukami T (2009) Discovery of pyridone-containing imidazolines as potent and selective inhibitors of neuropeptide Y Y_5 receptor. *Bioorg Med Chem* **17**:6106-6122.

Birnboim HC and Doly J (1979) A rapid alkaline extraction procedure for screening recombinant plasmid DNA. *Nucleic Acids Res* **7**:1513-1523.

Bischoff A, Puttmann K, Kotting A, Moser C, Buschauer A and Michel MC (2001) Limited signal transduction repertoire of human Y_5 neuropeptide Y receptors expressed in HEC-1B cells. *Peptides* **22**:387-394.

Criscione L, Rigollier P, Batzl-Hartmann C, Rueger H, Stricker-Krongrad A, Wyss P, Brunner L, Whitebread S, Yamaguchi Y, Gerald C, Heurich RO, Walker MW, Chiesi M, Schilling W, Hofbauer KG and Levens N (1998) Food intake in free-feeding and energy-deprived lean rats is mediated by the neuropeptide Y_5 receptor. *J Clin Invest* **102**:2136-2145.

Dautzenberg FM, Higelin J, Pflieger P, Neidhart W and Guba W (2005) Establishment of robust functional assays for the characterization of neuropeptide Y (NPY) receptors: identification of 3-(5-benzoyl-thiazol-2-ylamino)-benzonitrile as selective NPY type 5 receptor antagonist. *Neuropharmacology* **48**:1043-1055.

De los Frailes M and Diez E (2009) Screening technologies for G protein-coupled receptors: from HTS to uHTS. *Methods Mol Biol* **552**:15-37.

Gerald C, Walker MW, Criscione L, Gustafson EL, Batzl-Hartmann C, Smith KE, Vaysse P, Durkin MM, Laz TM, Linemeyer DL, Schaffhauser AO, Whitebread S, Hofbauer KG, Taber RI, Branchek TA and Weinshank RL (1996) A receptor subtype involved in neuropeptide-Y-induced food intake. *Nature* **382**:168-171.

Gerald C, Walker MW, Vaysse PJ, He C, Branchek TA and Weinshank RL (1995) Expression cloning and pharmacological characterization of a human hippocampal neuropeptide Y/peptide YY Y_2 receptor subtype. *Journal of Biological Chemistry* **270**:26758-26761.

Gessele K (1998) Zelluläre Testsysteme zur pharmakologischen Charakterisierung neuer Neuropeptid Y-Rezeptorantagonisten, Doctoral thesis, University of Regensburg, Germany

Grynkiewicz G, Poenie M and Tsien RY (1985) A new generation of Ca^{2+} indicators with greatly improved fluorescence properties. *J Biol Chem* **260**:3440-3450.

Kakui N, Tanaka J, Tabata Y, Asai K, Masuda N, Miyara T, Nakatani Y, Ohsawa F, Nishikawa N, Sugai M, Suzuki M, Aoki K and Kitaguchi H (2006) Pharmacological characterization and feeding-suppressive property of FMS586 [3-(5,6,7,8-tetrahydro-9-isopropyl-carbazol-3-yl)-1-methyl-1-(2-pyridin-4- yl-ethyl)-urea hydrochloride], a novel, selective, and orally active antagonist for neuropeptide Y Y_5 receptor. *J Pharmacol Exp Ther* **317**:562-570.

Kanatani A, Ishihara A, Iwaasa H, Nakamura K, Okamoto O, Hidaka M, Ito J, Fukuroda T, MacNeil DJ, Van der Ploeg LH, Ishii Y, Okabe T, Fukami T and Ihara M (2000) L-152,804: orally active and selective neuropeptide Y Y_5 receptor antagonist. *Biochem Biophys Res Commun* **272**:169-173.

Menon V, Ranganathn A, Jorgensen VH, Sabio M, Christoffersen CT, Uberti MA, Jones KA and Babu PS (2008) Development of an aequorin luminescence calcium assay for high-throughput screening using a plate reader, the LumiLux. *Assay Drug Dev Technol* **6**:787-793.

Moser C, Bernhardt G, Michel J, Schwarz H and Buschauer A (2000) Cloning and functional expression of the hNPY Y_5 receptor in human endometrial cancer (HEC-1B) cells. *Can J Physiol Pharmacol* **78**:134-142.

Sato N, Jitsuoka M, Shibata T, Hirohashi T, Nonoshita K, Moriya M, Haga Y, Sakuraba A, Ando M, Ohe T, Iwaasa H, Gomori A, Ishihara A, Kanatani A and Fukami T (2008) (9S)-9-(2-hydroxy-4,4-dimethyl-6-oxo-1-cyclohexen-1-yl)-3,3-dimethyl-2,3,4 ,9-tetrahydro-1H-xanthen-1-one, a selective and orally active neuropeptide Y Y_5 receptor antagonist. *J Med Chem* **51**:4765-4770.

Schneider E (2005) Development of Fluorescence-Based Methods for the Determination of Ligand Affinity, Selectivity and Activity at G-Protein Coupled Receptors, Doctoral thesis, University of Regensburg, Germany

Walker MW, Wolinsky TD, Jubian V, Chandrasena G, Zhong H, Huang X, Miller S, Hegde LG, Marsteller DA, Marzabadi MR, Papp M, Overstreet DH, Gerald CP and Craig DA (2009) The novel neuropeptide Y Y_5 receptor antagonist Lu AA33810 [N-[[trans-4-[(4,5-dihydro[1]benzothiepino[5,4-d]thiazol-2-yl)amino]cyclohexyl]methyl]-methanesulfonamide] exerts anxiolytic- and antidepressant-like effects in rat models of stress sensitivity. *J Pharmacol Exp Ther* **328**:900-911.

Ziemek R (2006) Development of binding and functional assays for the neuropeptide Y Y_2 and Y_4 receptors, Doctoral thesis, University of Regensburg, Germany

Chapter 5

5 Establishment of a steady-state GTPase assay for the human NPY Y_2 receptor

5.1 Introduction

5.1.1 Functional assays for the NPY Y_2 receptor

As the Y_2 receptor is known to couple to $G_{i/o}$ proteins (Michel *et al.*, 1998), initially, radiochemical assays based on the inhibition of forskolin-induced cAMP formation (Beck-Sickinger *et al.*, 1992; Goumain *et al.*, 2001) were devised. Later, assay formats more suitable for high throughput screening (HTS) were developed. For example, the need for prestimulation of the cells by forskolin was eluded by redirecting GPCR signaling to the PLC pathway via chimeric G proteins. Thus, receptor activation leads to an elevation of intracellular calcium, which is measured by Ca^{2+} chelating fluorescent probes (Dautzenberg *et al.*, 2005; Ziemek, 2006). Additionally, quantification of formation of tritiated IP_3 was applied (Berridge, 1983; Merten *et al.*, 2007) and a luminescence-based assay was developed by Ziemek (Ziemek *et al.*, 2006). Very recently, Brothers et al. (Brothers *et al.*, 2010) reported on a cAMP biosensor assay, which was applied for ligand screening at the hY_2R. For this purpose, HEK293 cells, stably expressing a cyclic nucleotide-gated channel (CNG) together with the hY_2R and a membrane potential sensitive fluorescent indicator were used to measure the polarization state of the cell membrane. Aiming at ultra HTS, complex industrial instrumentation is required, which is not ideal for laboratory research. Most of the mentioned functional assays are costly, laborious and time consuming, especially when, for example, cells have to be stably transfected, cell lines maintained at a given protein expression level or

membranes be prepared from mammalian cells, e.g. for GTPγS binding (Dautzenberg *et al.*, 2005). Given the advantages of the steady-state GTPase assay mentioned in section 1.3.3, especially regarding $G_{i/o}$ coupled receptors, the baculovirus/Sf9 cell system was exploited for the hY_2R.

5.1.2 Coupling of the NPY Y_2 receptor to $G_{i/o}$ proteins

High coupling efficiency of the GPCR to the preferred G protein should result in robust stimulation and favourable signal-to-noise ratio in a steady-state GTPase assay. According to literature G protein coupling has been investigated, both in native cells endogenously expressing hY_2Rs and in recombinant systems, giving contradictory results concerning G protein selectivity. For example, in SMS-KAN cells the hY_2R conveys signals predominantly via $G\alpha_{i3}$, but not $G\alpha_o$ (Freitag *et al.*, 1995), while a knockdown of $G\alpha_{i2}$ in renal proximal tubular cells is sufficient to abolish PYY-mediated effects (Voisin *et al.*, 1996a; Voisin *et al.*, 1996b) and purified $G\alpha_o$ protein mediates NPY effects, when infused into sensory neurons (Ewald *et al.*, 1988). The hY_2R was also reported to elevate intracellular calcium levels in transfected HEK293 cells (Gerald *et al.*, 1995). Recently, Misra et al (Misra *et al.*, 2004) co-expressed Y_1R, Y_2R, and Y_4R in smooth muscle cells and found that all three receptors preferentially coupled to $G\alpha_{i2}$, while the Y_2R and the Y_4R additionally activated $G\alpha_q$. However, coupling to $G\alpha_o$ in this cell line has not been investigated. As the hY_2R is largely expressed in the central nervous system with $G\alpha_o$ being the major neuronal G protein (Birnbaumer *et al.*, 1990), coupling of the receptor to this G protein is also of interest. Thus, in this work, the receptors were combined with the physiologically most prevalent representatives of the family of $G_{i/o}$ proteins in the Sf9 cell expression system.

5.2 Materials and Methods

5.2.1 Preparation of the SF-hY_2-His_6 construct by sequential overlap extension PCR

In order to direct the receptor towards the cell membrane the cDNA of the hY_2R was 5' terminally tagged with the cleavable signal peptide from influenza hemagglutinin flanked by the FLAG epitope, which is recognized by the M1 antibody. The sequence for the hexahistidine was attached at the C-terminus of the receptor for analytical purposes, for purification and to improve proteolytic stability. These modifications were generated by sequential overlap extension PCR in three steps (**Fig. 5.1**). In PCR 1a, the DNA sequence of the signal peptide (S) and the FLAG epitope (F) was amplified. A plasmid containing the SF sequence was used as template, the sense pGEM primer, which starts 5' of the *Sac*I site of the pGEM-3Z plasmid and an antisense primer encoding the final part of the FLAG sequence followed by the start codon of the receptor. In PCR 1b, the cDNA of the receptor was amplified using pcDNA3-hY_2 as template. PCR 1b was performed with the sense primer FLAG-hY_2R-sense encoding a C-terminal part of FLAG followed by the first 21 bp of the starting sequence for the receptor and an antisense primer 6His-hY_2-as comprising 18 bp of the C-terminal sequence of the receptor, followed by His_6, the stop codon and the *Xba*I restriction site. The two products from PCR 1a and 1b served as templates in PCR 2. The sense pGEM primer and the 6His-hY_2-as primer were used to generate the gene construct of *Sac*I restriction site followed by the signal sequence, the FLAG epitope, the hY_2R DNA, the hexahistidine tag, the stop codon and an *Xba*I restriction site.

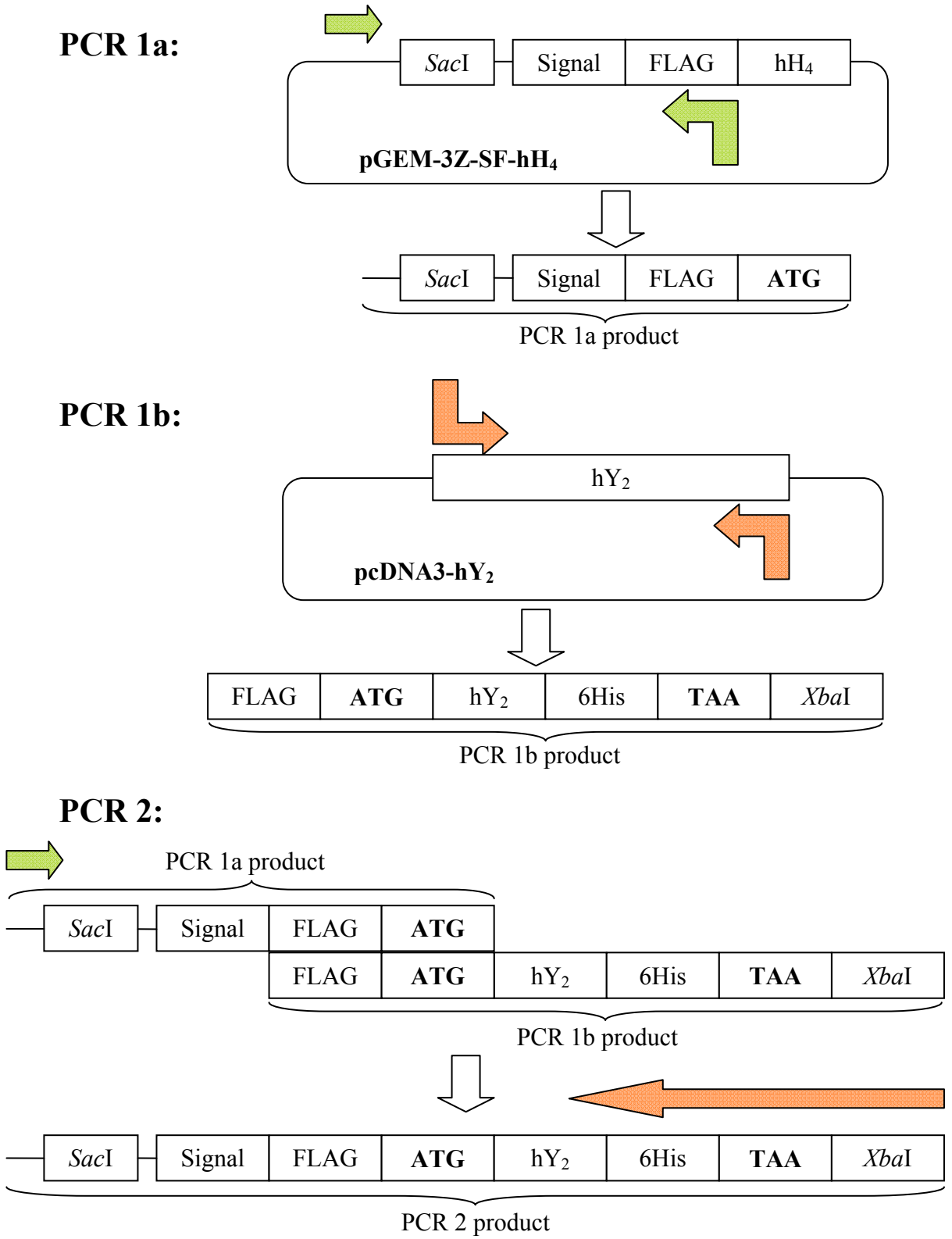

Fig. 5.1: Strategy for the construction of the insert SF-hY_2-His_6 by overlap extension PCR
Three sequential PCRs are required to tag the hY_2 receptor cDNA N-terminally with the signal and FLAG and C-terminally with the 6His sequences and to introduce the restriction sites for cloning. The template for PCR 2 are the products from the preceding PCRs annealing at the C-terminal FLAG sequence and the start codon (ATG) of the receptor. The stop codon (TAA) is shifted C-terminally behind the 6His-tag. Arrows represent primers. Angulate arrows bear the introduced sequences and do not anneal with templates in those regions. For further explanations see the text above.

5.2.1.1 PCR 1a for the hY_2R

In PCR 1a the cDNA containing the sequences for the *Sac*I restriction site and the SF followed by the start codon ATG were amplified using 100 ng of the plasmid pGEM-3Z-SF-hH_4-His_6, kindly provided by Dr. E. Schneider (Dept. of Pharmacology, University of Regensburg, Germany), as template. The primers were obtained from MWG (Ebersberg, Germany).

sense pGEM	5'-GCT CAC TCA TTA GGC ACC-3'
antisense pGEM	5'-CAT GGC GTC ATC ATC GTC-3'

All other reagents were from Fermentas Life Sciences (St. Leon-Rot, Germany), if not stated otherwise. PCR reaction mixtures contained 2.5 U of recombinant *Pfu* DNA Polymerase, 10 µl of 10x *Pfu* buffer, 3.5 mM $MgSO_4$, dNTP Mix (0.2 mM each), primers (0.5 µM each) and water up to a volume of 100 µl. PCR 1a was performed without (**Fig. 5.2 A**) or with (**Fig. 5.2 B**) 10 % DMSO to prevent annealing of template cDNA. PCR reactions were performed in a Mastercycle gradient Thermocycler (Eppendorf, Hamburg, Germany).

Cycling parameters were:

(1)	initial denaturation	95 °C, 3 min
(2)	denaturation	95 °C, 1 min
(3)	annealing	55 °C, 2 min
(4)	extension	72 °C, 2 min
(5)	final extension	72 °C, 5 min
(6)	hold	4 °C

Steps (2) to (4) were repeated 24 times.

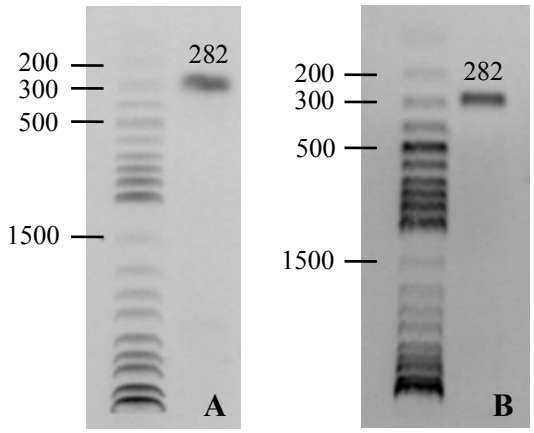

Fig. 5.2: Agarose gel electrophoresis of PCR 1a product, (A) without and (B) with DMSO 10 % in PCR reaction mixtures; Numbers indicate the sizes of bands in the DNA ladder in base pairs (bp).

The product of PCR 1a was expected to have 282 bp. As shown in the 1 % agarose gel in **Fig. 5.2** the band lies right above the 300 bp of the DNA ladder. Nucleotides and polymerase were removed and the PCR product desalted with the QIAquick PCR Purification Kit (Qiagen). The concentrations were estimated relative to the standard to 10 to 20 ng/µl (**Fig. 5.2**).

5.2.1.2 PCR 1b for the hY_2R

In PCR 1b, the cDNA of the receptor was amplified using pcDNA3-hY_2 as template. The vector pcDNA3-hY_2 was prepared by R. Ziemek (Ziemek, 2006), hY_2 sequence corresponding to the published sequence with the GenBank accession no. U32500 (Rose *et al.*, 1995). The **receptor sequence** was extended N-terminally by a part of the *FLAG* sequence and C-terminally by a hexahistidine tag followed by the shifted stop codon and the *Xba*I restriction site. These modifications were introduced via the primer pairs used at a final concentration of 0.5 µM each.

FLAG-hY_2R-sense	5'-*AAG GAC GAT GAT GAC GCC* **ATG GGT CCA ATA GGT GCA GAG**-3'
6His-hY_2-as	5'-GG TCC *TCT AGA* TTA GTG ATG GTG ATG ATG GTG **GAC ATT GGT AGC CTC TGT**-3'

Reaction mixtures were adjusted to a volume of 50 µl containing 1 U of Phusion™ High-Fidelity DNA Polymerase (New England Biolabs, Ipswich, MA) with 10 µl of either 5x Phusion™ HF buffer or 5x Phusion™ GC, dNTPs 0.2 mM each, 10 ng of template DNA, primers 0.5 µM each and DMSO 3%.

PCR reactions were conducted with a temperature gradient at 6 different temperatures as follows:

(1) initial denaturation	98 °C, 30 s
(2) denaturation	98 °C, 10 s
(3) annealing	62 °C, 30 s
(4) Gradient	10 °C, R=3 °C/s
(5) extension	72 °C, 21 s
(6) final extension	72 °C, 7 min
(7) hold	4 °C

Steps (2) to (5) were repeated 25 times.

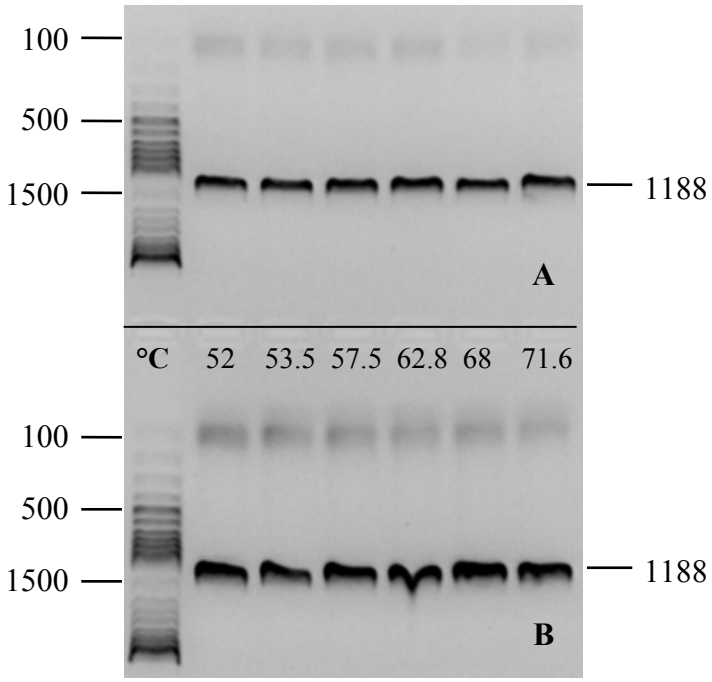

Fig. 5.3: Agarose gel electrophoresis of PCR 1b product for hY_2 performed with Phusion™ HF buffer (A) or with Phusion™ GC buffer (B) at different temperatures as indicated for each lane

Fig. 5.3 shows the expected products from PCR 1b for hY_2R at 1188 bp on a 1.5 % agarose gel. Both buffer systems, HF and GC (for GC rich DNA templates) are suitable for this PCR reaction, with the GC buffer yielding a higher amount of product. By products are found at ≈100 bp at all temperatures, however HF buffer and higher temperatures show less side bands (**Fig. 5.3 A**). All PCR preparations were pooled and purified with the QIAquick PCR Purification Kit without further separation from side products by gel electrophoresis. DNA concentration of the PCR 1b product amounted to ≈12 ng/µl (**Fig. 5.4**).

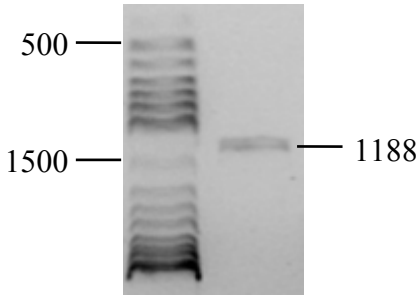

Fig. 5.4: Agarose (1.5 %) gel electrophoresis of purified PCR 1b product for the estimation of DNA concentration

5.2.1.3 PCR 2 for the hY_2R

The annealed products of PCR 1a and PCR 1b served as the template (5 or 10 ng each, cf. **Fig. 5.5**) for the amplification of the new insert SF-hY_2R-His_6 flanked by the restriction sites *Sac*I (at the 5' end) and *Xba*I (at the 3' end) in PCR 2 (cf. **Fig. 5.1**). The sense primer from PCR 1a (sense pGEM) and the antisense primer from PCR 1b (6His-hY_2-as) were used at a concentration of 0.5 µM each. All other reagents were used by analogy with 5.2.1.2 with the exception that only the 5x Phusion™ HF buffer was applied. Cycling conditions were the

same as for PCR 1b, but reactions were performed only at the four highest temperatures as indicated at the bottom of each lane in **Fig. 5.5**.

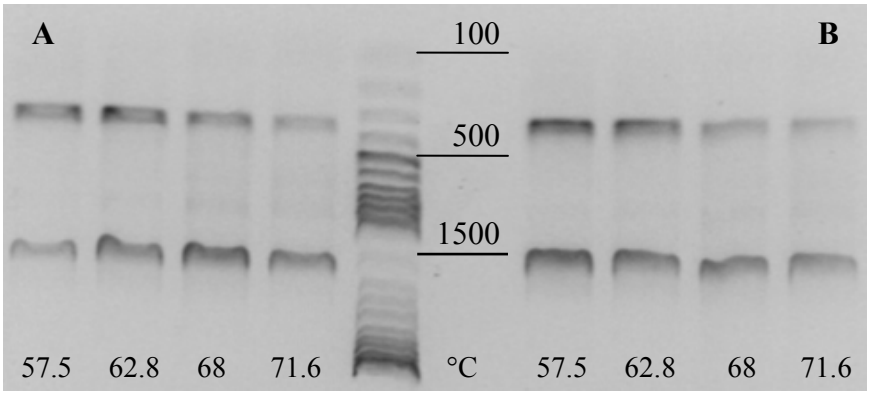

Fig. 5.5: Agarose gel electrophoresis of the products from PCR 2 with 5 ng of template DNA (A) and 10 ng of template DNA (B); Annealing temperatures are indicated at the bottom of each lane.

Agarose gel (1.5 %) electrophoresis showed comparable results for all conditions (**Fig. 5.5**). Expected bands with the size of 1454 bp were present in all PCR preparations, the same holds for side products of ≈350 bp. All products were pooled and purified with the QIAquick PCR Purification Kit. The DNA concentration of the insert SF-hY_2-His_6, (ca. 10 ng/µl) was estimated from the intensities of the bands relative to the DNA standard.

5.2.2 Subcloning of SF-hY_2-His_6 into pGEM-3Z

The SF-hY_2R-His_6 fragment was subcloned into a pGEM-3Z plasmid containing the restriction sites *Sac*I and *Xba*I in its multiple cloning site. After transformation and amplification in *E. coli* Top10 cells, the fragment from pGEM-3Z-SF-hY_2R-His_6 was subcloned into a baculovirus expression vector pVL1392 containing the same restriction sites in its multiple cloning site (see 5.2.3).

500 ng of the previously prepared pGEM-3Z-SF-hY_4-His_6 plasmid were digested with 10 U of *Sac*I (MBI Fermentas, St. Leon Rot, Germany) and 10 U of *Xba*I (MBI Fermentas) in a reaction mixture containing 2 µl of 10x Tango™ buffer (MBI Fermentas) in a final volume of 20 µl for 2 h at 37 °C. To prevent self ligation the plasmid was dephosphorylated by incubation with 0.04 U of calf intestinal phosphorylase (CIP, Boehringer Mannheim, Mannheim, Germany) for 1 h at 37 °C. Subsequently, CIP was inactivated by heating at 80 °C for 20 min. The eluate from PCR 2 obtained with the QIAquick PCR Purification Kit (~ 348 ng) was digested with *Sac*I and *Xba*I (10 U each) in 1x Tango™ buffer for 2 h at 37

°C. Thereafter, the digested DNA fragments were separated by agarose gel electrophoresis, and DNA was estimated by comparing the intensities of DNA fragments with those from bands in the DNA ladder of approximately the same size.

After extraction from the gel, ligation was performed with a tenfold molar excess of SF-hY_2-His_6 in a reaction mixture containing 5 U of T4 DNA Ligase (MBI Fermentas) and 1x Ligation buffer (MBI Fermentas) at room temperature overnight. The next day the sample was used for transformation.

Mini-Preps were prepared with colonies picked from ampicillin containing agar plates and plasmid DNA was analyzed by restriction enzyme digestion with *Sac*I and *Xba*I. A positive clone was chosen for Maxi-Prep. After double digestion with the same enzymes, expected bands were found in gel electrophoresis (insert 1293 bp and plasmide 2734 bp, **Fig. 5.6**). Sequencing with the SP6 and the T7 standard primers revealed a conservative mutation (A vs. G, in position 42 from the start codon) in the signal peptide sequence.

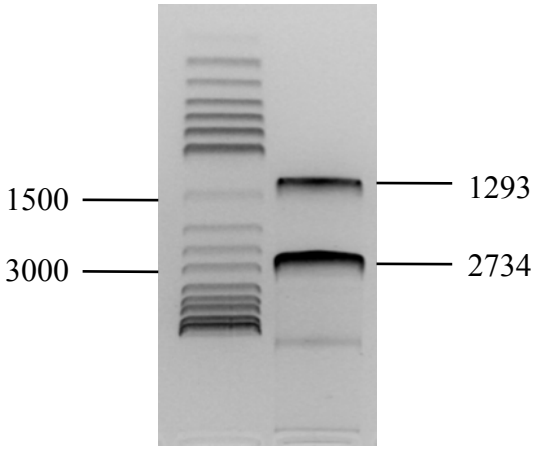

Fig. 5.6: Restriction analysis of the Maxiprep of pGEM3Z-SF-hY_2-His_6 with *Sac*I and *Xba*I; The insert (1293 bp) and the linearized plasmid (2734 bp) were found to have the correct sizes.

5.2.3 Subcloning of SF-hY_2-His_6 into pVL1392

Subcloning of the construct into the pVL-1392 vector was essentially carried out as described in 5.2.2. The insert was excised from the plasmid pGEM-3Z-SF-hY_2-His_6 with *Sac*I and *Xba*I. The previously prepared pVL-1392-SF-hY_4-His_6 was digested in the same way and dephosphorylated with 0.02 U of CIP. Ligation was performed at five-, ten- and twentyfold molar excess of insert to plasmid, and used for transformation. Minipreps were assessed for the existence of the *Xho*I restriction site, which is important for the following homologous recombination of the pVL1392 vector with the baculovirus DNA to form intact baculoviruses (section 1.3.3). For this purpose, plasmid preparations were double digested with *Xba*I and *Xho*I to yield fragments of 3535 bp and 7425 bp (**Fig. 5.7**). After Maxiprep with clone 52 the same silent mutation A42G (counted from the ATG of the signal peptide) as in the insert in pGEM-3Z was detected by sequencing.

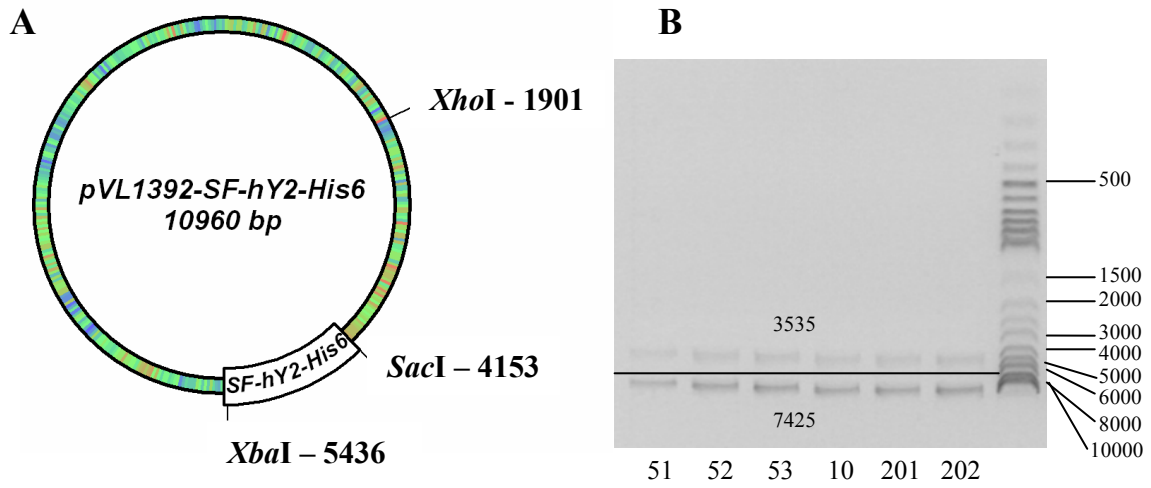

Fig. 5.7: Vector map of pVL1392-SF-hY_2-His_6 with given restriction sites *Xho*I, *Sac*I and *Xba*I (A) and restriction enzyme digestion of the Minipreps from the different ligation samples (numbers of clones given below each lane) with *Xho*I and *Xba*I (B)

5.2.4 Sf9 cell culture

Sf9 cells were cultured in SF 900 II medium (Invitrogen, Carlsbad, USA), supplemented with fetal calf serum (Biochrom, Berlin, Germany) to 5 % (v/v) and gentamicin sulfate (0.1 mg/ml, Cambrex Bio Science, Walkersville, MD) in 250 ml disposable Erlenmeyer flasks at 28 °C at 125 rpm in an incubation shaker (New Brunswick Scientific, model C24KC, Edison, NJ). Sf9 cells were maintained at a density of 0.5 to 6.0 · 10^6 cells/ml.

5.2.5 Generation of recombinant baculoviruses

Recombinant baculoviruses, encoding the FLAG- and hexahistidine-tagged hY_2 and hY_4 receptors, were generated using the BaculoGOLD transfection kit (PharMingen, San Diego, CA) according to the manufacturer's protocol. Briefly, Sf9 cells (3 ml) were seeded in 25 cm^2 culture flasks at a density of 1.3 · 10^6 cells/ml and were allowed to attach. For initial transfection, 5 µg of pVL-DNA were mixed with 0.45 µg of baculovirus DNA and added to the cells followed by an incubation of 4 h at 28 °C. Thereafter, transfection buffer was removed by suction, cells were washed and incubated in fresh medium (3 ml) for 7 days at 28 °C. To obtain high-titer virus stocks 1 ml of the supernatant (after centrifugation under sterile conditions) was used to infect Sf9 cells suspended in 50 ml medium in a 125 ml Erlenmeyer flask and the culture was incubated one week at 28 °C and 125 rpm. As a control for infectious viruses, 3 ml of this culture were transferred into a 25 cm^2 flask and kept at

28 °C in parallel. After one week of incubation, the release of baculoviruses in the 25 cm^2 control flask was confirmed microscopically, becoming obvious by the lysis of the cells. The cell debris was removed by centrifugation in a sterile 50 ml Falcon tube at 1,500 g and the supernatant (first amplification) was kept protected from light at 4 °C. In a second amplification step, cells seeded at $3.0 \cdot 10^6$ cells/ml in a 100 ml culture (250 ml Erlenmeyer flask) were infected with 5 ml of the supernatant from the first amplification and incubated for 48 h. The supernatant was harvested under sterile conditions and kept under protection from light at 4 °C. After the 48 h culture period, cells showed signs of infection (e.g. altered morphology, viral inclusion bodies) but most of them were still intact. For membrane preparation this high-titer virus stock was used to infect Sf9 cells at a ratio of 1:100.

Baculoviruses $G\alpha_{i1}$, $G\alpha_{i2}$ and $G\alpha_{i3}$ were gifts from Dr. A. G. Gilman (Dept. of Pharmacology, University of Southwestern Medical Center, Dallas, TX), whereas baculovirus encoding rat $G\alpha_{o1}$ was donated by Dr. J. C. Garrison (University of Virginia, Charlottesville, VA). Recombinant baculovirus encoding the $G\beta_1\gamma_2$ subunits was a kind gift of Dr. P. Gierschik (Dept. of Pharmacology and Toxicology, University of Ulm, Germany). Baculoviruses encoding RGS4 and GAIP were a kind gift from Dr. E. Ross (University of Texas Southwestern Medical Center, Dallas, TX).

5.2.6 Membrane preparation and determination of protein concentration

For membrane preparation buffers were prepared from following stock solutions which were pH adjusted, sterile filtered and stored at 4 °C or -20 °C (in case of protease inhibitors) until use:

10x PBS: 27 mM KCl, 15 mM KH_2PO_4, 81 mM Na_2HPO_4 and 1.37 M NaCl (all chemicals from Merck, Darmstadt, Germany) at pH 7.4 in millipore water

1 M Tris·HCl (usb, Staufen, Germany) adjusted to pH 7.4

0.5 M EDTA (Merck) adjusted to pH 7.4

Protease inhibitors: benzamide (Sigma, Deisenhofen, Germany) and leupeptin (Merck) 1 mg/ml in millipore water and PMSF 200 mM in isopropyl alcohol, all stored at -20 °C.

10x binding buffer: 750 mM Tris base (usb), 10 mM EDTA (Merck) and 125 mM $MgCl_2$ (Merck) adjusted to pH 7.4.

On the day of membrane preparation the following buffers were prepared:

PBS buffer

Lysis buffer: 10 mM Tris·HCl , 1 mM EDTA, 10 µg/ml benzamide , 10 µg/ml leupeptin and 200 µM PMSF.

Binding buffer.

For membrane sets 30 ml culture of $3.0 \cdot 10^6$ cells/ml in fresh medium were infected 1:100 with up to four different high-titer virus stocks, to combine receptors with G proteins and RGS proteins (cf. section 5.3.1) in 100 ml disposable Erlenmeyer flasks. All membrane preparation steps were conducted at 4 °C or on ice in 50 ml Falcon tubes. After incubation for 48 h, Sf9 cells were checked for signs of infection and harvested by centrifugation at 170 g for 10 min. The cells were re-suspended in the same volume of PBS with disposable 3 ml PE Pasteur pipettes (VWR, Darmstadt, Germany) and centrifuged again. The pellet was suspended in 10 ml of lysis buffer and cells were homogenised in a 15 ml Dounce homogenizer with 25 strokes. After 5 min centrifugation at 45 g, the loose pellet contained nuclei and residual cells. The supernatant with the membranes was carefully pipetted into a Sorvall tube. Membranes were spun down at 38,500 g for 20 min in a Sorvall RC-5B centrifuge, resuspended in fresh lysis buffer and the centrifugation step was repeated. After discarding the supernatant, the membrane pellet was suspended in 15 ml of binding buffer and homogenized with a 20 ml syringe equipped with a 0.9 mm (i. d.) cannula by 15 strokes. The membrane suspension was aliquoted into 15 tubes (1 ml each) and stored at -80 °C until use.

To study the effect of N-glycosylation on receptor structure and function, membranes were prepared from infected Sf9 cells grown in the absence and presence of tunicamycin (Sigma), an inhibitor of the GlcNAc-1P-transferase, at a final concentration of 10 µg/ml. The stock solution of tunicamycin (5 mg/ml) was prepared in 10 mM NaOH and stored at -20 °C until use.

To simulate the conditions of the steady-state GTPase assay, samples were frozen and thawn before using the Lowry based DC Protein Assay kit (BioRad, München, Germany) according to the manufacturer's instructions.

5.2.7 SDS Page and immunoblot analysis

Twofold concentrated sample buffer was prepared by dissolving 28.8 g of urea (Merck) in 20 ml of millipore water under heating. The solution was let to cool down to room temperature, and SDS (1.5 g, Sigma), DTT (1.8 g), 1.5 ml of Tris·HCl, pH 8.0 (1 M), 6.0 ml of glycerol (50 %, Merck) and 6.0 mg of bromphenol blue (Sigma) were added and dissolved. The sample buffer was aliquoted in 1.5 ml tubes and stored at -20 °C until use.

For SDS-PAGE membranes were thawn and centrifuged at 16,100 g and 4 °C for 10 min. The pellets were homogenized with a syringe (equipped with a 0.4 mm cannula) by 30 strokes in a volume of 10 mM Tris (pH 8.0) to a final protein concentration of 2 µg/µl. Subsequently, the equal volume of twofold concentrated sample buffer was added and mixed with the syringe by 3 strokes. Samples were stored at -80 °C.

For polyacrylamide gels and Western blotting buffers were prepared as follows:

Buffer A: 1.5 M Tris·HCl (pH 8.8) and 0.4 % (w/v) SDS

Buffer B: 0.5 M Tris·HCl (pH 6.8) and 0.4 % (w/v) SDS

APS 10 %: 1 g of ammonium peroxodisulfate (APS, Serva, Heidelberg, Germany) in 10 ml of millipore water, aliquoted to volumes of 100 µl each and stored at -20 °C

10x running buffer: 30 g of Tris base, 144 g of glycine (Merck) and 10 g of SDS were dissolved in 1000 ml of millipore water, pH was adjusted to 8.3 with concentrated HCl

Blotting buffer (always prepared freshly before use): 14 g of glycine and 3 g of Tris base were dissolved in 800 ml millipore water and mixed with 200 ml of methanol

10x TBS buffer (pH 7.6): 80 g of NaCl (VWR International, Haasrode, Belgium) were dissolved in 200 ml of Tris·HCl (1 M, pH 7.6) and millipore water to a volume of 1000 ml. The buffer was diluted 1:10 and 1000 µl/l of Tween 20 (Carl Roth GmbH, Karlsruhe, Germany) was added before use (TBS-T buffer).

5 % fat-free milk (always prepared freshly before use): 5 g of fat-free milk powder were dissolved in TBS-T buffer.

12 % separation gel mixtures contained 4.4 ml of millipore water, 4 ml of buffer A, 1.06 ml of glycerol (50 %) and 6.4 ml of acrylamide/bisacrylamide (30 % solution, acrylamide/bis-acrylamide = 29/1, Sigma) calculated for 2 gels. Polymerization was started by addition of 6.7 µL of N,N,N',N'-tetramethylethylenediamine (TEMED, Serva) and 66.7 µL of APS (10 %). The mixture was filled into gel chambers (10 x 10 x 0.8 cm) and covered with a layer of water-saturated isobutyl alcohol (Merck). After 45 min the gel was completely polymerized and the stacking gel was pipetted on top of the separation gel after the isobutyl alcohol had been washed away with water. Stacking gel (3 %) mixtures contained 6.5 - of millipore water, 2.5 ml of buffer B and 1 ml of acrylamide/bisacrylamide (30 %, see above). Polymerization was initiated by addition of 6.7 µL of TEMED and 100 µL of APS (10 %).

After loading the gel pockets with samples (10 µl) or 10 µl of the Prestained Protein Molecular Weight Marker #SM0441 (MBI Fermentas), , electrophoresis was performed in a PerfectBlue™ Double gel system Twin S (Peqlab, Erlangen, Germany) at 150 V for 1 – 1.5 h with the electrode chambers filled with running buffer.

Western blotting was achieved in a Perfect-Blue "Semi-Dry" electro blot apparatus (Peqlab) by placing the gels on top of a nitrocellulose membrane (0.2 μm, Peqlab) between 6 filter slides equilibrated in blotting buffer and blotted for 45 min at 250 mA. Then, the membrane was blocked by shaking for 2 h in fat-free milk (5 %). The membrane was washed twice for 5 - 10 min with TBS-T buffer and then incubated overnight with the primary antibody in a 50 ml Falcon tube under rotation (4 rpm). Primary antibodies were diluted (see **Table 5.1**) with TBS-T buffer containing 3 % BSA (VWR International) and 0.05 % sodium azide (Merck). The dilutions were kept at 4 °C and re-used (usually one year). The next day, membranes were washed three times for 15 min with TBS-T buffer and subsequently incubated with the secondary antibody for 1 h at room temperature. The secondary antibody, conjugated with horseradish peroxidase (see **Table 5.1**), was freshly diluted with fat-free milk (5 %). Then, washing was repeated and immunoreactive bands were visualized by enhanced chemoluminescence with the Pierce® ECL Western blotting substrate (Thermo Fisher Scientific, Bonn, Germany) according to the manufacturer's protocol.

Table 5.1: Overview of antibodies used for Western blot analysis of Sf9 membranes

Primary antibody	Dilution	Secondary antibody	Dilution
M1 (= anti-FLAG)[1]	1 : 1,000	Anti-mouse (goat)[1]	1 : 2,000
Anti-$G\alpha_{common}$ (AS 398/9)[2]	1 : 500	Anti-rabbit (donkey)[5]	1 : 10,000
Anti-$G\alpha_{i1/2}$[3]	1 : 1,000	Anti-rabbit[5]	1 : 10,000
Anti-$G\alpha_{o}$[3]	1 : 1,000	Anti-rabbit[5]	1 : 10,000
Anti-$G\beta_{common}$ (AS 266)[2]	1 : 1,200	Anti-rabbit[5]	1 : 10,000
Anti-RGS4[4]	1 : 500	Anti-goat (donkey)[5]	1 : 5,000
Anti-GAIP[4]	1 : 500	Anti-goat[5]	1 : 5,000

[1]from Sigma (Taufkirchen, Germany), [2]kindly provided by Dr. B. Nürnberg (Dept. of Biochemistry, University of Düsseldorf, Germany), [3]from Calbiochem (Bad Soden, Germany), [4]from Santa Cruz Biotechnology (Heidelberg, Germany), [5]from Amersham Biosciences (München, Germany).

The immunoblots were scanned with a calibrated GS-710 imaging densitometer (Bio-Rad Laboratories, München, Germany). Quantity One 4.0.3 software (Bio-Rad) was used for the analysis of band intensities.

For the estimation of receptor and G protein expression levels a standard Sf9 membrane, containing the FLAG-tagged human β_2-adrenoreceptor (FLAG-hβ_2-AR), and purified $G\alpha_{i2}$- and $G\alpha_{o2}$ proteins were used at appropriate dilutions. The standard membrane expressing 7.5 pmol/mg FLAG-hβ_2-AR was kindly provided by the institute of pharmacology, University of Regensburg. The expression level was determined by radioligand binding with [^{3}H]-dihydroalprenolol.

5.2.8 Y_2 receptor antagonists

The Y_2 receptor antagonists BIIE 0246 (**1**) and the structural analogs **2-5** were synthesized in our work group by A. Brennauer and were used as solutions in DMSO 50 %.

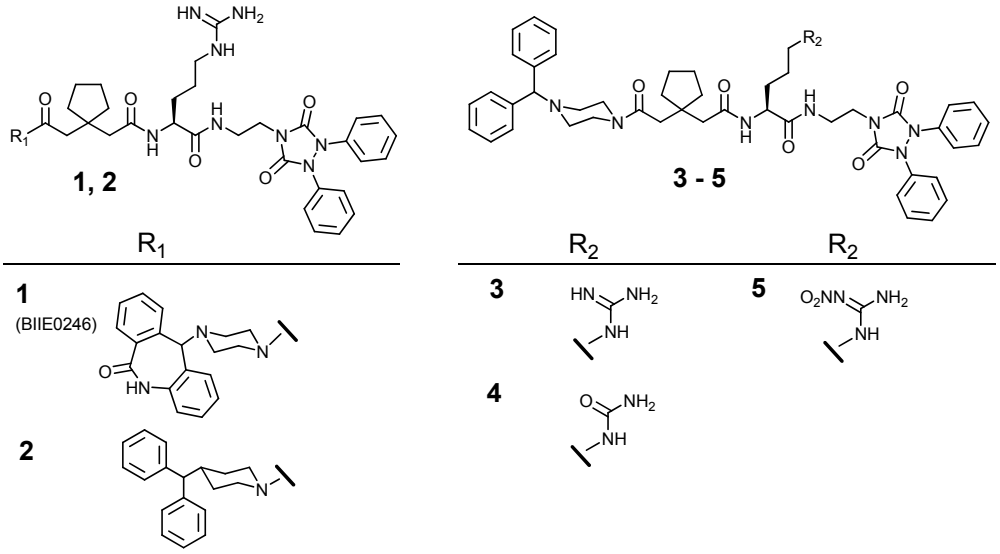

Fig. 5.8: Y_2 receptor antagonists used for GTPase assay validation

5.2.9 Steady-state GTPase assay

[γ-^{32}P]-GTP was prepared in our laboratory using GDP and [^{32}P]-orthophosphoric acid (150 mCi/ml, obtained from PerkinElmer, Pfaffenhofen, Germany) according to a previously described enzymatic labelling procedure (Walseth and Johnson, 1979).

Stock solutions and reagents for the steady-state GTPase assay were prepared as follows:

10 mM Tris·HCl (pH 7.4)

20 mM Tris·HCl (pH 7.4)

1 M Tris·HCl (pH 7.4), sterile filtered

10 mM EDTA (pH 7.4)

100 mM $MgCl_2$

10 mM adenosine triphosphate (ATP, Roche, Mannheim, Germany): aliquoted to 1 ml and stored at –20 °C

10 µM guanosine triphosphate (GTP, Roche): aliquoted to 1 ml and stored at –20 °C

10 mM adenylyl imidodiphosphate (AppNHp, Roche): aliquoted to 1 ml and stored at –20 °C

6.7 % (w/v) bovine serum albumin (BSA, VWR International)

Creatinin kinase / creatine phosphate (CK, Sigma / CP, Roche): 1 mg CK, 30 mg CP and 15 µl of BSA 6.7% ad 1000 µl with millipore water

Slurry: 50 g of activated charcoal (Merck) and 50 ml of 1 M NaH_2PO_4 (pH 2; Merck) ad 1000 ml with millipore water, stored at 4 °C

If not stated otherwise, stocks were stored at room temperature.

Steady-state GTPase assays were performed for hY_2R and hY_4R in analogy. Following descriptions relate to both receptors, differences are indicated.

For experiments regarding sensitivity of $hY_{2/4}Rs$ towards monovalent salts (cf. sections 5.3.3 and 6.3.3) a dilution series of 20x concentrated salt solutions were prepared out of freshly prepared 3 M stocks of LiCl, LiBr, LiI, NaCl, NaBr, NaI, KCl, KBr, KI (salts obtained from Merck or Fluka).

Steady-state GTPase assays were essentially performed as previously described (Preuss *et al.*, 2007).

Briefly, 10 µl of 10x concentrated ligand dilution or solvent were pipetted into assay tubes. For experiments regarding sensitivity of $hY_{2/4}Rs$ towards monovalent salts (cf. sections 5.3.3 and 6.3.3), 20x concentrated ligand and salt solutions (5 µl each) were applied, respectively. Then, reaction mixture containing 100 mM Tris·HCl, 200 µM EDTA, 2 mM $MgCl_2$, 200 µM ATP, 200 nM GTP, 200 µM AppNHp, 0.4 % BSA, 2 µg of CK and 2.4 mM CP was prepared from stock solutions and pipetted 50 µl per assay tube. For experiments run in the antagonist mode, the reaction mixture additionally contained 100 nM pNPY (for hY_2R) or 100 nM hPP (for hY_4R). Membranes were thawn, sedimented by centrifugation at 16,100 g at 4 °C and sequentially homogenized with syringes, equipped with hollow needles of 0.7 and 0.4 mm i. d., respectively, in 10 mM Tris·HCl, pH 7.4. The membrane suspension was then pipetted 20 µl/tube (i.e. usually 10 µg protein/tube).

[γ-^{32}P]-GTP (calculated as 0.1 µCi/tube) was added to 20 mM Tris·HCl (the volume calculated as 20 µl/tube) and stored on ice. Then, assay tubes were pre-incubated for 2 min each in a heating unit. Reactions were started by addition of [γ-^{32}P]-GTP (20 µl/tube) and proceeded for 20 min at 25 - 27 °C, until 900 µl of slurry was pipetted for termination. Nucleotides are adsorbed to charcoal, but not $^{32}P_i$. After centrifugation of the samples at 16,100 g and 4 °C, 600 µl of the supernatant were transferred into scintillation vials filled with 3 ml of water, and Cherenkov radiation was measured in a TRI-CARB 2800 TR liquid scintillation analyzer (PerkinElmer, Rodgau, Germany).

To consider spontaneous hydrolysis of [γ-^{32}P]-GTP, samples containing an excess of GTP (1 mM) instead of ligand were incubated in parallel. GTP competes with the binding of

[γ-^{32}P]-GTP and thereby inhibits the enzymatic degradation of the labeled nucleotide by G proteins. Spontaneous hydrolysis (blank) amounted to < 1 %. The chosen conditions ensured that no more than 10 % of the total amount added of [γ-^{32}P]-GTP was consumed.
GTPase activities (as pmol P_i released per mg of protein per minute) of membranes were calculated according to the following equation:

$$GTPase\ activty = \frac{(cpm\ reaction - cpm\ blank) \cdot pmol\ unlabeled\ GTP \cdot 1.67}{cpm\ total \cdot mg\ \ protein \cdot \min\ incubation} \left[pmol \cdot mg^{-1} \cdot \min^{-1}\right]$$

Equation 1

Explanations:

cpm reaction	radioactivity counted in 600 µl of samples except those with 1 mM unlabeled GTP
cpm blank	radioactivity counted in 600 µl of samples containing 1 mM unlabeled GTP; spontaneous hydrolysis of [γ-^{32}P]-GTP
pmol unlabeled GTP	absolute amount of GTP present in the assay tubes, i.e. 10 pmol
1.67	factor accounting for the fact that only 600 µl of the 1000 µl samples were counted
cpm total	counts resulting from total [γ-^{32}P]-GTP added to each tube (no charcoal addition)
mg protein	amount of membrane protein present in each tube (usually 0.01 or 0.02 mg)
min incubation	incubation period (duration of the enzymatic reaction, usually 20 min)

5.3 Results and Discussion

5.3.1 Immunoblot analysis of membranes

In order to study the G protein specificity of the hY_2 receptor, two identical batches of a set of 16 membranes were prepared comprising different combinations of the GPCR (hY_2R) with different $G\alpha_{i/o}$ proteins and RGS proteins. $G\alpha$ subunits were always co-expressed with $G\beta_1\gamma_2$. To keep protein expression approximately at the same level, the individual sets were prepared on the same day. An overview of such a set of membranes is given in **Table 5.2**.

Table 5.2: Overview of the set of membranes generated for the hY_2R (SF-hY_2-His_6)

Membrane preparation	Receptor	Gα	Gβγ	RGS protein	Protein [µg/ml]
B27	SF-hY_2-His_6	$G\alpha_{i1}$	$G\beta_1\gamma_2$	-	472 ± 48
B28	SF-hY_2-His_6	$G\alpha_{i1}$	$G\beta_1\gamma_2$	RGS 4	604 ± 25
B29	SF-hY_2-His_6	$G\alpha_{i1}$	$G\beta_1\gamma_2$	GAIP	592 ± 10
B30	SF-hY_2-His_6	$G\alpha_{i2}$	$G\beta_1\gamma_2$	-	559 ± 26
B31	SF-hY_2-His_6	$G\alpha_{i2}$	$G\beta_1\gamma_2$	RGS 4	515 ± 9
B32	SF-hY_2-His_6	$G\alpha_{i2}$	$G\beta_1\gamma_2$	GAIP	559 ± 26
B33	SF-hY_2-His_6	$G\alpha_{i3}$	$G\beta_1\gamma_2$	-	582 ± 10
B34	SF-hY_2-His_6	$G\alpha_{i3}$	$G\beta_1\gamma_2$	RGS 4	534 ± 31
B35	SF-hY_2-His_6	$G\alpha_{i3}$	$G\beta_1\gamma_2$	GAIP	549 ± 28
B36	SF-hY_2-His_6	$G\alpha_{o1}$	$G\beta_1\gamma_2$	-	599 ± 12
B37	SF-hY_2-His_6	$G\alpha_{o1}$	$G\beta_1\gamma_2$	RGS 4	354 ± 13
B38	SF-hY_2-His_6	$G\alpha_{o1}$	$G\beta_1\gamma_2$	GAIP	210 ± 9
B39	SF-hY_2-His_6	-	-	-	330 ± 4
B40	SF-hY_2-His_6	-	-	RGS 4	417 ± 55
B41	SF-hY_2-His_6	-	-	GAIP	465 ± 17
B42	-	$G\alpha_{i2}$	$G\beta_1\gamma_2$	-	750 ± 9

Membranes were analyzed by immunoblotting with the antibodies listed in **Table 5.1**. Receptor expression was confirmed with the M1 antibody, which recognizes the FLAG epitope of the tagged hY_2R at its extracellular N-terminus. The predicted molecular weight of the hY_2R is ≈43 kDa. Somewhat diffuse bands (**Fig. 5.9 A**) were found at ≈50 kDa, probably due to differently glycosylated forms of the receptor, which possesses one potential extracellular N-glycosylation site in its N-terminus.

Using the anti-$G\alpha_{common}$ antibody, only the membranes expressing mammalian Gα proteins showed bands at the expected molecular weight ≈40 kDa. However, no bands within this range were visible for $G\alpha_{i1}$ expressing membranes (B27 – B29) (**Fig. 5.9 B**). When reacted with the more selective antibody anti-$G\alpha_{i1/2}$ only very slight bands for $G\alpha_{i1}$ appeared (**Fig. 5.9 C**). Using the anti-$G\alpha_o$ antibody bands were only detected with the membranes B36 – B38 (**Fig. 5.9 D**). In studies by Kleemann et al. (2008) and Schnell et al (2010) the authors observed a lower expression level for $G\alpha_{i1}$, when compared to other mammalian G proteins of the $G\alpha_{i/o}$ family. This is an intrinsic property of $G\alpha_{i1}$ heterologously expressed in Sf9 cells (cf. section 6.3.2) and does not affect its ability to interact effectively with GPCRs (Kleemann *et al.*, 2008), which is also shown in sections 5.3.2 and 6.3.3. With the anti-$G\beta_{common}$ antibody - as expected - bands at ≈37 kDa became obvious (**Fig. 5.9 E**) and RGS proteins in RGS4 and

GAIP expressing membranes are seen at somewhat higher molecular weights ≈30 kDa than expected (≈ 23 – 24 kDa, **Fig. 5.9 F-G**). The varying protein expression levels among the membranes were probably due to handling during preparation, determination of protein concentration or pipetting into gel pockets. The results for the second set of membranes were identical (not shown).

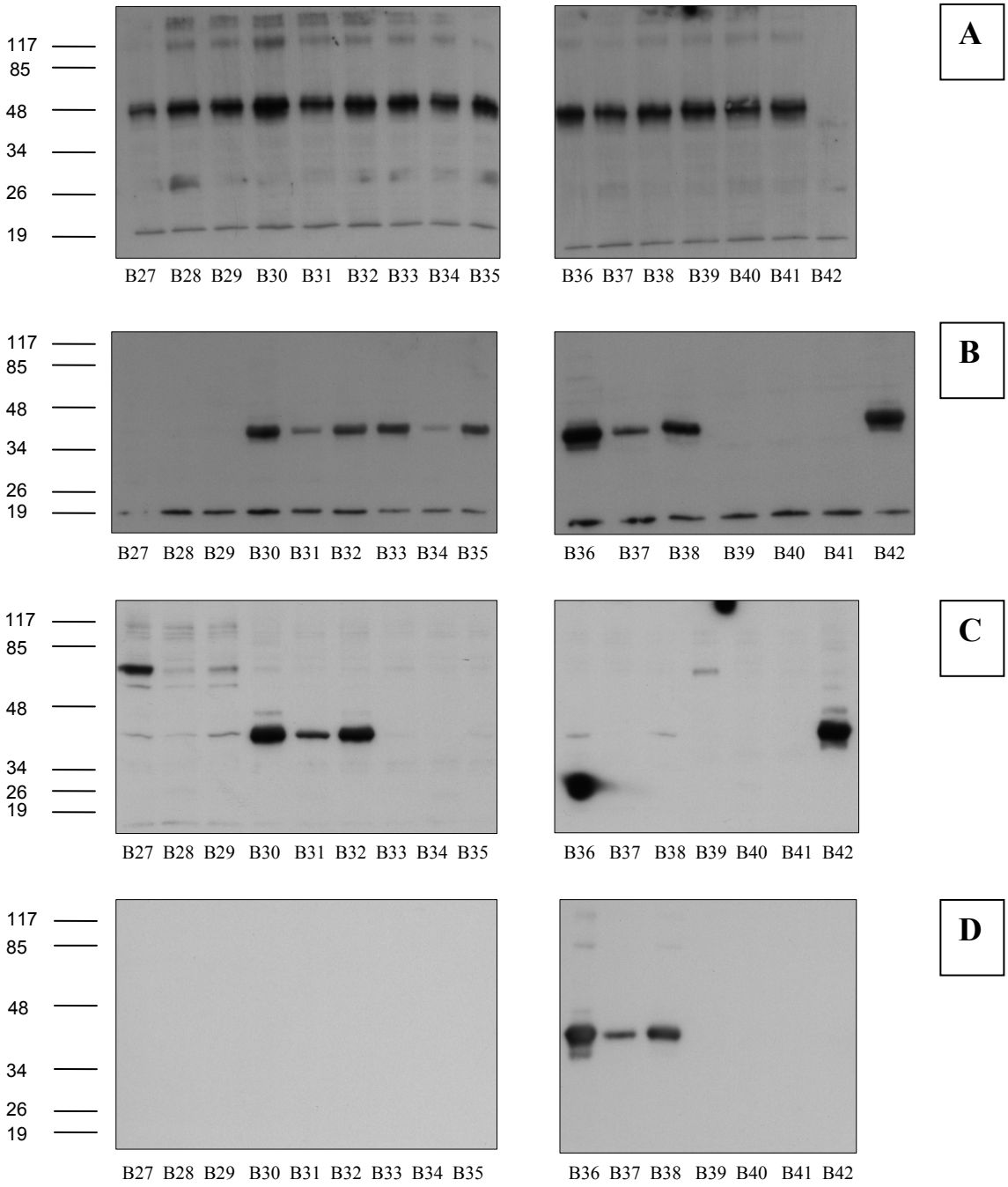

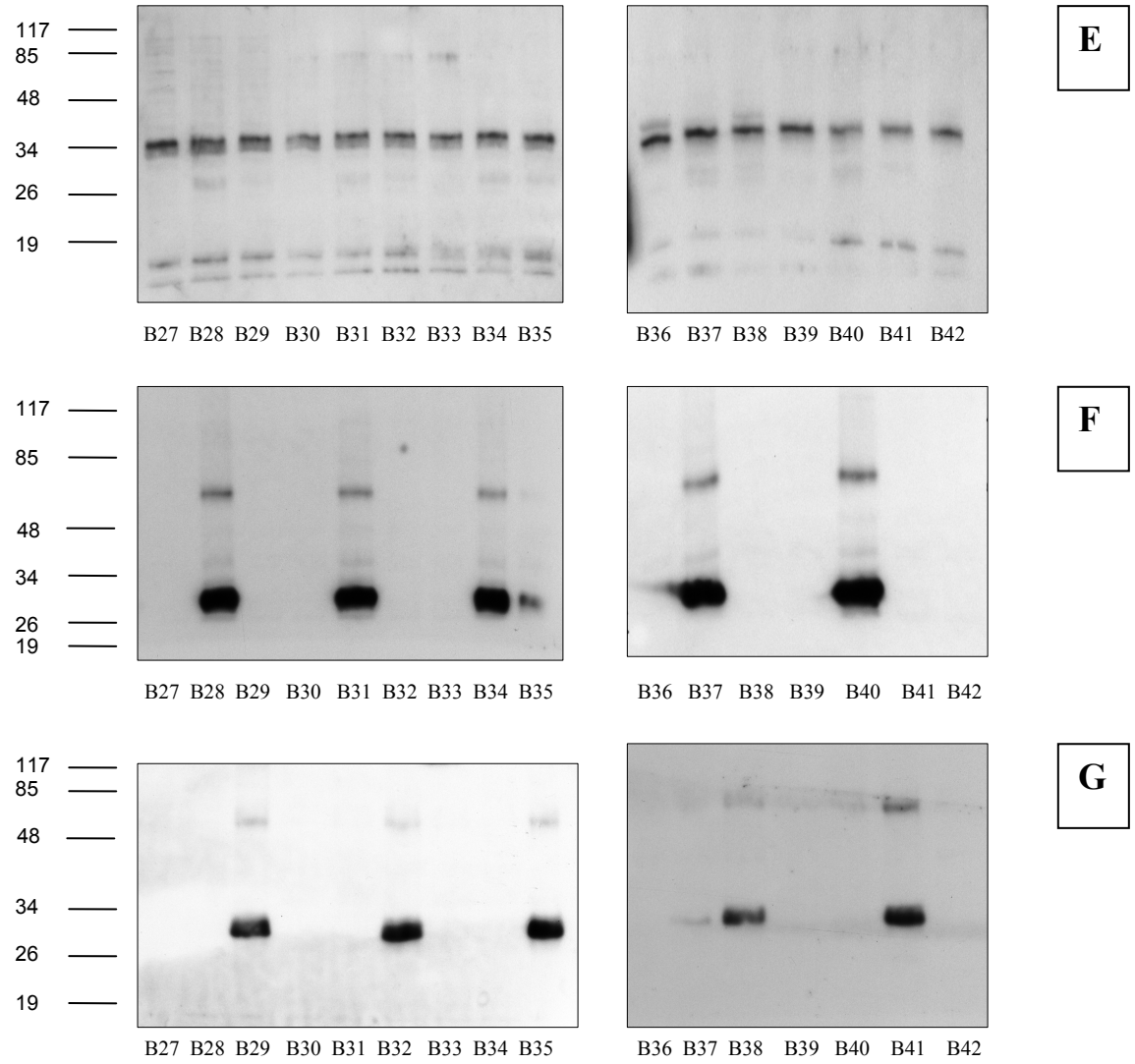

Fig. 5.9: Immunochemical detection of recombinant proteins expressed in Sf9 insect cells; 10 µg of protein from each membrane of set (B27 - B42) were loaded on each lane. Bands were detected with the following antibodies: (A) anti-FLAG, (B) anti-$G\alpha_{common}$, (C) anti-$G\alpha_{i1/2}$, (D) anti-$G\alpha_{o}$, (E) anti-$G\beta_{common}$, (F) anti-RGS4 and (G) anti-GAIP. Numbers on the left designate masses of marker proteins in kDa.

The hY_2R possesses one potential N-glycosylation site at its N-terminus. Therefore, the effect of N-glycosylation on the receptor's molecular weight and function (cf. section 5.3.4) was studied in membranes prepared from infected Sf9 cells grown in the presence and absence of the GlcNAc-1P-transferase, tunicamycin. The M1 antibody recognized both, glycosylated and non glycosylated receptors. A pronounced band for the monomeric hY_2R was detected at ≈46 kDa, while dimers and oligomers were found at ≈103 kDa and higher molecular weights (**Fig. 5.10**) for membranes engineered both from cell cultures with and without tunicamycin. The intensities of the bands were comparable to those of the FLAG-$h\beta_2AR$ at ≈57 kDa, but the signal was weaker in case of the tunicamycin treated membrane (lanes marked by arrows). A rough estimation of receptor expression levels was performed by comparison with

increasing protein amounts of a standard membrane expressing FLAG-hβ_2AR at 7.5 pmol/mg. For the glycosylated hY_2R a B_{max} value of ≈4.9 pmol/mg was determined, while a decrease to ≈3.4 pmol/mg was seen with tunicamycin treatment (**Fig. 5.10**).

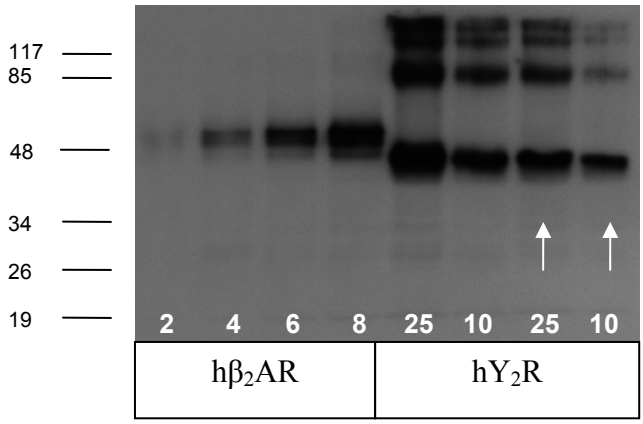

Fig. 5.10: Quantitative immunoblot analysis of two membranes expressing the hY_2R from tunicamycin treated (lanes marked by an arrow) and non-treated cells with the anti-FLAG (M1) antibody; A dilution of a reference membrane preparation with the expression of 7.5 pmol/mg hβ_2AR was used to estimate the receptor expression level of the hY_2. White numbers on the bottom of each lane indicate the amount of protein in µg loaded onto the gel. Expression levels for glycosylated hY_2R were ≈4.9 pmol/mg and for non glycosylated ≈3.4 pmol/mg.

When isolated from mammalian tissues, for example rat hippocampus (Sheikh and Williams, 1990), rabbit kidney (Sheikh and Williams, 1990; Sheikh *et al.*, 1991) or porcine brain (Wimalawansa, 1995), N-glycosylation of the Y_2 receptor usually makes up to ≈ 10 – 20 kDa, that is the receptor molecular weights found in these studies were ≈ 50 – 60 kDa. According to the above described immunoblot analyses, the hY_2R expressed in Sf9 cells shows a molecular mass of ≈ 46 - 50 kDa, which lies in the lower range of molecular weight compared to literature. However, this is not surprising, because Sf9 insect cells are known to have very simple glycosylation patterns compared to mammalian cells (Massotte, 2003). Tunicamycin treatment has virtually no effect on receptor molecular weight (**Fig. 5.10**). However the expression level of receptor is lowered by ≈1.5 pmol/mg with tunicamycin, which can be taken as a hint to the implication of N-glycosylation in the proper folding of the receptor protein and/or its targeting to the membrane.

5.3.2 Coupling efficiency of the hY_2R to $G\alpha_{i/o}$ proteins

In view of the establishment of a steady-state GTPase assay with a co-expression system for ligand screening purposes offering high signal-to-noise ratios, the preferential G protein for hY_2R had to be determined. Thus, with the two batches of membranes combining the hY_2R with different Gα-subunits (always co-expressed with $G\beta_1\gamma_2$) the coupling efficiency of hY_2R to $G\alpha_{i/o}$ proteins was investigated. RGS proteins, RGS4 and GAIP, were co-expressed to identify possible beneficial effects on signal enhancement.

Steady-state GTPase assays were performed with 100 nM of pNPY and under control conditions. Thus, stimulated and basal GTPase activities were determined, and signal-to-noise ratios expressed in % of basal GTPase activity were calculated for each membrane. In **Fig. 5.11** hY_2R coupling to mammalian $G\alpha_{i/o}$ proteins and endogenous Sf9 insect cell G proteins is shown. Low basal GTPase activities are found throughout all membranes in comparison to the ones co-expressing $G\alpha_o$. The hY_2R showed stimulation in combination with all mammalian G proteins, but was poorly activated, when co-expressed with endogenous Sf9 insect cell G proteins only. In fact, the hY_2R co-expressed with $G\alpha_{i3}$ and RGS4 or GAIP, yielded highest stimulations (≈ 290 - 310 % of basal GTPase activity in **Fig. 5.11 B**). However, robust signals were also obtained from hY_2R + $G\alpha_{i2}$ and hY_2R + $G\alpha_o$ + RGS4 or GAIP. Because of the lower basal GTPase activity and the high signal-to-noise ratio further examinations were mainly performed with hY_2R + $G\alpha_{i2}$. $G\alpha_{i2}$ expressed in control membranes exhibited no elevated GTPase activity upon stimulation with 100 nM pNPY.

In contrast to literature, these results show that the hY_2R couples with comparable efficiency to all $G\alpha_i$ proteins and also to $G\alpha_o$, although to a somewhat less extent. Endogenous G proteins of Sf9 cells are activated only poorly by hY_2Rs. Both RGS4 and GAIP enhance signaling via $G\alpha_{i3}$, $G\alpha_o$ and endogenous G proteins. The combination hY_2R + $G\alpha_{i2}$ + $G\beta_1\gamma_2$ showed a high signal-to-noise ratio allowing the investigation of constitutive receptor activity and the pharmacological characterisation of ligands as full/partial agonists, neutral antagonists or inverse agonists and thus providing a well suited system for ligand screening.

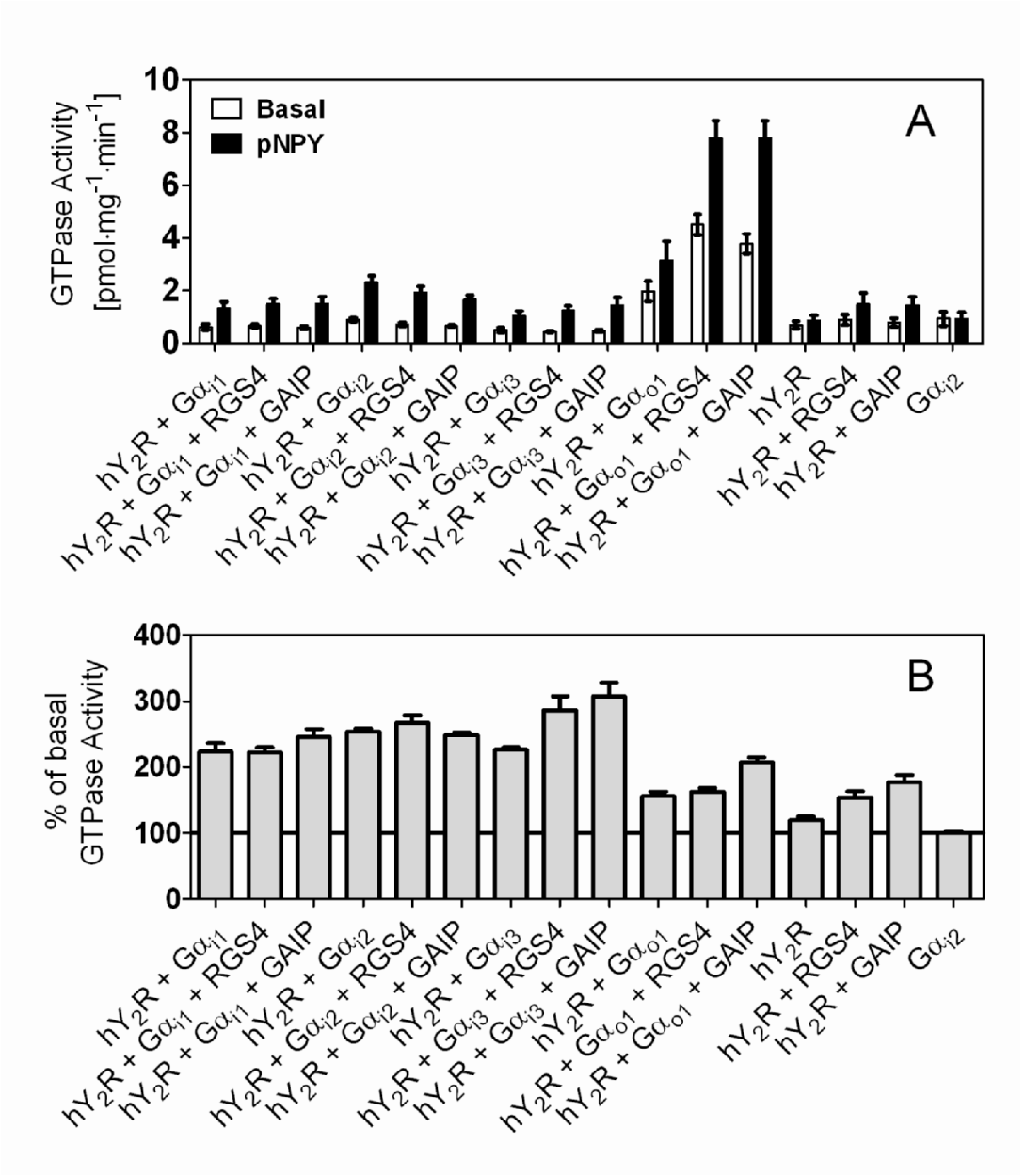

Fig. 5.11: Comparison of the coupling efficiency of hY_2R to $G\alpha_{i/o}$ proteins in the presence and absence of RGS4 or GAIP; The human Y_2R was co-expressed with $G\alpha_{i1}$, $G\alpha_{i2}$, $G\alpha_{i3}$ and $G\alpha_{o1}$ each with $G\beta_1\gamma_2$ and with or without RGS4 or GAIP, respectively. Control membranes contained hY_2R alone, hY_2R in combination with RGS4 or GAIP and $G\alpha_{i2}$ + $G\beta_1\gamma_2$. (A) Absolute GTPase activities under control conditions open bars (basal) and upon stimulation with 100 nM pNPY (black bars). (B) GTPase activities relative to basal expressed in percent. Data are means ± S.E.M. of at least 3 independent experiments performed in duplicate with two membrane batches prepared on one day each.

5.3.3 Effects of monovalent salts on the GTPase activity

It is well established that Na^+ acts as an allosteric inverse agonist at several $G_{i/o}$-coupled GPCRs and stabilizes the inactive state of the receptors (Seifert and Wenzel-Seifert, 2001; Seifert and Wenzel-Seifert, 2002). Therefore, basal and stimulated GTP hydrolysis was

measured in the presence of increasing concentrations of monovalent salts, and concentration response curves were constructed (**Fig. 5.12**).

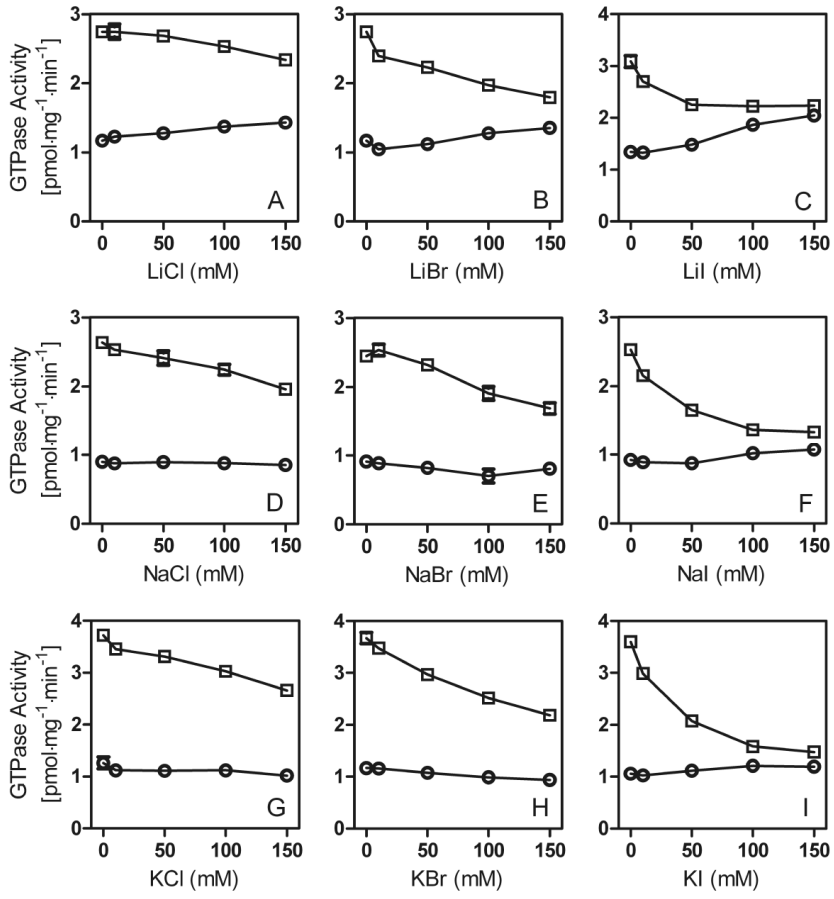

Fig. 5.12: Basal and ligand-stimulated GTPase activity depending on the concentration of various monovalent salts as indicated on the abscissa; High-affinity GTPase activity was determined with a Sf9 membrane expressing $hY_2R + G\alpha_{i2} + G\beta_1\gamma_2$ under control conditions (○) and upon stimulation with 100 nM pNPY (□). Data are means ± S.E.M. of one representative experiment performed in duplicate.

Major effects become obvious for anions rather than for cations at the hY_2R co-expressed with $G\alpha_{i2}$ and $G\beta_1\gamma_2$. The concentration response curves of the chlorides (**Fig. 5.12 A, D, G**) show stable basal GTPase activity with a slight drop of stimulated GTPase activity at higher salt concentrations. The same is true for the bromides (**Fig. 5.12 B, E, H**), although the decrease in stimulated GTPase activity is steeper. The most pronounced effect is observed with the iodides (**Fig. 5.12 C, F, I**), where the response of activated hY_2R almost equals the value of basal GTPase activity at a concentration of 150 mM. The Li^+ salts seem to elevate basal GTPase activity in ascending order $Cl^- < Br^- < I^-$ (**Fig. 5.13 A - C**), whereas no reduction of basal GTPase activity in the presence of Na^+ was observed, indicating that the

hY_2R is devoid of constitutive activity (**Fig. 5.12 D - F**). The same results were obtained, when GAIP was present in the membrane (data not shown).

The effect of NaCl on hY_2R was studied in combination with mammalian $G\alpha_{i1}$, $G\alpha_{i3}$ and $G\alpha_o$, however no differences in concentration response curves were found (**Fig. 5.13**).

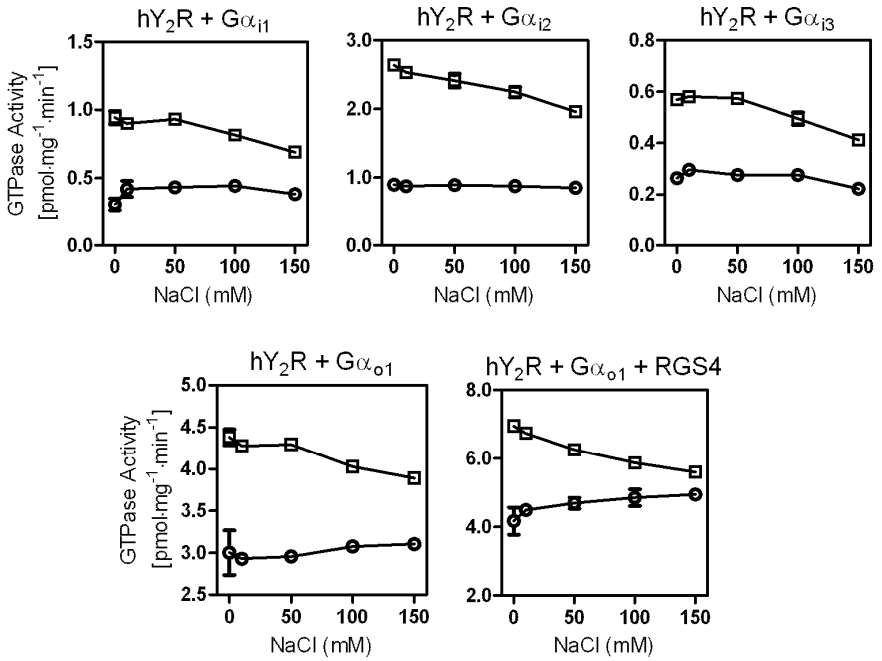

Fig. 5.13: Basal and stimulated GTPase activity depending on the concentration of NaCl; High-affinity GTPase activity was determined with membranes expressing the hY_2R in combination with different Gα-subunits as indicated in titles above graph panels (always along with $G\beta_1\gamma_2$). Data are means ± S.E.M. of one representative experiment performed in duplicate.

5.3.4 Effect of N-glycosylation on receptor function

According to immunoblot analyses (cf. section 5.3.1) the molecular weight of hY_2R is not affected by treatment with the GlcNAc-1P-transferase inhibitor, tunicamycin, but the expression level of protein suffers a loss of ≈1.5 pmol/mg. To investigate the influence of N-glycosylation on receptor function, steady-state GTPase assays were performed and concentration response curves for pNPY recorded (**Fig. 5.14**). After tunicamycin treatment the concentration-response curve was comparable to the control with untreated membranes. However, the maximal response was only 30 % relative to that of the control, which probably reflects an impaired expression in the presence of the GlcNAc phosphotransferase inhibitor. The determined EC_{50} (17.8 ± 7.3 nM) for pNPY at the tunicamycin treated membrane was in agreement with the EC_{50} (11.7 ± 3.0 nM) at control membranes. Thus, the unglycosylated

receptor retains its function, however with a decreased efficacy for its physiological ligand. This could be due to the lower expression level as N-glycosylation probably confers to correct receptor folding and targeting to the membrane.

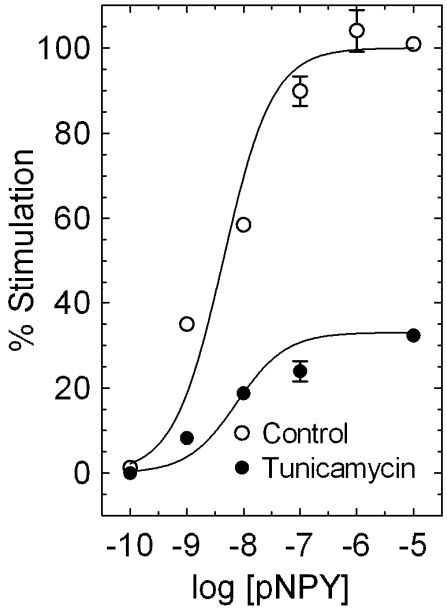

Fig. 5.14: Concentration response curves of pNPY at hY_2R, $G\alpha_{i2}$ and $G\beta_1\gamma_2$ expressing membranes from Sf9 cells grown in the presence (●) and absence (○) of tunicamycin; Data are means ± S.E.M. from representative experiments performed in duplicate.

5.3.5 Evaluation of the expression system $hY_2R + G\alpha_{i2} + G\beta_1\gamma_2$

For assay validation, concentration response curves of peptidergic ligands were recorded (**Fig. 5.16 A**) at membranes expressing $hY_2R + G\alpha_{i2} + G\beta_1\gamma_2$ and EC_{50} values calculated. Furthermore, non peptidergic Y_2 receptor antagonists with known affinities were tested in the steady-state GTPase assay by constructing inhibition curves from obtained data (**Fig. 5.15 B**). The concentration response curves yielded EC_{50} values of 11.7 ± 3.0 nM for pNPY, 23.7 ± 6.2 nM for $pNPY_{13-36}$ and 7.5 ± 1.2 nM for pPYY, which are in good agreement with data from other assay formats (Dautzenberg *et al.*, 2005; Ziemek *et al.*, 2006; Merten *et al.*, 2007). The antagonistic activities of nonpeptidergic Y_2 receptor antagonists were determined in the presence of 50 nM pNPY. Likewise the IC_{50} value of **1** (64.5 ± 8.1 nM) was in good agreement with data from the literature (Doods *et al.*, 1999; Dautzenberg, 2005; Ziemek *et al.*, 2006). There was a tendency towards higher IC_{50} values in the case of the BIIE 0246 derivatives (compounds **2-5**), probably due to variable assay parameters, such as the period of incubation and adsorption effects to materials used in the different assays. However there was a good correlation between the K_b values from this work and those determined in an aequorin

assay, established by Ziemek *et al.* (2006) in our work group. Pharmacological data from the steady-state GTPase assay are summarized in **Table 5.3**.

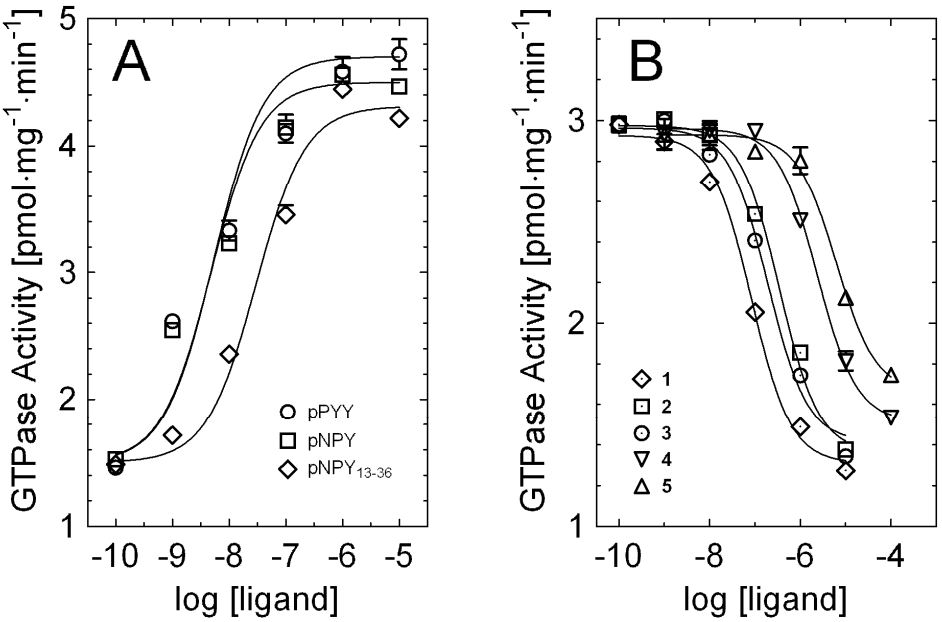

Fig. 5.15: Concentration-response curves of peptidergic ligands (A) and inhibition curves of compounds **1-5** at Sf9 membranes containing hY_2R, $G\alpha_{i2}$ and $G\beta_1\gamma 2$ (B); Inhibition curves were recorded in the presence of 50 nM pNPY. Data are means ± S.E.M. from representative experiments performed in duplicate.

5.4 Summary and conclusions

The baculovirus Sf9 insect cell system has proven to be suitable for the functional reconstitution of the hY_2R in combination with different $G_{i/o}$ proteins. The receptor coupled with comparable efficiency to $G\alpha_{i1}$, $G\alpha_{i2}$ and $G\alpha_{i3}$, respectively, while with $G\alpha_o$ the signal-to-noise ratio was poor. RGS proteins enhanced ligand stimulated signal in expression systems with $G\alpha_{i3}$, $G\alpha_o$ and endogenous insect cell G proteins. The combination of hY_2R and $G\alpha_{i2}$ yielded a high signal-to-noise ratio and was chosen for validation with peptidergic and non-peptidergic ligands. Pharmacological data obtained are in good agreement with literature and are summerized in **Table 5.3**.

Table 5.3: Pharmacological data of hY_2R ligands determined in the steady-state GTPase assay with membranes expressing the $hY_2R + G\alpha_{i2} + G\beta_1\gamma_2$

Peptide	EC_{50} [nM]	E_{max}
pNPY	11.7 ± 3.0 (n=8)	-
pNPY (Tun)	17.8 ± 7.3 (n=3)	-
$pNPY_{13-36}$	23.7 ± 6.2 (n=3)	0.94 ± 0.1
pPYY	7.5 ± 1.2 (n=3)	1.0 ± 0.03
Antagonist	**IC_{50} [nM]**	**K_b [nM]**
1	64.5 ± 8.1 (n=5)	10.2 ± 1.8
2	377.6 ± 33.8 (n=3)	71.7 ± 6.4
3	289.4 ± 61.5 (n=3)	54.9 ± 11.7
4	2,139 ± 261 (n=3)	406.0 ± 49.7
5	6,079 ± 214 (n=3)	1,154 ± 41

Mean values ± S.E.M. of at least three independent experiments performed in duplicate. Data derived from membranes engineered in the presence of tunicamycin are marked with (Tun). IC_{50} values were determined in the presence of 50 nM pNPY and K_b values of antagonists were calculated using the Cheng-Prusoff equation.

The chosen expression system allows not only for the screening of new ligands at the hY_2, but also renders investigations on receptor structure and function depending on N-glycosylation possible. Furthermore, the influence of monovalent salts on receptor function can be easily assessed, because in contrast to cell based assays, the salt concentration at the receptor can be defined exactly. Thus, with the steady-state GTPase assay for the hY_2R a powerful and versatile tool has been established.

5.5 References

Beck-Sickinger AG, Grouzmann E, Hoffmann E, Gaida W, van Meir EG, Waeber B and Jung G (1992) A novel cyclic analog of neuropeptide Y specific for the Y_2 receptor. *Eur J Biochem* **206**:957-964.

Berridge MJ (1983) Rapid accumulation of inositol trisphosphate reveals that agonists hydrolyse polyphosphoinositides instead of phosphatidylinositol. *Biochem J* **212**:849-858.

Birnbaumer L, Abramowitz J and Brown AM (1990) Receptor-effector coupling by G proteins. *Biochim Biophys Acta* **1031**:163-224.

Brothers SP, Saldanha SA, Spicer TP, Cameron M, Mercer BA, Chase P, McDonald P, Wahlestedt C and Hodder PS (2010) Selective and brain penetrant neuropeptide Y Y_2 receptor antagonists discovered by whole-cell high-throughput screening. *Mol Pharmacol* **77**:46-57.

Dautzenberg FM (2005) Stimulation of neuropeptide Y-mediated calcium responses in human SMS-KAN neuroblastoma cells endogenously expressing Y_2 receptors by co-expression of chimeric G proteins. *Biochem Pharmacol* **69**:1493-1499.

Dautzenberg FM, Higelin J, Pflieger P, Neidhart W and Guba W (2005) Establishment of robust functional assays for the characterization of neuropeptide Y (NPY) receptors: identification of 3-(5-benzoyl-thiazol-2-ylamino)-benzonitrile as selective NPY type 5 receptor antagonist. *Neuropharmacology* **48**:1043-1055.

Doods H, Gaida W, Wieland HA, Dollinger H, Schnorrenberg G, Esser F, Engel W, Eberlein W and Rudolf K (1999) BIIE0246: a selective and high affinity neuropeptide Y Y_2 receptor antagonist. *Eur J Pharmacol* **384**:R3-5.

Ewald DA, Sternweis PC and Miller RJ (1988) Guanine nucleotide-binding protein G_o-induced coupling of neuropeptide Y receptors to Ca^{2+} channels in sensory neurons. *Proceedings of the National Academy of Sciences of the United States of America* **85**:3633-3637.

Freitag C, Svendsen AB, Feldthus N, Lossl K and Sheikh SP (1995) Coupling of the human Y_2 receptor for neuropeptide Y and peptide YY to guanine nucleotide inhibitory proteins in permeabilized SMS-KAN cells. *Journal of Neurochemistry* **64**:643-650.

Gerald C, Walker MW, Vaysse PJ, He C, Branchek TA and Weinshank RL (1995) Expression cloning and pharmacological characterization of a human hippocampal neuropeptide Y/peptide YY Y_2 receptor subtype. *Journal of Biological Chemistry* **270**:26758-26761.

Goumain M, Voisin T, Lorinet AM, Ducroc R, Tsocas A, Roze C, Rouet-Benzineb P, Herzog H, Balasubramaniam A and Laburthe M (2001) The peptide YY-preferring receptor mediating inhibition of small intestinal secretion is a peripheral Y_2 receptor: pharmacological evidence and molecular cloning. *Mol Pharmacol* **60**:124-134.

Kleemann P, Papa D, Vigil-Cruz S and Seifert R (2008) Functional reconstitution of the human chemokine receptor CXCR4 with G_i/G_o-proteins in Sf9 insect cells. *Naunyn Schmiedebergs Arch Pharmacol* **378**:261-274.

Massotte D (2003) G protein-coupled receptor overexpression with the baculovirus-insect cell system: a tool for structural and functional studies. *Biochimica et Biophysica Acta* **1610**:77-89.

Merten N, Lindner D, Rabe N, Römpler H, Mörl K, Schöneberg T and Beck-Sickinger AG (2007) Receptor subtype-specific docking of $Asp^{6.59}$ with C-terminal arginine residues in Y receptor ligands. *J Biol Chem* **282**:7543-7551.

Michel MC, Beck-Sickinger A, Cox H, Doods HN, Herzog H, Larhammar D, Quirion R, Schwartz T and Westfall T (1998) XVI. International Union of Pharmacology recommendations for the nomenclature of neuropeptide Y, peptide YY, and pancreatic polypeptide receptors. *Pharmacol Rev* **50**:143-150.

Misra S, Murthy KS, Zhou H and Grider JR (2004) Coexpression of Y_1, Y_2, and Y_4 receptors in smooth muscle coupled to distinct signaling pathways. *J Pharmacol Exp Ther* **311**:1154-1162.

Preuss H, Ghorai P, Kraus A, Dove S, Buschauer A and Seifert R (2007) Constitutive activity and ligand selectivity of human, guinea pig, rat, and canine histamine H_2 receptors. *J Pharmacol Exp Ther* **321**:983-995.

Rose PM, Fernandes P, Lynch JS, Frazier ST, Fisher SM, Kodukula K, Kienzle B and Seethala R (1995) Cloning and functional expression of a cDNA encoding a human type 2 neuropeptide Y receptor. *Journal of Biological Chemistry* **270**:22661-22664.

Schnell D, Burleigh K, Trick J and Seifert R (2010) No evidence for functional selectivity of proxyfan at the human histamine H_3 receptor coupled to defined G_i/G_o protein heterotrimers. *J Pharmacol Exp Ther* **332**:996-1005.

Seifert R and Wenzel-Seifert K (2001) Unmasking different constitutive activity of four chemoattractant receptors using Na^+ as universal stabilizer of the inactive (R) state. *Receptors Channels* **7**:357-369.

Seifert R and Wenzel-Seifert K (2002) Constitutive activity of G-protein-coupled receptors: cause of disease and common property of wild-type receptors. *Naunyn Schmiedebergs Arch Pharmacol* **366**:381-416.

Sheikh SP, Hansen AP and Williams JA (1991) Solubilization and affinity purification of the Y_2 receptor for neuropeptide Y and peptide YY from rabbit kidney. *Journal of Biological Chemistry* **266**:23959-23966.

Sheikh SP and Williams JA (1990) Structural characterization of Y_1 and Y_2 receptors for neuropeptide Y and peptide YY by affinity cross-linking. *Journal of Biological Chemistry* **265**:8304-8310.

Voisin T, Lorinet AM and Laburthe M (1996a) Partial knockdown of $G\alpha_{i2}$ protein is sufficient to abolish the coupling of PYY receptors to biological response in renal proximal tubule cells. *Biochemical and Biophysical Research Communications* **225**:16-21.

Voisin T, Lorinet AM, Maoret JJ, Couvineau A and Laburthe M (1996b) $G\alpha_i$ RNA antisense expression demonstrates the exclusive coupling of peptide YY receptors to G_{i2} proteins in renal proximal tubule cells. *Journal of Biological Chemistry* **271**:574-580.

Walseth TF and Johnson RA (1979) The enzymatic preparation of [α-^{32}P]nucleoside triphosphates, cyclic [^{32}P] AMP, and cyclic [^{32}P] GMP. *Biochim Biophys Acta* **562**:11-31.

Wimalawansa SJ (1995) Purification and biochemical characterization of neuropeptide Y_2 receptor. *Journal of Biological Chemistry* **270**:18523-18530.

Ziemek R (2006) Development of binding and functional assays for the neuropeptide Y Y_2 and Y_4 receptors, Doctoral thesis, University of Regensburg, Germany

Ziemek R, Brennauer A, Schneider E, Cabrele C, Beck-Sickinger AG, Bernhardt G and Buschauer A (2006) Fluorescence- and luminescence-based methods for the determination of affinity and activity of neuropeptide Y_2 receptor ligands. *European Journal of Pharmacology* **551**:10-18.

Chapter 6

6 Establishment of a steady-state GTPase assay for the human NPY Y_4 receptor

6.1 Introduction

Due to the common signaling of Y receptors via $G_{i/o}$ proteins, the same assay formats as already mentioned for the Y_2 receptor were essentially applied for the Y_4R. For example, measurements of the inhibition of forskolin induced cAMP formation (Parker *et al.*, 1998; Voisin *et al.*, 2000), the accumulation of tritiated IP_3 (Berridge, 1983; Merten *et al.*, 2007) or the elevation of intracellular Ca^{2+} utilizing fluorescent probes (Dautzenberg *et al.*, 2005) or bioluminescence (Ziemek *et al.*, 2007) as well as GTPγS binding (Dautzenberg *et al.*, 2005) have been reported. Besides, Chen *et al.* (2000) used Xenopus laevis melanophores, transfected with $hY_{1/2/4}R$, to assess constitutive activity of these GPCRs and suggested this system for the screening of ligands. According to these authors the hY_4R indeed showed elevated basal activity as it changed the transmittance of incident light by cells without being stimulated. However, in literature this assay format is not widely used for GPCRs, probably due to the variability of these cells (Suska *et al.*, 2008) giving spurious results in conventional macroscopic evaluations. By contrast, the baculovirus/Sf9 expression system with its broad usability in binding and functional experiments has been successfully applied for plenty of G protein coupled receptors (Massotte, 2003). In view of the lack of potent and selective Y_4 antagonists we were aiming at a screening system for ligands, especially antagonists, at the hY_4R. One potent and selective Y_4 receptor agonist reported lately (Balasubramaniam *et al.*, 2006) has been identified in a radioimmuno cAMP assay and probed in feeding studies on mice after i. p. application. Since no potent antagonists are available, knockout animals lacking the Y_4 receptor gene were the negative control and seem to be broadly in use

(Wultsch *et al.*, 2006; Painsipp *et al.*, 2008; Tasan *et al.*, 2009). Thus, the development of reliable small molecule receptor ligands is still a challenging task and would greatly facilitate and accelerate investigations and drug discovery. For this purpose reliable functional assays are needed.

6.2 Materials and Methods

6.2.1 Preparation of SF-hY$_4$R-His$_6$ construct by overlap extension PCR

Overlap extension PCR was essentially performed as described in section 5.2.1. However, for PCR 1b and PCR 2 different DNA polymerases and cycling conditions were applied.

The PCR 1a was accomplished as described for the hY$_2$R (section 5.2.1.1).

In PCR 1b, pcDNA3-hY$_4$, prepared by R. Ziemek (2006) was used as template. The hY$_4$ nucleotide sequence corresponds to GenBank accession no. U35232 published by Bard *et al.* (1995). Again, the **receptor sequence** was extended N-terminally by a part of the *FLAG* sequence and C-terminally by a hexahistidine tag, followed by the shifted stop codon and the *Xba*I restriction site. These modifications were introduced via the following primer pairs (MWG) used at a final concentration of 0.5 µM each.

FLAG-hY$_4$R-sense	5'- *AAG GAC GAT GAT GAC GCC* **ATG AAC ACC TCT CAC CTC CTG** -3'
6His-hY$_4$-as	5'- GG TCC *TCT AGA* TTA GTG ATG GTG ATG ATG GTG **AAT GGG ATT GGA CCT GCC** -3'

Reaction mixtures were prepared to a volume of 100 µl containing 5 U of *PfuTurbo*® DNA Polymerase (Stratagene, La Jolla, CA) with 10 µl of 10× Cloned *Pfu* DNA Polymerase Reaction buffer (Stratagene), $MgSO_4$ (3.5 mM), dNTPs 50 µM each, 100 ng of template DNA, primers 0.5 µM each and DMSO 10 %. Cycling conditions were as follows:

(1)	initial denaturation	95 °C, 5 min
(2)	denaturation	95 °C, 1 min
(3)	annealing	65 °C, 2 min
(4)	extension	72 °C, 1.5 min
(5)	final extension	72 °C, 10 min
(6)	hold	4 °C

Steps (2) to (4) were repeated 24 times.

10 µl of PCR 1b product were analyzed by agarose gel electrophoresis. The expected band was found at 1175 bps (**Fig. 6.1**).

PCR 2 was carried out by analogy with PCR 1b using purified products of PCR 1a and PCR 1b (2 µl each) as template and the sense pGEM and 6His-hY_4-as primers (**Fig. 6.2**).

After purification the PCR 2 product was subcloned into a pGEM-3Z and a pVL1392 plasmid as described for the hY_2R in sections 5.2.2. and 5.2.3. The sequence of the construct SF-hY_4R-His_6 was verified and one conservative mutation A66G (counted from the ATG of the receptor) was found.

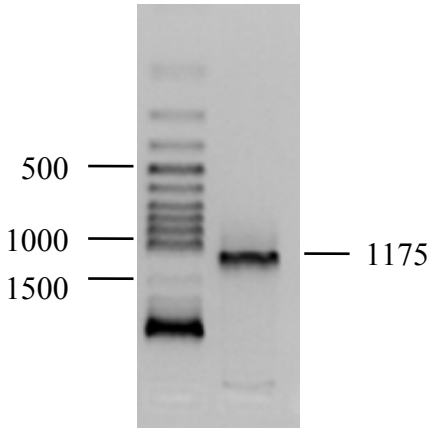

Fig. 6.1: Agarose (1.5 %) gel electrophoresis of PCR 1b product.; Sizes of DNA bands are indicated in bps.

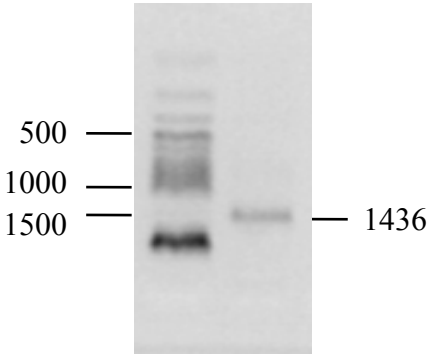

Fig. 6.2: Agarose (1.5 %) gel electrophoresis of PCR 2 product; Sizes of DNA bands are indicated in bps.

All subsequent steps including the GTPase assays were conducted as already described for the hY_2R.

6.2.2 Y_4 receptor ligands

The peptides hPP, K^4-hPP, BW1911U90, rPP, pNPY, pPYY were kindly provided by Prof. Dr. C. Cabrele, (Ruhr-University of Bochum, Germany). GW1229 (also designated GR231118 or 1229U91) was a gift from Dr. J. Daniels, Glaxo Wellcome Inc., USA. The compounds AK 49, AK 377 and AK 472 were synthesized by A. Kraus and the compounds PI 284, PI 317 and PI 330 were prepared by P. Igel (both from University of Regensburg, Germany).

Table 6.1: Compounds tested at the hY_4R

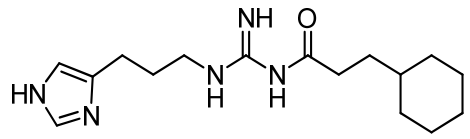 AK 49	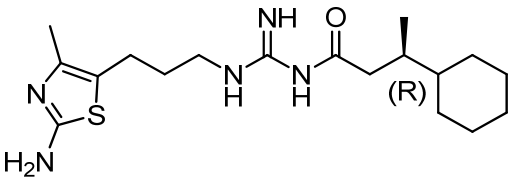 AK 377
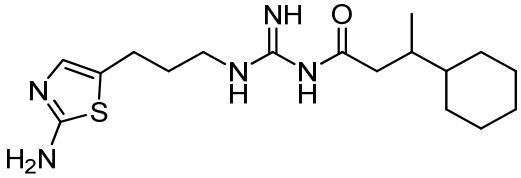 AK 472	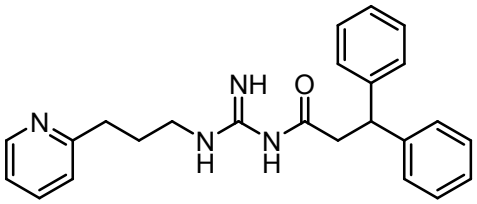 PI 284
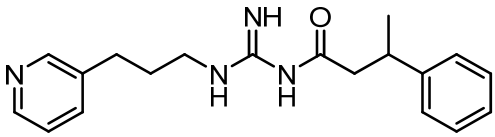 PI 317	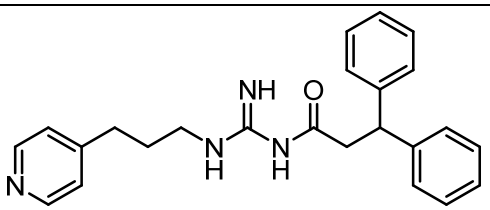 PI 330

6.3 Results and Discussion

6.3.1 Immunoblot analysis of membranes

6.3.1.1 Protein expression in membrane batch

By analogy with the hY_2R, a batch comprising a set of 16 membranes with different combinations of the hY_4R with G proteins and RGS proteins was prepared as summarized in **Table 6.2**.

Table 6.2: Overview of the set of membranes generated for the hY_4R

Membrane preparation	Receptor	Gα	Gβγ	RGS protein	Protein [µg/ml]
1644	SF-hY_4-His_6	$G\alpha_{i2}$	$G\beta_1\gamma_2$	-	276
1645	SF-hY_4-His_6	$G\alpha_{i2}$	$G\beta_1\gamma_2$	RGS 4	1316
1646	SF-hY_4-His_6	$G\alpha_{i2}$	$G\beta_1\gamma_2$	GAIP	1232
1647	SF-hY_4-His_6	$G\alpha_{i1}$	$G\beta_1\gamma_2$	-	1286
1648	SF-hY_4-His_6	$G\alpha_{i1}$	$G\beta_1\gamma_2$	RGS 4	1612
1649	SF-hY_4-His_6	$G\alpha_{i1}$	$G\beta_1\gamma_2$	GAIP	1349
1650	SF-hY_4-His_6	$G\alpha_{i3}$	$G\beta_1\gamma_2$	-	1396
1651	SF-hY_4-His_6	$G\alpha_{i3}$	$G\beta_1\gamma_2$	RGS 4	1299
1652	SF-hY_4-His_6	$G\alpha_{i3}$	$G\beta_1\gamma_2$	GAIP	1344
1653	SF-hY_4-His_6	$G\alpha_{o1}$	$G\beta_1\gamma_2$	-	1539
1654	SF-hY_4-His_6	$G\alpha_{o1}$	$G\beta_1\gamma_2$	RGS 4	1499
1655	SF-hY_4-His_6	$G\alpha_{o1}$	$G\beta_1\gamma_2$	GAIP	1279
1656	SF-hY_4-His_6	-	-	-	1076
1657	-	$G\alpha_{i2}$	$G\beta_1\gamma_2$	-	1039
1658	SF-hY_4-His_6	-	-	RGS 4	1379
1659	SF-hY_4-His_6	-	-	GAIP	1502

After the preparation of membranes as described in section 5.2.6, 10 µg of samples were loaded onto 12 % SDS gels each, and blotted after electrophoresis onto nitrocellulose membranes, which were then reacted with antibodies as indicated in **Fig. 6.3**. Bands were found at molecular weights expected for each protein: Gα-subunits at 43 kDa, Gβ-subunits at 36 kDa and RGS4 and GAIP at somewhat higher molecular weights than expected at 29 and 31 kDa, respectively. Dimers and oligomers were found for the GAIP at 64 kDa and higher (**Fig. 6.3 E**). Protein expression levels were approximately the same in all membranes, except for the $G\alpha_{i1}$-subunit, which showed weaker bands than the other Gα-subunits (**Fig 6.3 B**). $G\alpha_{i2}$ in the control membrane (1657) showed a very pronounced band at 43 kDa giving account of the fact that in this case the cells had been infected with only two baculoviruses (encoding for $G\alpha_{i2}$ and the dimer $G\beta_1\gamma_2$) instead of up to four. The FLAG-tagged hY_4 receptor was expressed at approximately the same level in all membranes. Somewhat divergent band

intensities could be due to the determination of protein concentration performed only in single measurements. The receptor molecular weight found by immunoblot analysis was 45 kDa, which corresponds to the unglycosylated protein. However, the hY_4R is a glycoprotein with four potential N-glycosylation sites, with glycosylation acconting for up to 20 kDa.

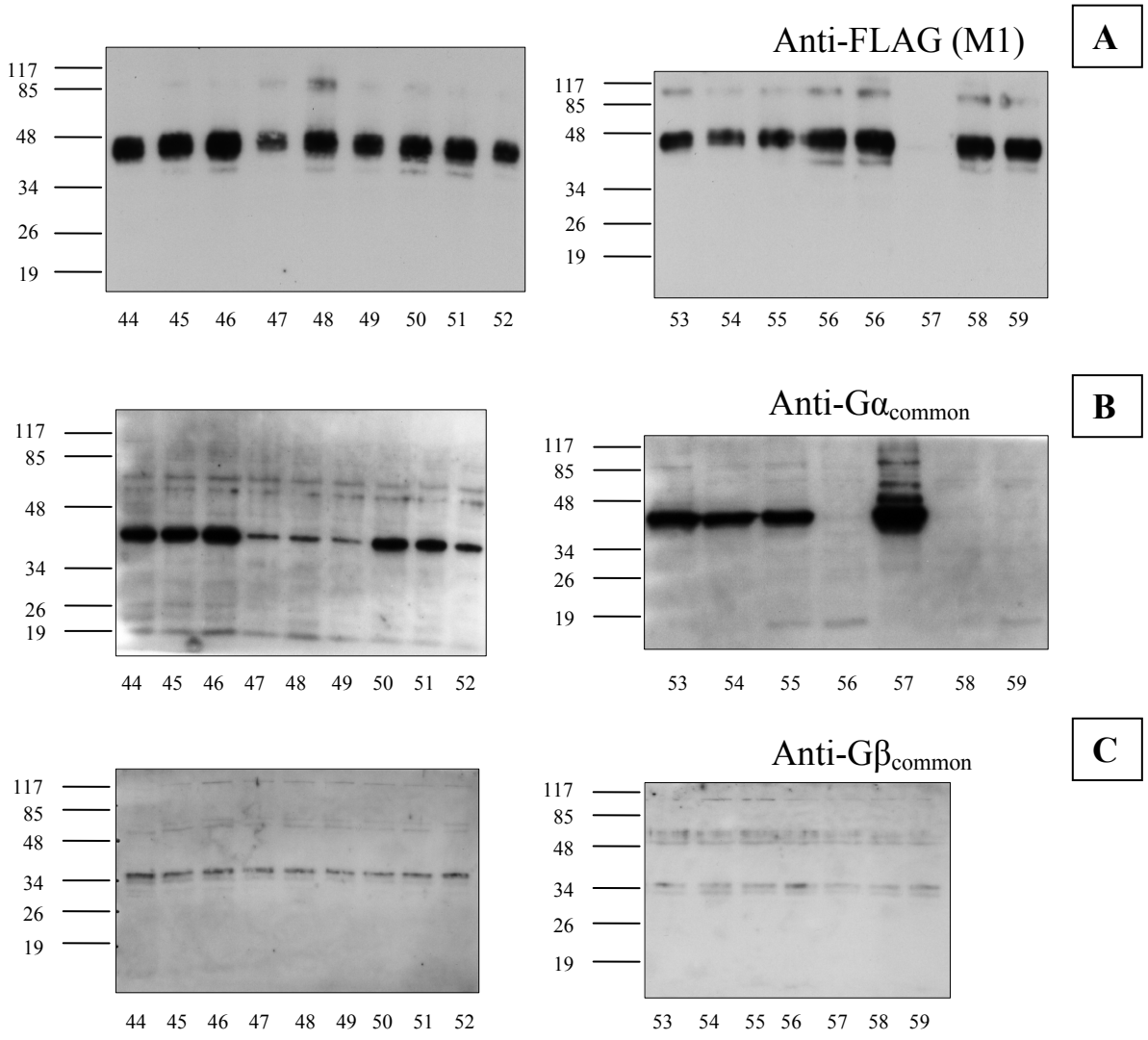

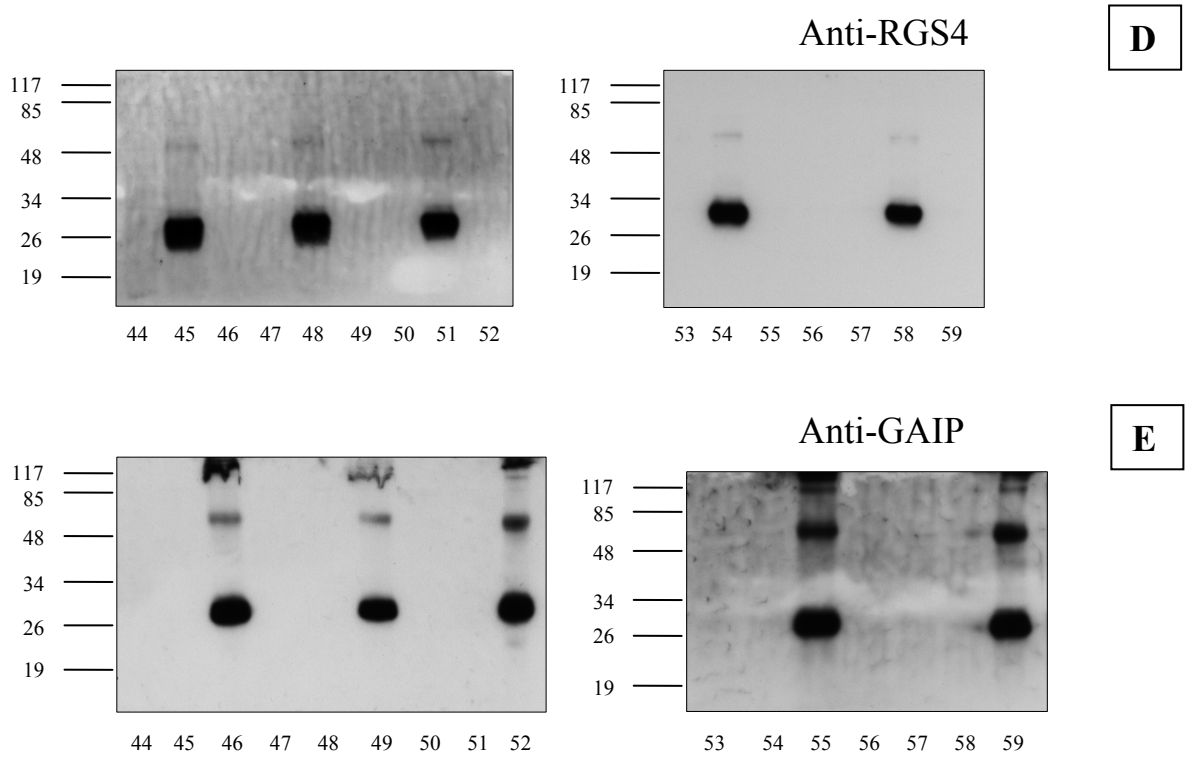

Fig. 6.3: Immunological detection of recombinant proteins expressed in Sf9 insect cells; 10 µg of protein from each membrane of the batch (1644-1659) were loaded on each lane. Numbers of membranes are shortened to the last two digits. Bands were detected with the following antibodies: (A) anti-FLAG, (B) anti-$G\alpha_{common}$, (C) anti-$G\beta_{common}$, (D) anti-RGS4 and (E) anti-GAIP. Figures on the left side of the blots designate masses of marker proteins in kDa.

6.3.1.2 Quantitative immunoblot analysis

To assess the receptor and G protein expression level of membranes, quantitative immunoblot analyses were performed. A high G protein/GPCR ratio ensures that the signal transduction of the hY_4R is not compromised by limited availability of G proteins (Kenakin, 1997). Therefore, membranes, expressing hY_4R + $G\alpha_{i2}$ + RGS4 and hY_4R + $G\alpha_{o1}$ + RGS4 (always along with $G\beta_1\gamma_2$), were subjected to quantification of GPCR and G protein expression by immunoblot analysis (**Fig. 6.4** and **6.5**). With 1.4 and 1.8 pmol/mg the hY_4R is expressed at comparable levels in all membrane preparations. $G\alpha_{i2}$ amounted to ≈300 pmol/mg, while $G\alpha_{o1}$ is present at ≈150 pmol/mg, so the GPCR/Gα results in a ratio of ≈ 1:200 and ≈ 1:80, respectively (**Table 6.3**).

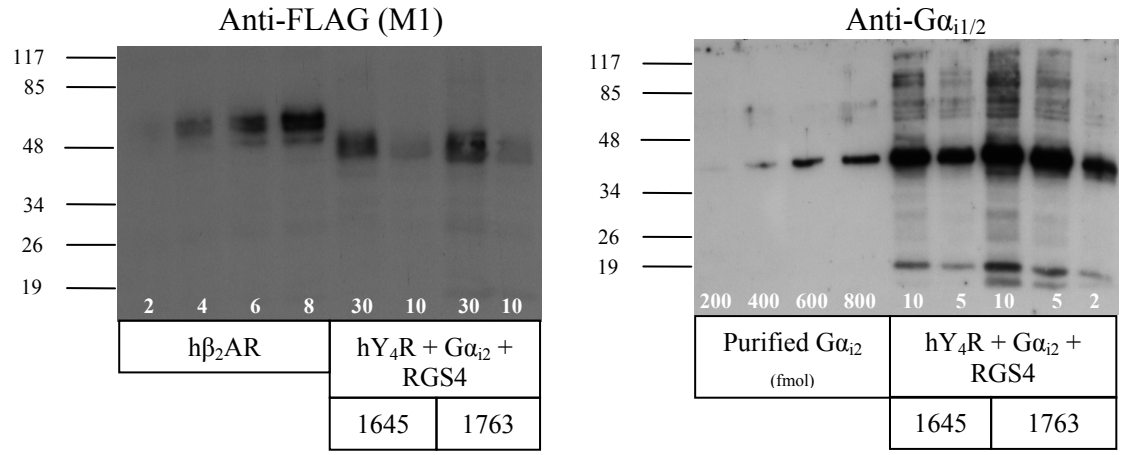

Fig. 6.4: Quantitative immunoblot analysis of two membranes (1645 and 1763) expressing the hY_4R + $G\alpha_{i2}$ + $G\beta_1\gamma_2$ + RGS4 with the anti-FLAG (M1) and the anti $G\alpha_{i1/2}$ antibody; A dilution of a reference membrane with the expression of 7.5 pmol/mg $h\beta_2AR$ and defined amounts of purified $G\alpha_{i2}$ were used to estimate receptor and G protein expression levels. The figures on the bottom of each lane indicate the amount of membrane protein in µg or purified protein in fmol ($G\alpha_{i2}$) loaded onto the gel.

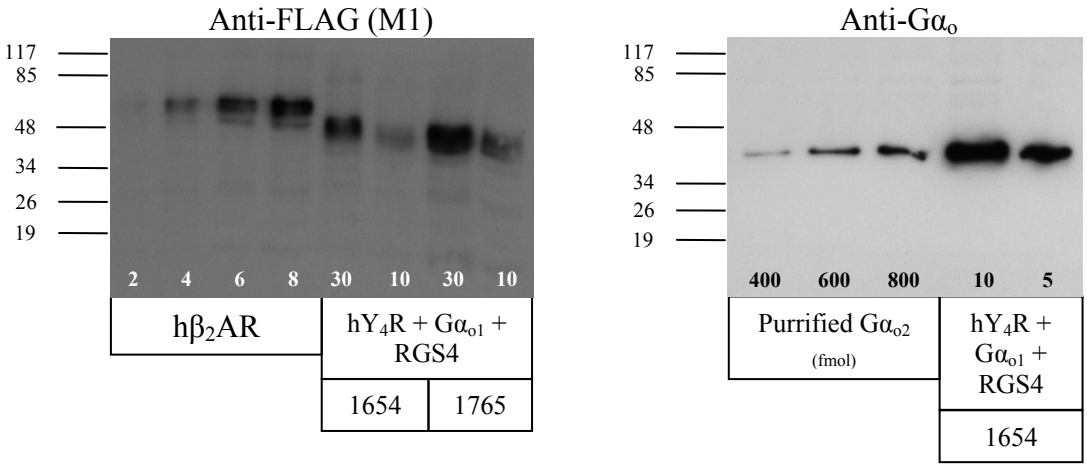

Fig. 6.5: Quantitative immunoblot analysis of two membranes (1654 and 1765) expressing the hY_4R + $G\alpha_{o1}$ + $G\beta_1\gamma_2$ + RGS4 with the anti-FLAG (M1) and the anti $G\alpha_o$ antibody; A dilution of a reference membrane, expressing 7.5 pmol/mg $h\beta_2AR$ and defined amounts of purified $G\alpha_{o2}$ were used to estimate receptor and G protein expression levels. Figures on the bottom of each lane indicate the amount of membrane protein in µg or purified protein in fmol ($G\alpha_{o2}$) loaded onto the gel.

Table 6.3: Expression levels and ratios of proteins in Sf9 membranes

Parameter	**hY_4R + $G\alpha_{i2}$ + RGS4**	**hY_4R + $G\alpha_{o1}$ + RGS4**
hY_4R expression level [pmol/mg]	1.4 ± 0.5[1] (n=5)	1.8 ± 1.1[2] (n=3)
Gα expression level [pmol/mg]	293 ± 138[3] (n=3)	146 ± 42[2] (n=1)
hY_4R/Gα ratio	1 : 205	1 : 81

All membranes contained proteins as indicated along with $G\beta_1\gamma_2$. [1]determined with 3 different membrane preparations; [2]determined with one membrane preparation; [3]determined with 2 different membrane preparations.

This is in good agreement with ratios determined for other $G_{i/o}$ coupled receptors in Sf9 membranes, for example the human histamine H_3 receptor (Schnell *et al.*, 2010), the human histamine H_4 receptor (Schneider *et al.*, 2009) or the human cannabinoid receptors CB_1 and CB_2 (Nickl *et al.*, 2008).

6.3.1.3 Effect of N-glycosylation on the structure and the expression level of the hY_4R

Defective N-glycosylation of GPCRs can affect receptor function, as shown, e.g., for the human formyl peptide receptor FPR (Wenzel-Seifert and Seifert, 2003), as well as receptor expression. For example, the expression level of non glycosylated hY_1R, which possesses four potential extracellular N-glycosylation sites (like the hY_4R), suffered a dramatic loss in the methylotrophic yeast *Pichia pastoris* compared to the glycosylated protein (Yurugi-Kobayashi *et al.*, 2009). Therefore, structural and functional (see section 6.3.4) analysis of glycosylated and non glycosylated hY_4R have been performed via immunoblot and steady-state GTPase assays.

When expressed in CHO cells, Voisin et al (Voisin *et al.*, 2000) found a molecular weight for the hY_4R of ≈60 kDa, which was reduced to ≈43 kDa after incubation with PNGase F, a N-glycanase, and the rhesus Y_4R had a size of ≈80 kDa expressed in HEK293 cells (Berglund *et al.*, 2003a). By contrast, immunoblot analysis of membranes from Sf9 cells revealed a molecular weight of ≈45 kDa for the glycosylated (see also section 6.3.1.1) and of ≈36 kDa for the non glycosylated receptor, when the cells were cultured in the presence of 10 µg/ml tunicamycin (**Fig. 6.6**). Several explanations can be given for this discrepancy: for example Fabre *et al.* (1993) reported on diverse molecular weights for the VIP receptor, when prepared

from different tissues, and Sf9 cells are known to have very simple glycosylation patterns compared to mammalian cells (Grünewald *et al.*, 1996; Massotte, 2003). In addition, several GPCRs, expressed in Sf9, cells have been found to migrate atypically in SDS-polyacrylamide gels such the dopamine D_{2S} receptor (Grünewald *et al.*, 1996), a mutant of the formyl peptide receptor (FPR-C126W) (Seifert and Wenzel-Seifert, 2001) or the guinea pig histamine H_1 receptor (Seifert *et al.*, 2003). Thus, the differing molecular weights of the hY_4R from those reported in literature are presumably due to both, differential N-glycosylation in Sf9 cells, and abnormal protein migration in SDS gels. Tunicamycin treatment decreased the molecular weight of the hY_4R by about 9 kDa, which is in agreement with four potential N-glycosylation sites. However, this reduction in weight is quite small, when compared to the results of the aforementioned studies. Regarding the protein expression level, a moderate decrease from ≈1.7 to ≈1.3 pmol/mg was found.

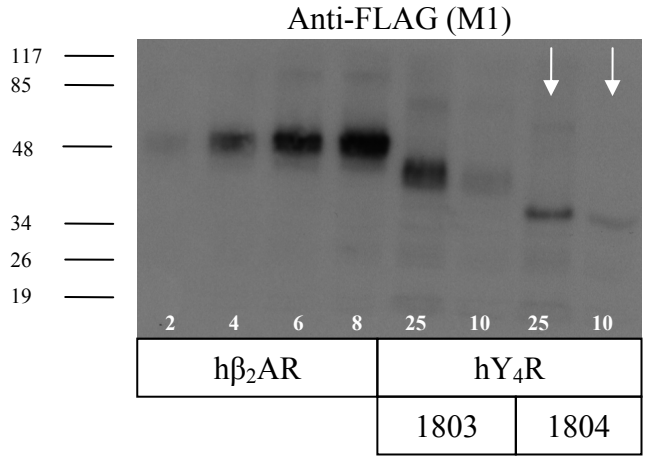

Fig. 6.6: Quantitative immunoblot analysis of two membranes, expressing the hY_4R from tunicamycin treated (lanes marked by an arrow) and untreated cells, with the anti-FLAG (M1) antibody; A dilution of a reference membrane (7.5 pmol/mg $h\beta_2AR$) was used to estimate the expression level of the hY_4 receptor. Figures on the bottom of each lane indicate the amount of protein in µg loaded onto the gel. Expression levels were ≈1.7 pmol/mg and ≈1.3 pmol/mg for the glycosylated and the non glycosylated hY_4R, respectively.

6.3.2 Coupling efficiency of the hY_4R to $G\alpha_{i/o}$ proteins

As described for the hY_2R in section 5.3.2, the coupling efficiency of the hY_4R was determined, using hPP as ligand. **Fig. 6.7** shows the results as basal and stimulated GTPase activity in **A** and as relative to basal GTPase activity in **B**.

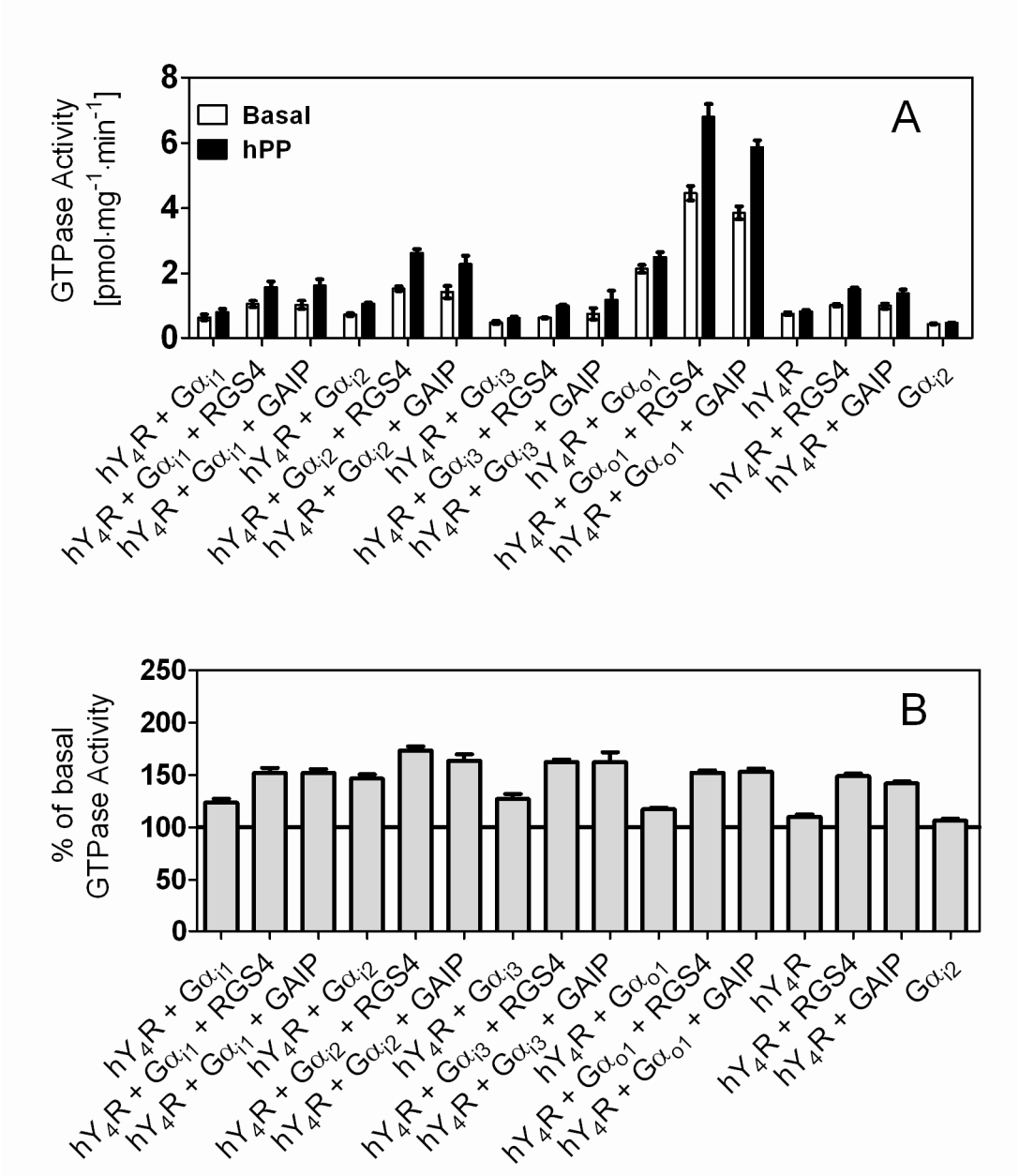

Fig. 6.7: Comparison of the coupling efficiency of hY_4R to $G\alpha_{i/o}$ proteins in the presence and absence of RGS4 or GAIP; The human Y_4R was co-expressed with $G\alpha_{i1}$, $G\alpha_{i2}$, $G\alpha_{i3}$ and $G\alpha_{o1}$, each with $G\beta_1\gamma_2$ and with or without RGS4 or GAIP, respectively. Control membranes contained hY_4R alone, hY_4R in combination with RGS4 or GAIP and $G\alpha_{i2} + G\beta_1\gamma_2$. (A) Absolute GTPase activities under control conditions (open bars, basal) and upon stimulation with 100 nM hPP (black bars); (B) GTPase activities relative to basal expressed in percent; The data are means ± S.E.M. of at least 3 independent experiments performed in duplicate with one membrane batch prepared on one day.

Although G protein coupling of the hY_4R has less been described in literature, reports are limited to the inhibition of forskolin stimulated cAMP formation via $G_{i/o}$ proteins in transfected HEK293 cells (Dautzenberg *et al.*, 2005) and inhibition of forskolin stimulated cAMP formation via $G_{i/o}$ proteins and calcium mobilization in hY_4 transfected $LMTK^-$ cells (Bard *et al.*, 1995). Recently, Misra *et al.* (2004) co-expressed Y_1R, Y_2R, and Y_4R in smooth muscle cells and found that all three receptors preferentially coupled to $G\alpha_{i2}$, while Y_2R and Y_4R additionally activated $G\alpha_q$.

Our results (**Fig. 6.7**) show that the hY_4R couples with comparable efficiency to all $G\alpha_i$ proteins and also to $G\alpha_o$, although to a somewhat lesser extent. Endogenous G proteins of Sf9 cells are activated only poorly by hY_4R. Both RGS4 and GAIP enhance signaling considerably regarding mammalian and endogenous insect cell G proteins. The combinations hY_4R + $G\alpha_{i2}$ + RGS4 and hY_4R + $G\alpha_o$ + RGS4 always co-expressed with $G\beta_1\gamma_2$ showed high signal-to-noise ratios, allowing the investigation of constitutive receptor activity, the pharmacological characterisation of ligands being full/partial agonists, neutral antagonists or inverse agonists and thus providing a well suited system for ligand screening.

6.3.3 Effects of monovalent salts on the GTPase activity

By analogy with section 5.3.3, the hY_4R has been studied with respect to its sensitivity to monovalent salts in the $hY_4R + G\alpha_{i2} + G\beta_1\gamma_2$ + RGS4 Sf9 expression system (**Fig. 6.8**).

NaCl decreased basal and stimulated GTPase activity (**Fig. 6.8 A, D, G**), which reveals a moderate constitutive activity of the hY_4R, while LiCl and KCl showed much less effect. This is in accordance with elevated hY_4R activity observed by Chen *et al.* when the receptor was expressed in melanophores (Chen *et al.*, 2000). The efficacy of hPP was also affected by anions in the same range order of potency, $Cl^- < Br^- < I^-$, as has been seen at the hY_2R. Lately, Lindner *et al.* (2008) reported on ligand-receptor interactions for the NPY receptor family at the molecular level. The authors postulated two ionic interaction sites for pNPY at the hY_2R compared to only one for hPP at the hY_4R. This would mean that the hY_2R binds its ligand tighter than the hY_4R, thus being less sensitive to interferences by monovalent salts.

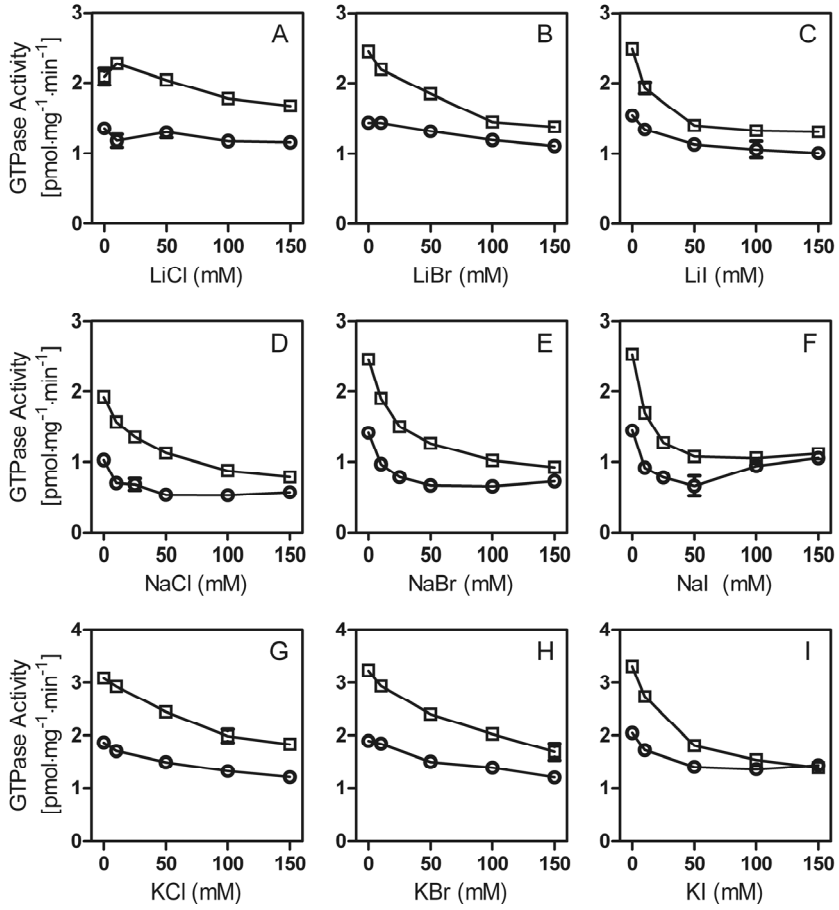

Fig. 6.8: Basal and ligand-stimulated GTPase activity depending on the concentration of various monovalent salts as indicated on the abscissa; High-affinity GTPase activity was determined with a Sf9 membrane expressing $hY_4R + G\alpha_{i2} + G\beta_1\gamma_2$ + RGS4 under control conditions (○) and upon stimulation with 100 nM hPP (□). Data are means ± S.E.M. of one representative experiment performed in duplicate.

The effect of NaCl on hY_4R was studied also in combination with mammalian $G\alpha_{i1}$, $G\alpha_{i3}$, $G\alpha_o$ and with endogenous Sf9 insect cell proteins (always along with RGS4). No differences in concentration-response curves were found (**Fig. 6.9**).

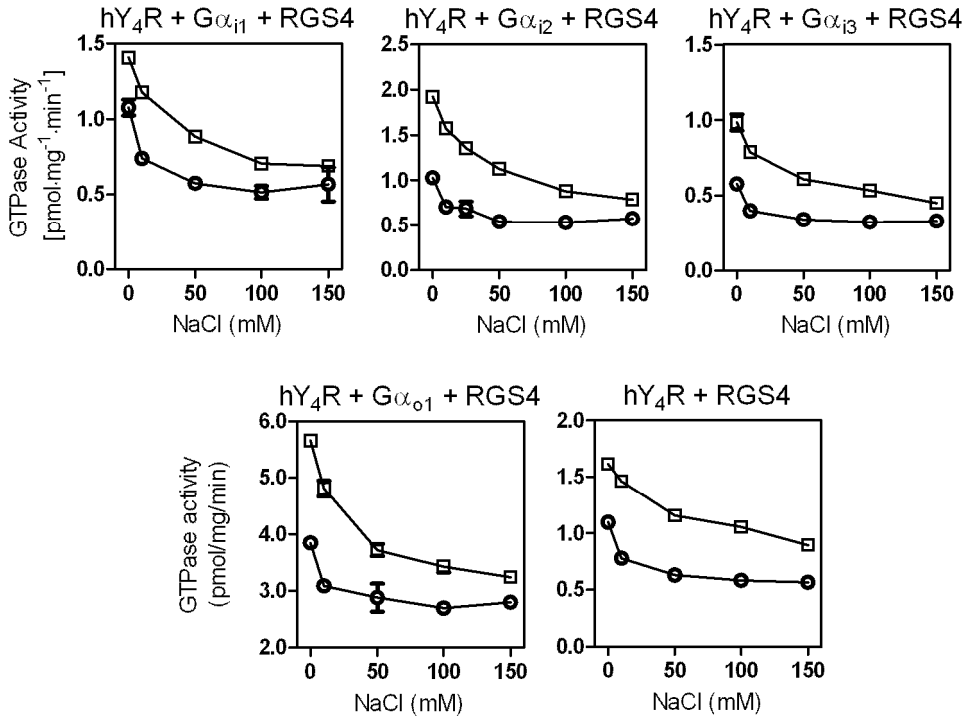

Fig. 6.9: Basal and stimulated GTPase activity depending on the concentration of NaCl; High-affinity GTPase activity was determined with membranes expressing the hY_4R in combination with different Gα-subunits and RGS4 as indicated in titles above graph panels (always along with $G\beta_1\gamma_2$). Data are means ± S.E.M. of one representative experiment performed in duplicate.

6.3.4 Effect of N-glycosylation on receptor function

According to immunoblot analysis (section 6.3.1.3) inhibition of N-glycosylation by tunicamycin causes a drop of ≈9 kDa of the receptor mass and a ≈0.5 pmol/mg decrease in receptor expression level. As revealed by the steady-state GTPase assay, the non-glycosylated hY_4R loses its function and can no longer be stimulated with hPP (**Fig. 6.10**). This highlights the necessity of N-glycosylation for the hY_4R.

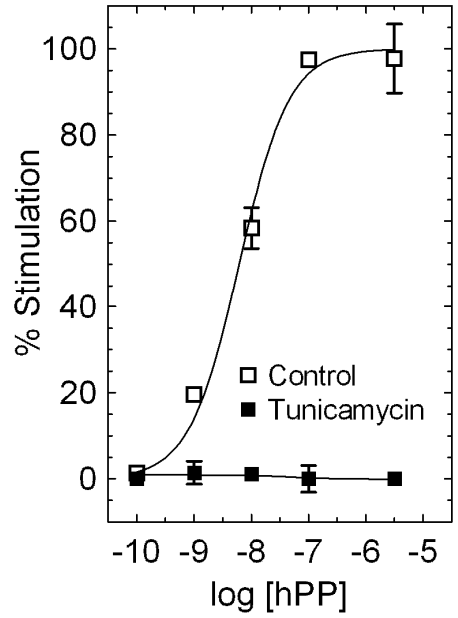

Fig. 6.10: Concentration-response curves of hPP at hY_4R, $G\alpha_{i2}$, $G\beta_1\gamma_2$ and RGS4 expressing membranes from Sf9 cells grown in the presence (■) and absence (□) of tunicamycin; Data are means ± S.E.M. from a representative experiment performed in duplicate.

6.3.5 Evaluation of the hY_4R Sf9 expression systems

To investigate G protein specific effects on ligand potency, as described e.g. for the β2-AR (Wenzel-Seifert and Seifert, 2000), experiments for the construction of hPP concentration-response curves and the calculation of hPP potency at membranes combining the GPCR and different Gα-subunits in the presence and absence of RGS4 were run (**Fig. 6.11** and **Table 6.4**).

The shapes of the concentration-response curves are similar with all membranes used. The hPP potencies are in good agreement. Whether the EC_{50} values from hY_4R + $G\alpha_{i1}$ + RGS4 and hY_4R + $G\alpha_{i3}$ + RGS4 (always co-expressed with $G\beta_1\gamma_2$) are significantly different from those obtained with other membranes, has to be evaluated in further experiments.

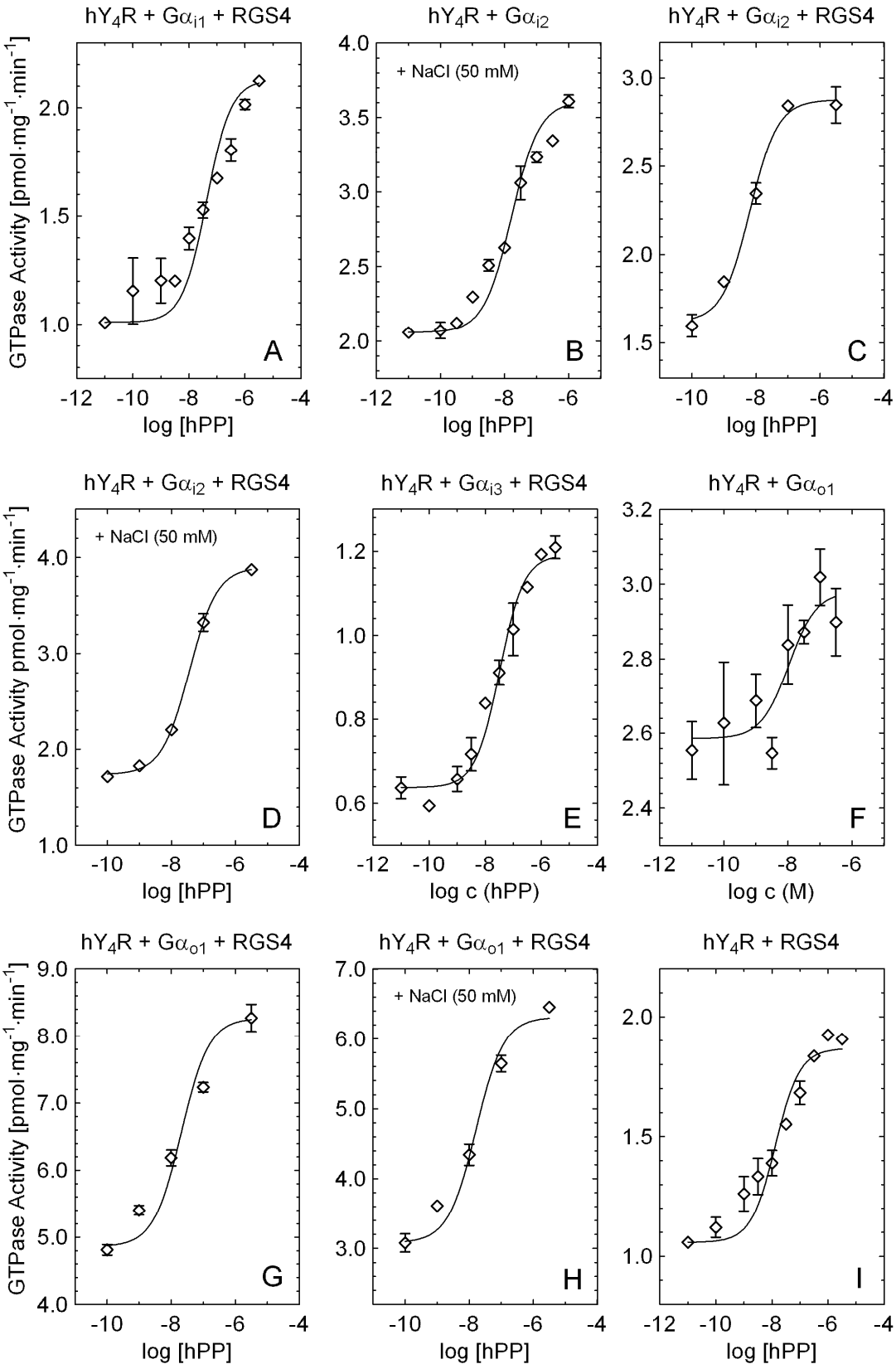

Fig. 6.11: Concentration-response curves of hPP at different co-expression systems (always along with $G\beta_1\gamma_2$ except in I) as indicated on top of each graph; Curves were constructed from data in means ± S.E.M from one experiment each performed in duplicate or triplicate. NaCl was present in some experiments at a concentration of 50 mM (B, D, H).

Table 6.4: EC_{50} values of hPP, determined with different co-expression systems

hY_4R +	$G\alpha_{i1}$ + RGS4	$G\alpha_{i2}$	$G\alpha_{i2}$ + RGS4	$G\alpha_{i3}$ + RGS4	$G\alpha_{o1}$	$G\alpha_{o1}$ + RGS4	RGS4
EC_{50} [nM]	42.2[1]	-	11.0 ± 3.6	32.5[1]	10.5[1]	17.9 ± 1.4	16.5 ± 3.3[2]
EC_{50} [nM][3]	-	16.4[1]	28.3 ± 5.3	-	-	14.3 ± 3.6	-

Membranes contained proteins as indicated in the head row of the table always along with $G\beta_1\gamma_2$ except for the last column. Data are means ± S.E.M. or single values from experiments performed in duplicate or triplicate. [1]n=1, [2]n=2, [3]EC_{50} determined in the presence of 50 mM NaCl

To further validate the steady-state GTPase assay as a sensitive and reliable test system for hY_4R ligands, the two membranes that yielded best signal-to-noise ratios (hY_4R + $G\alpha_{i2}$ + RGS4 and hY_4R + $G\alpha_{o1}$ + RGS4, always co-expressed with $G\beta_1\gamma_2$), were characterized pharmacologically with hY_4R selective peptidergic ligands.

Due to the sensitivity of the hY_4R to sodium ions, experiments with hPP and GW1229 were performed in the presence of 50 mM NaCl and under control conditions. Representative curves are shown in **Fig. 6.12**. There is a noteworthy decrease in basal GTPase activity and maximal response, and the EC_{50} value increases significantly ($p < 0.05$) for hPP (from 11.0 ± 3.6 nM to 28.3 ± 5.3 nM in the presence of 50 mM NaCl) with $G\alpha_{i2}$. However, at the hY_4R + $G\alpha_{o1}$ + RGS4 the EC_{50} value of hPP remains unchanged with 17.9 ± 1.4 nM (control) and 14.3 ± 3.6 nM in the presence of 50 mM NaCl. Regarding GW1229, there is a significant ($p < 0.001$) eightfold increase in EC_{50} from 0.55 ± 0.15 nM to 4.6 ± 0.2 nM in the presence of 50 mM NaCl at the membrane expressing hY_4R + $G\alpha_{i2}$ + RGS4. Likewise at the hY_4R + $G\alpha_{o1}$ + RGS4 the potency drops significantly ($p < 0.05$) by a factor of approximately five from 1.0 ± 0.3 nM to 5.2 ± 1.2 nM in the presence of 50 mM NaCl. These findings are in accordance with reported K_I values for hPP and GW1229 at rY_4R differing in the presence and absence of NaCl (145 mM) (Parker *et al.*, 2002).

Intriguingly, the applied salt concentration raised the intrinsic activity of GW1229 from 82 % to approximately 100 % at both membranes. GW1229 has been reported both as a partial (Berglund *et al.*, 2003b; Ziemek *et al.*, 2007) and a full agonist (Parker *et al.*, 1998; Berglund *et al.*, 2003a).

The ratio of stimulated (3 µM hPP) to basal GTPase activity was improved in the presence of 50 mM NaCl by a factor of 1.4 with $G\alpha_{i2}$ and 1.2 with $G\alpha_{o1}$, respectively (**Table 6.5**).

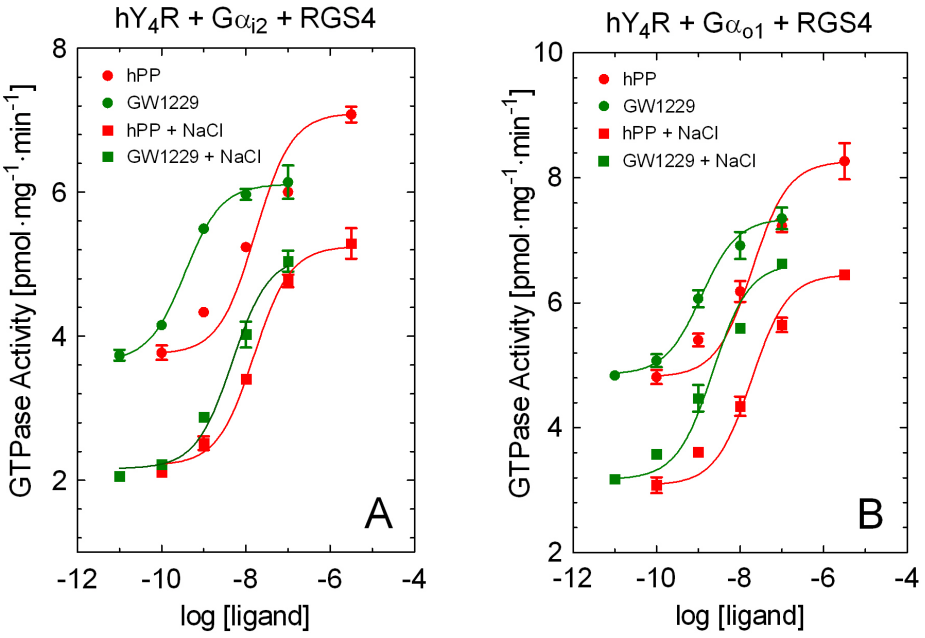

Fig. 6.12: Concentration-response curves of hPP and GW1229 at different co-expression systems (always along with $G\beta_1\gamma_2$) as indicated on top of graphs; Curves were constructed from means ± S.E.M from one representative experiment performed in duplicate. NaCl was present in experiments at a concentration of 50 mM as indicated in the legends.

Table 6.5: Signal-to-noise ratios determined with ligands at two different co-expression systems in the presence and absence of NaCl

	Signal-to-noise ratios at membranes:	
Ligand	**$hY_4R + G\alpha_{i2} + RGS4$**	**$hY_4R + G\alpha_{o1} + RGS4$**
hPP	1.90 ± 0.07	1.63 ± 0.07
+ NaCl (50 mM)	2.37 ± 0.08**	2.11 ± 0.02*
GW1229	1.70 ± 0.05	1.64 ± 0.05
+ NaCl (50 mM)	2.26 ± 0.07***	2.03 ± 0.04***

Signal-to-noise ratios were determined by dividing maximum (at hPP 3 µM or GW1229 100 nM) by basal GTPase activities. Membranes contained proteins as indicated always along with $G\beta_1\gamma_2$. Data are means ± S.E.M. from at least three ($n \geq 3$) independent experiments performed in duplicate. Ratios were compared in the unpaired two-tailed *t* test with a confidence interval of 95 % (*$p < 0.05$, **$p < 0.01$, ***$p < 0.001$).

Additional peptides were tested in the steady-state GTPase assay at both membranes for the hY_4R system (**Fig. 6.13**). Generally, the pharmacological data were in the same range as known from literature (Dautzenberg *et al.*, 2005; Ziemek, 2006).

BW1911U90, a moderately potent Y_4R agonist, pancreatic polypeptide from the rat (rPP) and pNPY were significantly ($p < 0.05$) more potent at membranes expressing $G\alpha_{o1}$. Surprisingly, BW1911U90 was 18 (with $G\alpha_{i2}$), respectively 40 (with $G\alpha_{o1}$) times more potent than reported

in literature (Parker *et al.*, 1998). K^4-hPP was chosen because of its use as fluorescently labeled ligand at the hY_4R in binding assays in our work group (Ziemek *et al.*, 2007). The potencies correspond very well to the data determined by Ziemek (2006) in the aequorin assay. The reported EC_{50} values of the peptide pPYY range from ≈13 to ≈106 nM (Dautzenberg *et al.*, 2005; Parker *et al.*, 2005) or even up to ≈600 nM (hPYY) (Merten *et al.*, 2007) depending on the assay system applied. Pharmacological data are summarized in **Table 6.6** (section 6.3).

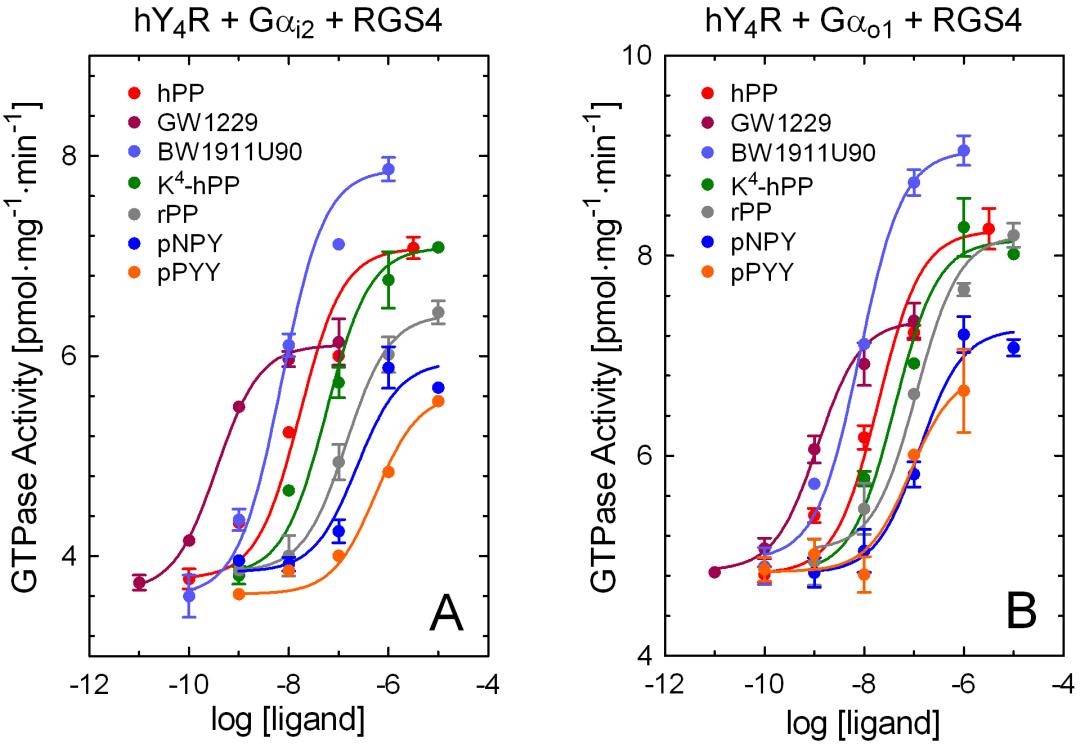

Fig. 6.13: Concentration-response curves of agonistic peptides at different co-expression systems (always along with $G\beta_1\gamma_2$) as indicated on top of graphs; Curves were constructed from means ± S.E.M from one representative experiment performed in duplicate.

6.3.6 Screening of potential NPY Y_4R ligands

Due to a lack of potent non-peptidic antagonists for the hY_4R, a small library of chemical compounds prepared in our work group was screened for activity and affinity to the hY_4R in aequorin assays as well as in flow cytometric binding assays as described by Ziemek (2006) for a pre-selection in order to be applied in the newly established steady-state GTPase assay. First the substances were tested at a concentration of 100 µM for their inhibition of the Ca^{2+}-signal triggered by 100 nM hPP in the antagonist mode. Compounds were chosen that suppressed the hPP signal to a value of less than 30 %. Then, the agonist mode was applied to

select compounds that did not evoke a luminescence signal greater than 35 % of the hPP signal within the cells at 100 µM. Inhibition curves of the chosen potential Y_4 antagonists have been recorded in the aequorin assay (**Fig. 6.14**). Curves were fitted and IC_{50} values were calculated with the GraphPad Prism 5.01 software. Finally some of these substances were tested in a flow cytometric binding assay for their ability to displace the fluorescently labeled Cy5-K^4-hPP (3 nM). Curves were fitted and IC_{50} values were determined with the GraphPad Prism 5.01 software (**Fig. 6.15**).

Though promising results were obtained from the aequorin assay (for pIC_{50} values see **Fig. 6.15**) with AK 377 and PI 284 being somewhat more potent than AK 49, which was described by Ziemek *et al.* (2007) as the first non-peptidic antagonist for the hY_4R, the affinities of the substances were not higher than that of AK 49 (**Fig. 6.15**).

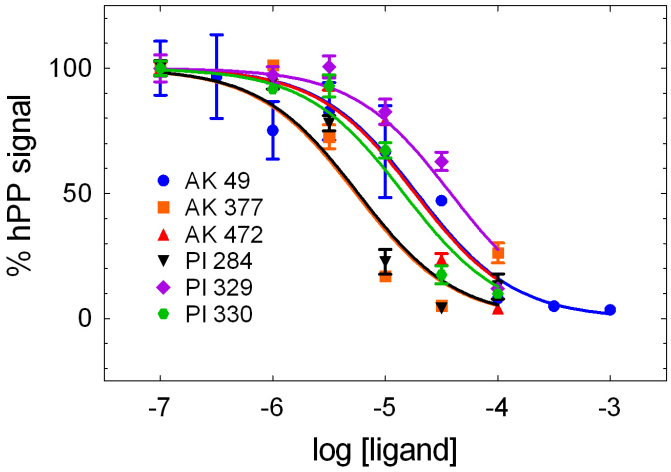

Fig. 6.14: Inhibition curves of non-peptidergic ligands at CHO-hY_4R-$G\alpha_{qi5}$-mtAEQ in the aequorin assay; hPP was present at 100 nM (mean values ± S.E.M., from one experiment, n = 3). pIC_{50} ± S.E.M values were:

AK 49	4.7 ± 0.1	(19.2 µM)
AK 377	5.3 ± 0.1	(5.4 µM)
AK 472	4.7 ± 0.1	(18.3 µM)
PI 284	5.2 ± 0.1	(5.7 µM)
PI 317	4.4 ± 0.1	(38.2 µM)
PI 330	4.8 ± 0.1	(14.6 µM)

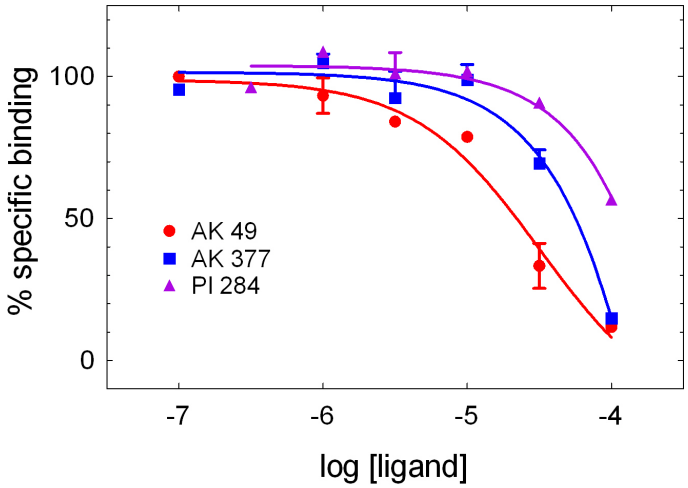

Fig. 6.15: Competition binding of non-peptidergic ligands at CHO-hY_4R-$G\alpha_{qi5}$-mtAEQ in the flow cytometric binding assay; Cy5-K^4-hPP was present at 3 nM. (mean values ± S.E.M., from one representative experiment, n = 3);
IC_{50} values were:
AK 49: ≈32 µM
AK 377: > 100 µM
PI 284: > 100 µM

The compounds were also investigated in the newly established steady-state GTPase assay for their inhibition of the hPP (50 nM) induced signal at membranes containing hY_4R + $G\alpha_{i2}$ +

$G\beta_1\gamma_2$ + RGS4. Intriguingly, AK 49 had the poorest potency (> 500 µM), while the other substances showed IC_{50} values between 100 and 500 µM (**Fig. 6.16 A**). However, hPP stimulated GTPase activity was suppressed to values below basal (except for PI 317). Due to the very high concentrations used, presumably, receptor independent effects take place. Concentration-response curves of hPP in the absence and presence of PI 330 and PI 284 were recorded (**Fig. 6.16 B**). Potential negative effects of the solvent of the ligands were checked. However curves from experiments with and without 1 % DMSO were not different from each other. Determined pEC_{50} values for hPP in these experiments were somewhat higher than usual (7.25 ± 0.09 and 7.31 ± 0.07). As shown in **Fig. 6.16 B** PI 330 (30 and 50 µM) and PI 284 (50 µM) both shifted the concentration-response curve of hPP to the right yielding pEC_{50} values of 6.71 ± 0.09, 6.73 ± 0.08 and 6.82 ± 0.08, respectively. As the maximum signal was depressed by both substances by 15 – 25 %, PI 330 and PI 284 do not behave as typical competitive antagonists.

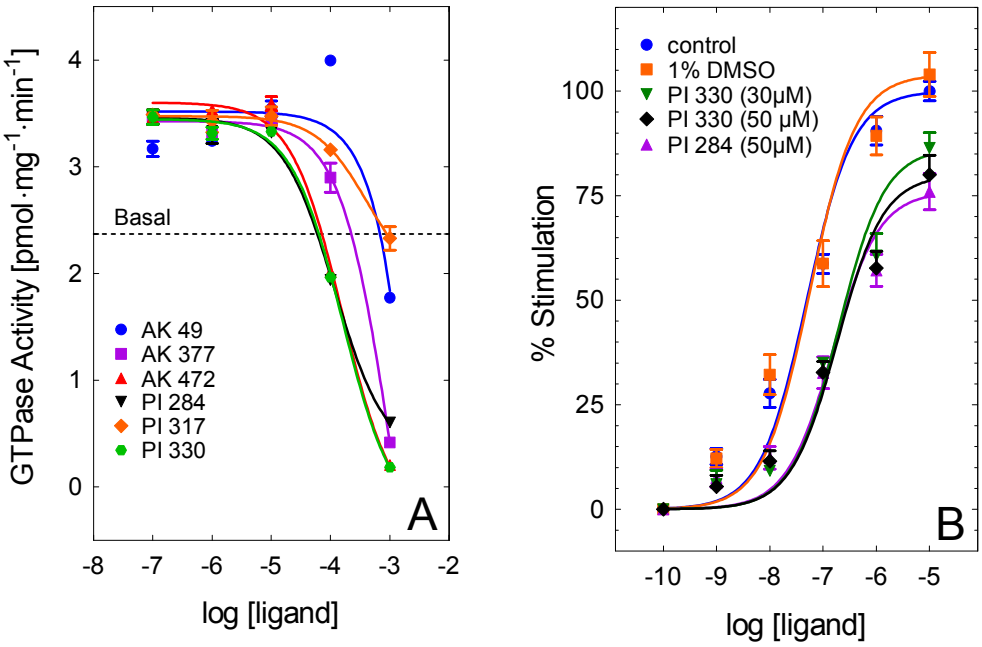

Fig. 6.16: Inhibition and concentration-response curves of potential non peptidergic ligands at membranes containing hY_4R + $G\alpha_{i2}$ + $G\beta_1\gamma_2$ + RGS4 in the steady-state GTPase assay; (A) Inhibition curves were recorded in the presence of 50 nM hPP, basal GTPase activity of non stimulated membranes is indicated as a dotted line. Means ± S.E.M from one representative experiment performed in duplicate. (B) Concentration-response curves of hPP under control conditions, in the presence of 1% DMSO, 30, respectively 50 µM PI 330 and 50 µM PI 284. Means ± S.E.M from three independent experiments performed in duplicate.

Taken together, the promising results obtained with substances in the aequorin assay could not be reproduced with the steady-state GTPase assay. This is presumably due to receptor-independent effects of the compounds as the affinities were not higher than in the case of

AK 49 in the flow cytometric binding assay. Furthermore, as membranes are used for the GTPase assay, there is no physiological barrier for the substances to prevent their direct interaction with, e.g., G proteins at the very high concentrations (obvious from the dramatic drop of GTPase activity at concentrations > 100 μM). However, with the rightward-shift of curves by PI 330 and PI 284 two additional substances have been identified to further optimize binding and antagonism of ligands at the hY_4R.

6.4 Summary and conclusions

The functional reconstitution of the hY_4R together with mammalian $G_{i/o}$ proteins and RGS proteins in Sf9 cells was successful. Characterization of cell membranes containing the GPCR, $G_{i/o}$ proteins and RGS proteins by immunoblotting revealed expression levels of proteins and GPCR/G protein ratios comparable to values from other GPCR co-expression systems reported in literature. Functional characterization of membranes in a steady-state GTPase assay showed that the hY_4R couples with comparable efficiency to all mammalian $G_{i/o}$ proteins applied. The sensitivity of the hY_4R towards monovalent cations revealed its moderate constitutive activity, as the basal receptor activity dropped in the presence of 50 mM NaCl. Furthermore, N-glycosylation of the hY_4R showed to be essential for receptor function. The co-expression systems hY_4R + $G\alpha_{i2}$ + RGS4 and hY_4R + $G\alpha_{o1}$ + RGS4 (always along with $G\beta_1\gamma_2$) were chosen to determine pharmacological parameters of peptidergic ligands (cf. **Table 6.6**), which were in good agreement with data reported in literature. Moreover, hY_4R + $G\alpha_{i2}$ + $G\beta_1\gamma_2$ + RGS4 has been successfully applied for ligand screening.

Table 6.6: Pharmacological parameters of hY_4R ligands determined in the steady-state GTPase assay

Ligand	**hY_4R + $G\alpha_{i2}$+RGS4**		**hY_4R + $G\alpha_{o1}$+RGS4**	
	EC_{50} [nM]	E_{max}	EC_{50} [nM]	E_{max}
hPP	11.0 ± 3.6	-	17.9 ± 1.4	-
+ 50mM NaCl	28.3 ± 5.3^{+}	-	14.3 ± 3.6	-
GW1229	0.55 ± 0.15	0.82 ± 0.04	0.97 ± 0.3	0.82 ± 0.02
+ 50mM NaCl	4.6 ± 0.2^{+++}	0.97 ± 0.03^{+}	5.2 ± 1.2^{+}	1.03 ± 0.01^{++}
K^4-hPP	143.0 ± 24.4	1.02 ± 0.06	76.7 ± 10.9	0.98 ± 0.06
BW1911U90	8.9 ± 1.5	1.28 ± 0.03	4.2 ± 0.4*	1.09 ± 0.01**
rPP	274. 8 ± 49.2	0.86 ± 0.03	127.4 ± 31.0*	0.97 ± 0.04
pNPY	416.9 ± 42.0	0.56 ± 0.05	218.1 ± 39.4*	0.59 ± 0.08
pPYY	400.2 ± 311.2[1]	0.61 ± 0.04[1]	84.9[2]	0.66[2]

Mean values ± S.E.M. of at least three independent experiments (unless indicated otherwise) performed in duplicate; EC_{50} and E_{max} values were compared in the unpaired two-tailed Sudent´s t-test with a confidence interval of 95 %. ($^{+}$experiments with the same ligand and the same membrane performed in the presence of 50 mM NaCl in comparison with experiments performed under control conditions, *comparison of membranes expressing the hY_4R + $G\alpha_{i2}$ + RGS4 versus membranes, expressing the hY_4R + $G\alpha_{o1}$ + RGS4 (always along with $G\beta_1\gamma_2$), one symbol: $p < 0.05$, two symbols: $p < 0.01$, three symbols: $p < 0.001$), [1] n=2; [2] n=1.

Thus, the newly established steady-state GTPase assay together with the Sf9 insect cell expression system proved to be reliable and sensitive tools not only for ligand screening but also for investigations on the molecular level, for instance, regarding receptor glycosylation and G protein coupling.

6.5 References

Balasubramaniam A, Mullins DE, Lin S, Zhai W, Tao Z, Dhawan VC, Guzzi M, Knittel JJ, Slack K, Herzog H and Parker EM (2006) Neuropeptide Y (NPY) Y_4 receptor selective agonists based on NPY(32-36): development of an anorectic Y_4 receptor selective agonist with picomolar affinity. *J Med Chem* **49**:2661-2665.

Bard JA, Walker MW, Branchek TA and Weinshank RL (1995) Cloning and functional expression of a human Y_4 subtype receptor for pancreatic polypeptide, neuropeptide Y, and peptide YY. *J Biol Chem* **270**:26762-26765.

Berglund MM, Schober DA, Esterman MA and Gehlert DR (2003a) Neuropeptide Y Y_4 receptor homodimers dissociate upon agonist stimulation. *J Pharmacol Exp Ther* **307**:1120-1126.

Berglund MM, Schober DA, Statnick MA, McDonald PH and Gehlert DR (2003b) The use of bioluminescence resonance energy transfer 2 to study neuropeptide Y receptor agonist-induced β-arrestin 2 interaction. *Journal of Pharmacology and Experimental Therapeutics* **306**:147-156.

Berridge MJ (1983) Rapid accumulation of inositol trisphosphate reveals that agonists hydrolyse polyphosphoinositides instead of phosphatidylinositol. *Biochem J* **212**:849-858.

Chen G, Way J, Armour S, Watson C, Queen K, Jayawickreme CK, Chen WJ and Kenakin T (2000) Use of constitutive G protein-coupled receptor activity for drug discovery. *Molecular Pharmacology* **57**:125-134.

Dautzenberg FM, Higelin J, Pflieger P, Neidhart W and Guba W (2005) Establishment of robust functional assays for the characterization of neuropeptide Y (NPY) receptors: identification of 3-(5-benzoyl-thiazol-2-ylamino)-benzonitrile as selective NPY type 5 receptor antagonist. *Neuropharmacology* **48**:1043-1055.

Fabre C, el Battari A, Karamanos Y, Couvineau A, Salomon R, Laburthe M, Marvaldi J, Pichon J and Luis J (1993) Glycosylation of VIP receptors: a molecular basis for receptor heterogeneity. *Peptides* **14**:483-489.

Grünewald S, Haase W, Reiländer H and Michel H (1996) Glycosylation, palmitoylation, and localization of the human D_{2S} receptor in baculovirus-infected insect cells. *Biochemistry* **35**:15149-15161.

Kenakin T (1997) Differences between natural and recombinant G protein-coupled receptor systems with varying receptor/G protein stoichiometry. *Trends Pharmacol Sci* **18**:456-464.

Lindner D, Stichel J and Beck-Sickinger AG (2008) Molecular recognition of the NPY hormone familiy by their receptors. *Nutrition* **24**:907-917.

Massotte D (2003) G protein-coupled receptor overexpression with the baculovirus-insect cell system: a tool for structural and functional studies. *Biochimica et Biophysica Acta* **1610**:77-89.

Merten N, Lindner D, Rabe N, Römpler H, Mörl K, Schöneberg T and Beck-Sickinger AG (2007) Receptor subtype-specific docking of $Asp^{6.59}$ with C-terminal arginine residues in Y receptor ligands. *J Biol Chem* **282**:7543-7551.

Misra S, Murthy KS, Zhou H and Grider JR (2004) Coexpression of Y_1, Y_2, and Y_4 receptors in smooth muscle coupled to distinct signaling pathways. *J Pharmacol Exp Ther* **311**:1154-1162.

Nickl K, Gardner EE, Geiger S, Heilmann J and Seifert R (2008) Differential coupling of the human cannabinoid receptors hCB_1R and hCB_2R to the G-protein $G\alpha_{i2}\beta_1\gamma_2$. *Neurosci Lett* **447**:68-72.

Painsipp E, Wultsch T, Edelsbrunner ME, Tasan RO, Singewald N, Herzog H and Holzer P (2008) Reduced anxiety-like and depression-related behavior in neuropeptide Y Y_4 receptor knockout mice. *Genes Brain Behav* **7**:532-542.

Parker EM, Babij CK, Balasubramaniam A, Burrier RE, Guzzi M, Hamud F, Mukhopadhyay G, Rudinski MS, Tao Z, Tice M, Xia L, Mullins DE and Salisbury BG (1998) GR231118 (1229U91) and other analogues of the C-terminus of neuropeptide Y are potent neuropeptide Y Y_1 receptor antagonists and neuropeptide Y Y_4 receptor agonists. *European Journal of Pharmacology* **349**:97-105.

Parker MS, Lundell I and Parker SL (2002) Pancreatic polypeptide receptors: affinity, sodium sensitivity and stability of agonist binding. *Peptides* **23**:291-303.

Parker MS, Sah R, Sheriff S, Balasubramaniam A and Parker SL (2005) Internalization of cloned pancreatic polypeptide receptors is accelerated by all types of Y_4 agonists. *Regul Pept* **132**:91-101.

Schneider EH, Schnell D, Papa D and Seifert R (2009) High constitutive activity and a G-protein-independent high-affinity state of the human histamine H_4-receptor. *Biochemistry* **48**:1424-1438.

Schnell D, Burleigh K, Trick J and Seifert R (2010) No evidence for functional selectivity of proxyfan at the human histamine H_3 receptor coupled to defined G_i/G_o protein heterotrimers. *J Pharmacol Exp Ther* **332**:996-1005.

Seifert R and Wenzel-Seifert K (2001) Defective G_i protein coupling in two formyl peptide receptor mutants associated with localized juvenile periodontitis. *Journal of Biological Chemistry* **276**:42043-42049.

Seifert R, Wenzel-Seifert K, Bürckstümmer T, Pertz HH, Schunack W, Dove S, Buschauer A and Elz S (2003) Multiple differences in agonist and antagonist pharmacology between human and guinea pig histamine H_1-receptor. *Journal of Pharmacology and Experimental Therapeutics* **305**:1104-1115.

Suska A, Ibanez AB, Filippini D and Lundstrom I (2008) Addressing variability in a Xenopus laevis melanophore cell line. *Assay Drug Dev Technol* **6**:569-576.

Tasan RO, Lin S, Hetzenauer A, Singewald N, Herzog H and Sperk G (2009) Increased novelty-induced motor activity and reduced depression-like behavior in neuropeptide Y (NPY)-Y_4 receptor knockout mice. *Neuroscience* **158**:1717-1730.

Voisin T, Goumain M, Lorinet AM, Maoret JJ and Laburthe M (2000) Functional and molecular properties of the human recombinant Y_4 receptor: resistance to agonist-promoted desensitization. *Journal of Pharmacology and Experimental Therapeutics* **292**:638-646.

Wenzel-Seifert K and Seifert R (2000) Molecular analysis of β_2-adrenoceptor coupling to G_s-, G_i-, and G_q-proteins. *Mol Pharmacol* **58**:954-966.

Wenzel-Seifert K and Seifert R (2003) Critical role of N-terminal N-glycosylation for proper folding of the human formyl peptide receptor. *Biochem Biophys Res Commun* **301**:693-698.

Wultsch T, Painsipp E, Donner S, Sperk G, Herzog H, Peskar BA and Holzer P (2006) Selective increase of dark phase water intake in neuropeptide-Y Y_2 and Y_4 receptor knockout mice. *Behav Brain Res* **168**:255-260.

Yurugi-Kobayashi T, Asada H, Shiroishi M, Shimamura T, Funamoto S, Katsuta N, Ito K, Sugawara T, Tokuda N, Tsujimoto H, Murata T, Nomura N, Haga K, Haga T, Iwata S and Kobayashi T (2009) Comparison of functional non-glycosylated GPCRs expression in Pichia pastoris. *Biochem Biophys Res Commun* **380**:271-276.

Ziemek R (2006) Development of binding and functional assays for the neuropeptide Y Y_2 and Y_4 receptors, Doctoral thesis, University of Regensburg, Germany

Ziemek R, Schneider E, Kraus A, Cabrele C, Beck-Sickinger AG, Bernhardt G and Buschauer A (2007) Determination of affinity and activity of ligands at the human neuropeptide Y Y_4 receptor by flow cytometry and aequorin luminescence. *Journal of Receptor and Signal Transduction Research* **27**:217-233.

Chapter 7

7 Summary

For the pharmacological characterization of GPCR ligands in addition to binding data, the determination of the quality of action, agonistic potency or antagonistic activity is a must. There are numerous methods to determine potency and efficacy of ligands at the GPCR of interest, each of which has its specific applications, advantages and disadvantages. Therefore, a maximum of information on a given GPCR is obtained by combining complementary approaches. This thesis aimed at the development of functional assays exploiting FRET-, bioluminescence- and radioactive techniques.

The FRET-based cAMP biosensor Epac2-camps was expressed in SK-N-MC cells to establish an assay to identify potential Y_1R ligands in High Throughput Screening. Thereby changes in CFP/YFP signal ratio due to altered intracellular cAMP levels in response to adenylyl cyclase stimulation with forskolin and inhibition via Y_1R activation are measured. Spectra of SK-N-MC-Epac2-camps cells were recorded in suspension and background corrected. Upon treatment with forskolin and the PDE inhibitor IBMX, the CFP/YFP ratio, calculated from intensities of the maximum emission peaks, increased. According to theory, this is because the fluorophores move away from each other due to unfolding of the protein upon binding of cAMP. The initial results were irreproducible, presumably due to poor stable transfection efficiency and low Epac2-camps expression. Therefore the same experiment was conducted on single cells using a confocal microscope equipped with a Meta detector for spectrum acquisition. However, meaningful changes in ratios were not observed, although adequate cAMP formation in SK-N-MC cells was shown previously by conventional methods. Thus, further investigation of Epac2-camps was discontinued.

HEC-1B-hY_5 cells, stably expressing the hY_5R were considered a suitable starting point to develop functional fluorescence- and bioluminescence-based Ca^{2+} assays. While only small

Ca^{2+} transients were measured in a flow cytometric assay upon stimulation with pNPY in these cells, a robust signal was elicited when the cells were expressing $G\alpha_{qi5}$. This effect was receptor specific because it was inhibited by the Y_5R antagonist CGP 71683A. The concentration response curve of pNPY revealed an EC_{50} comparable to values reported in literature. Since the expression of chimeric G protein declined over time, the parent cells were newly transfected with $G\alpha_{qi5}$ and $G\alpha_{qi9}$, respectively. All resulting transfectants showed only poor Ca^{2+} mobilization in flow cytometric and fluorimetric measurements, though high pNPY concentrations were used. In an additional approach, HEC-1B-hY_5-$G\alpha_{qi5/9}$ cells were transfected with mitochondrially targeted apoaequorin and tested for their ability to emit luminescence upon treatment with the non ionic detergent, triton-X-100. Signals were only obtained from cells expressing $G\alpha_{qi9}$. The measured response was weak compared to that obtained with CHO cells, stably expressing $hY_{2/4}R$, $G\alpha_{qi5}$ and mtAEQ. Thus, an aequorin assay for the hY_5R was not fully established. Nevertheless, optimization of the generation and selection of stable HEC-1B-hY_5 transfectants might pave the way for versatile functional calcium assays.

Finally, with the establishment of a steady-state GTPase assay a classical radioactive technique was applied. For this purpose, baculoviruses encoding the sequences of hY_2R and hY_4R were generated. Functional reconstitution of the receptors with different members of the $G_{i/o}$ protein family and RGS proteins in Sf9 insect cells enabled the determination of coupling efficiencies to G proteins and the identification of the best co-expression systems to yield robust stimulation and high signal-to-noise ratios. Evaluation of membranes, expressing hY_2R + $G\alpha_{i2}$ + $G\beta_1\gamma_2$, hY_4R + $G\alpha_{i2}$ + $G\beta_1\gamma_2$ + RGS4 and hY_4R + $G\alpha_{o1}$ + $G\beta_1\gamma_2$ + RGS4, was performed with peptidergic agonists and non-peptidic antagonists (Y_2R) yielding pharmacological data in good agreement with values reported in literature. The hY_4R stimulated GTPase activity proved to be sensitive to monovalent cations, indicating moderate constitutive receptor activity. Interestingly, only the hY_4R showed a pronounced decrease in molecular weight and a loss of function, when expressed in the presence of tunicamycin, which inhibits N-glycosylation. The hY_2R was much less affected. Thus, with the steady-state GTPase assay a well characterized system and a very useful model to search for potent Y_2 and Y_4 antagonists and inverse agonists has been established.

Ich erkläre hiermit an Eides statt, dass ich die vorliegende Arbeit ohne unzulässige Hilfe Dritter und ohne Benutzung anderer als der angegebenen Hilfsmittel angefertigt habe; die aus anderen Quellen direkt oder indirekt übernommenen Daten und Konzepte sind unter Angabe des Literaturzitats gekennzeichnet.

Regensburg, ……..

Nathalie Pop